

**ENHANCING EFFECT OF L-GLUTAMATE ON  
METHYLMERCURY-INDUCED TOXICITY**

**SIRIRAT AMONPATUMRAT**

**A THESIS SUBMITTED IN PARTIAL FULFILLMENT  
OF THE REQUIREMENTS FOR  
THE DEGREE OF DOCTOR OF PHILOSOPHY  
(TOXICOLOGY)  
FACULTY OF GRADUATE STUDIES  
MAHIDOL UNIVERSITY**

**2008**

**COPYRIGHT OF MAHIDOL UNIVERSITY**

Thesis  
Entitled

**ENHANCING EFFECT OF L-GLUTAMATE ON  
METHYLMERCURY-INDUCED TOXICITY**

.....  
Ms. Sirirat Amonpatumrat  
Candidate

.....  
Prof. Pawinee Piyachaturawat  
Ph.D.  
Major-Advisor

.....  
Prof. Yoshikatsu Kanai  
M.D., Ph.D.  
Co-Advisor

.....  
Assoc. Prof. Suda Riengrojpitak  
Ph.D.  
Co-Advisor

.....  
Assist. Prof. Surawat Jariyawat  
Ph.D.  
Co-Advisor

.....  
Asst. Prof. Auemphorn Mutchimwong.  
Ph.D  
Acting Dean  
Faculty of Graduate Studies

.....  
Prof. Skorn Mongkolsuk  
Ph.D.  
Chair  
Doctor of Philosophy Programme  
in Toxicology  
Faculty of Science

Thesis  
Entitled

**ENHANCING EFFECT OF L-GLUTAMATE ON  
METHYLMERCURY-INDUCED TOXICITY**

was submitted to the Faculty of Graduate Studies, Mahidol University  
for the degree of Doctor of Philosophy (Toxicology)

on

27 October 2008

.....

Ms. Sirirat Amonpatumrat

Candidate

.....

Assoc. Prof. Mayuree Tantisira

Ph.D.

Chair

.....

Assoc. Prof. Krongtong Yoovathaworn

Ph.D.

Member

.....

Prof. Pawinee Piyachaturawat

Ph.D.

Member

.....

Assoc. Prof. Suda Riengrojpitak

Ph.D.

Member

.....

Assist. Prof. Surawat Jariyawat

Ph.D.

Member

.....

Asst. Prof. Auemphorn Mutchimwong.

Ph.D.

Acting Dean

Faculty of Graduate Studies

Mahidol University

.....

Prof. Skorn Mongkolsuk

Ph.D.

Dean

Faculty of Science

Mahidol University

## **ACKNOWLEDGEMENTS**

I would like to express my deepest gratitude and appreciation to my major advisor, Prof. Dr. Pawinee Piyachaturawat for her guidance, supervision, helpful suggestion and encouragement throughout my study. Equal gratitude is also expressed to my co-advisors, Prof. Dr. Yoshikatsu Kanai, Assoc. Prof. Dr. Suda Riengrojpitak, Assist. Prof. Dr. Surawat Jariyawat as well as examination committee, Assoc. Prof. Dr. Mayuree Tantisira and Assoc. Prof. Dr. Krongtong Yoovathaworn for their valuable suggestions and comments on this thesis. I sincerely thank to Prof. Dr. Yoshikatsu Kanai for giving me the valuable opportunity to perform my work in Japan and he always gave a wise suggestion and direction of the experiment throughout my work. I specially thank Prof. Dr. Hiroyuki Sakurai who continuous supported, encouraged and gave a great suggestion during the preparation of my manuscript. I really thank all staff and friends of Department of Pharmacology and Toxicology, Kyorin University, School of Medicine for their supporting, kindness, and friendship. I also thank all friends and all staff of Toxicology Graduate Program and Department of Physiology, Faculty of Science, Mahidol University for their helpfulness and kindness.

This research work is supported by the grant from the Post-Graduate Education, Training and Research Program in Environmental Science, Technology and Management under Higher Education Development Project of Ministry of University Affairs.

Moreover, I would like to thank the grants from Development and Promotion of Science and Technology (DPST) and Ministry of Education, Culture, Sports, Science and Technology (MEXT) scholarship for supporting a part of my study.

Finally, I am very grateful to my parent and my family for their encouragement, kindness, support and understanding throughout my life.

Sirirat Amonpatumrat

**ENHANCING EFFECT OF L-GLUTAMATE ON METHYLMERCURY-INDUCED TOXICITY****SIRIRAT AMONPATUMRAT 4636543 SCTX/D****Ph.D. (TOXICOLOGY)****THESIS ADVISORS: PAWINEE PIYACHATURAWAT, Ph.D., YOSHIKATSU KANAI, M.D., Ph.D., SUDA RIENGROJPITAK, Ph.D., SURAWAT JARIYAWAT, Ph.D.****ABSTRACT**

Methylmercury (MeHg) is a well-known environmental toxicant. With its lipophilic nature and high reactivity to sulfhydryl groups, it is widely distributed and accumulated in the body and causes cells damage. The present study aimed to investigate the enhancing effect of L-Glutamate (L-Glu) on MeHg cytotoxicity in HeLa S3 cells. The results showed that among 20 natural L-amino acids, only L-Glu markedly enhanced the MeHg-induced toxicity. L-Glu exhibited concentration-dependent enhancement in MeHg cytotoxicity. Furthermore, the effect of Glu-related amino acid on the MeHg induced toxicity revealed that L-Glu and L-AAD were similarly effective in enhancing MeHg toxicity, whereas D-Glu, L-Asp and D-Asp were not effective in enhancing the MeHg toxicity. Thus, MeHg toxicity was specifically enhanced by L-Glu. The molecular mechanism underlying the phenomena was then investigated using DNA microarray analysis. Gene expression profile and Gene Ontology (GO) analysis implicated that the induction of stress and apoptosis were involved. We further showed that the enhancement of the toxicity was accompanied by the enhanced apoptosis as indicated by the loss of mitochondrial membrane potential ( $\Delta\Psi_m$ ), the increases in externalized phosphatidylserine (PS) level and activation of caspase-3 activity. Moreover, L-Glu also enhanced MeHg-induced production of reactive oxygen species (ROS) and the depleted intracellular GSH levels. Pretreatment with the anti-oxidant, *N*-acetylcysteine (NAC) greatly alleviated the cytotoxicity, suggesting an enhanced oxidative stress associated with L-Glu-elicited increase of MeHg toxicity. The role of the transport system  $x_C^-$  in the enhancement of MeHg cytotoxicity by L-Glu was then studied, and the results found that co-treatment with MeHg plus L-Glu increased the expression of xCT mRNA, supporting the role of oxidative stress as the underlying mechanism in the enhancement of toxicity. The activity of  $x_C^-$  slightly increased by treating it with L-Glu or MeHg, but greatly increased by co-treatment with MeHg plus L-Glu. In addition, the increased [ $^{14}\text{C}$ ]L-cystine uptake in the cells treated with MeHg and/or L-Glu was competitively inhibited by unlabeled cystine as well as by L-Glu and L-AAD but not by L-Asp. The glutamate receptor agonists; NMDA, KA, and AMPA, failed to enhance the MeHg toxicity, suggesting the inhibition of system  $x_C^-$  by L-Glu underlying its enhancement of MeHg cytotoxicity. The enhancement was highly synergistic as MeHg and L-Glu alone exhibited little toxic effect on the conditions used. This synergism also occurred in neural cells (neuroblastoma cell lines), suggesting that the similar mechanisms may underlie the neural toxicity of MeHg.

**KEY WORDS: METHYLMERCURY/ L-GLUTAMATE/ CYTOTOXICITY/  
OXIDATIVE STRESS/ TRANSPORT SYSTEM  $x_C^-$** 

124 pp.

# ผลของสารแอลกลูตาเมตในการเสริมความเป็นพิษของสารเมทิลเมอร์คิวรี (ENHANCING EFFECT OF L-GLUTAMATE ON METHYLMERCURY-INDUCED TOXICITY)

สิริรัตน์ อมรปทุมรัตน์ 4636543 SCTX/D

ปร.ด. (พิษวิทยา)

คณะกรรมการควบคุมวิทยานิพนธ์: ภาวิณี ปิยะจตุรวัฒน์, ปร.ด., Yoshikatsu Kanai, M.D., Ph.D., สุดา เรียงโรจน์พิทักษ์, Ph.D., สุรวุฒน์ จริยาวัฒน์, ปร.ด.

## บทคัดย่อ

สารเมทิลเมอร์คิวรี (MeHg) เป็นสารพิษที่ปนเปื้อนอยู่ทั่วไปในสิ่งแวดล้อม จากคุณสมบัติการละลายในไขมันได้ดีของสารและว่องไวต่อการรวมตัวกับหมู่ซัลไฟด์ทำให้ MeHg สามารถแพร่กระจายไปในที่ต่างๆ ได้ดีและสะสมไปทั่วร่างกาย ก่อให้เกิดความเป็นพิษต่อเซลล์ การศึกษานี้มีวัตถุประสงค์เพื่อศึกษาฤทธิ์ของ L-Glutamate (L-Glu) ต่อการเสริมความเป็นพิษของ MeHg โดยใช้เซลล์มะเร็งปากมดลูก (HeLa S3) เนื่องจากมีความทนต่อพิษของ MeHg ผลการศึกษาพบว่าในบรรดากรดอะมิโนทั้งหมด 20 ชนิดมีเฉพาะ L-Glu เท่านั้นที่เสริมความเป็นพิษของ MeHg เป็นข้อมูลยืนยัน L-Glu มีความจำเพาะต่อการเสริมความเป็นพิษ การศึกษากลไกของการเสริมความเป็นพิษของ L-Glu ต่อ MeHg ในระดับโมเลกุลนั้นโดยในเบื้องต้นได้ทำการวิเคราะห์ด้วย DNA microarray เพื่อตรวจสอบการแสดงออกของยีน ค้นหาหน้าที่และความสัมพันธ์ของกลุ่มยีนด้วย Gene Ontology พบว่าการออกฤทธิ์เสริมความเป็นพิษของ L-Glu ต่อ MeHg เกี่ยวข้องกับการกระตุ้นให้เกิดภาวะออกซิเดทีฟและการชักนำให้เกิดการตายของเซลล์ตามมาแบบอะพอพโทซิส โดย L-Glu ออกฤทธิ์เสริมความเป็นพิษชักนำให้เซลล์เกิดการตายแบบอะพอพโทซิสเพิ่มมากยิ่งขึ้น L-Glu ยังทำให้เกิดอนุมูลอิสระ (ROS) ในเซลล์เพิ่มขึ้น และลดระดับของกลูตาไทโอนภายในเซลล์ที่ได้รับ MeHg ลงไปอีก ในทางตรงกันข้ามการตายของเซลล์ลดน้อยลงเมื่อเซลล์ให้สาร *N*-acetylcysteine ก่อนชักนำให้เกิดความเป็นพิษ เนื่องจากความจำเพาะของ L-Glu ที่เสริมความเป็นพิษของ MeHg ผลที่ได้นี้สอดคล้องกับบทบาทในการทำงานของระบบการขนส่ง  $x_c^-$  ที่เกี่ยวข้องกับ L-Glu ร่วมกับ MeHg เมื่อเทียบกับเซลล์ที่ได้รับ L-Glu หรือ MeHg เพียงอย่างเดียว การทำงานของ  $x_c^-$  เพิ่มขึ้นเพียงเล็กน้อยเท่านั้น นอกจากนี้พบว่าการขนส่ง [ $^{14}$ C]L-cystine ที่เพิ่มขึ้นในเซลล์ที่ได้รับ L-Glu และ/หรือ MeHg สามารถถูกยับยั้งได้โดย cystine, L-Glu และ L-AAD ซึ่งเป็นตัวยับยั้งที่จำเพาะต่อการขนส่ง [ $^{14}$ C]L-cystine อย่างไรก็ตาม L-Asp ไม่สามารถยับยั้งการขนส่ง [ $^{14}$ C]L-cystine ได้ นอกจากนี้ เมื่อเซลล์ได้รับตัวยับยั้งจำเพาะต่อ Glu receptor ได้แก่ NMDA, KA และ AMPA พบว่าสารดังกล่าวไม่ทำให้ความเป็นพิษของ MeHg เพิ่มขึ้น จากข้อมูลการศึกษาทั้งหมดนี้แสดงให้เห็นว่า L-Glu มีความจำเพาะในการออกฤทธิ์เสริมความเป็นพิษของ MeHg โดยกลไกการทำงานผ่านกลไกการยับยั้งระบบขนส่ง  $x_c^-$  ความเป็นพิษที่เพิ่มขึ้นหลังจากเซลล์ได้รับทั้ง L-Glu และ MeHg เป็นการเสริมฤทธิ์ซึ่งกันและกัน เนื่องจากเมื่อเซลล์ได้รับเพียง L-Glu หรือ MeHg จะเกิดความเป็นพิษเพียงเล็กน้อยเท่านั้น จากกลไกที่ได้กล่าวมาข้างต้นอาจจะนำไปใช้อธิบายความเป็นพิษที่เกิดจากการออกฤทธิ์เสริมกันของ L-Glu และ MeHg ที่พบได้ในเซลล์ประสาท (neuroblastoma cell lines) และระบบประสาท

## CONTENTS

	<b>Page</b>
<b>ACKNOWLEDGEMENTS</b>	iii
<b>ABSTRACT</b>	iv
<b>LIST OF TABLES</b>	vii
<b>LIST OF FIGURES</b>	viii
<b>LIST OF ABBREVIATIONS</b>	x
<b>CHAPTER</b>	
<b>I INTRODUCTION</b>	1
<b>II LITERATURE REVIEW</b>	5
I) Mercury	5
1. Methylmercury (MeHg)	6
2. Toxicity of MeHg	7
2.1 Mechanism of MeHg cytotoxicity	7
2.2 Cell death induced by MeHg	14
II) Glutamate (Glu)	20
1. Glu as neurotransmitter and intermediary molecule	20
2. Glu in the peripheral tissues	23
3. Mechanism of Glu-induced toxicity	23
4. Effect of oxidative stress on $x_c^-$ transporter system	29
<b>III MATERIALS AND METHODS</b>	31
<b>IV RESULTS</b>	51
<b>V DISCUSSION</b>	91
<b>VI CONCLUSION</b>	100
<b>REFERENCE</b>	102
<b>APPENDIX</b>	120
<b>BIOGRAPHY</b>	124

## LIST OF TABLES

<b>TABLE</b>	<b>Page</b>
A. Transport system for cystine and/or glutamate	27
M1. List of 20 amino acids used in this experiment	41
M2. Chemical structure of Glu-related amino acids	42
1. Comparative effect of various L-amino acids on MeHg-induced toxicity in HeLa S3 cells	57
2. Gene ontology (GO) of up-regulated differentially expressed genes between MeHg alone and MeHg plus L-Glu treated for 3 h	65
3. List of up-regulated gene associated with stress-response in MeHg plus L-Glu for 3 h of exposure	67
4. List of up-regulated gene associated with apoptosis in MeHg plus L-Glu for 3 h of exposure	67
5. Comparison of genes which be classified into both stress-response and apoptosis process in MeHg plus L-Glu treatment at various times	68
6. Effect of glutamate receptor agonist on MeHg cytotoxicity	87



## LIST OF FIGURES

FIGURE	Page
A. Mercury cycle in biological system	5
B. Glutathione synthesis pathway	10
C. Glutathione redox cycling	10
D. Dysregulation of intracellular $\text{Ca}^{2+}$ lead to mitochondrial dysfunction and ultimately cytotoxicity	12
E. Morphological change of the apoptotic and necrotic cell death process	14
F. Extrinsic and intrinsic apoptotic pathway	15
G. Chemical structure of glutamate	20
H. Classification of glutamate receptors	21
I. Glutamate acts as the intermediary molecule in the metabolism process	22
J. Overstimulation of glutamate receptor leads to excitotoxicity	25
K. Oxidative glutamate toxicity	26
L. Structure of cystine/glutamate exchanger $\text{x}_c^-$	28
M1. Schematic diagram showing time course of treatment and sample collection	40
M2. Schematic diagram showing the step of sample collection for microarray experiment	43
M3. Schematic diagram showing the period of NAC pretreatment and experimental treatment group	47
1. Concentration- and time-effect of MeHg cytotoxicity in HeLa S3 cells	52
2. Effect of L-Glu on MeHg cytotoxicity in HeLa S3 cells	53
3. Concentration-dependent effect of L-Glu to enhance cytotoxicity of 8 $\mu\text{M}$ MeHg at 12 h of exposure	55
4. Effect of Glu-related amino acids on MeHg cytotoxicity	59
5. Scatter plot analysis comparing the hybridization signals of MeHg alone and MeHg plus L-Glu at various time points	61
6. Distribution of fold change of the gene in the cells co-treated with MeHg and L-Glu for 3 h using microarray analysis	63

## LIST OF FIGURES (Cont.)

FIGURE	Page
7. Representative histogram of FACS analysis of mitochondrial membrane potential ( $\Delta\Psi_m$ )	70
8. Change of mitochondrial membrane potential ( $\Delta\Psi_m$ ) in MeHg and/or L-Glu treatment with time	71
9. Representative dot plot analysis of an Annexin V-FITC staining cell population after MeHg and/or L-Glu treatment	73
10. Effect of MeHg and L-Glu on caspase-3 activity	75
11. Representative histograms showing the level of ROS in MeHg and/or L-Glu treated cell by FACS	77
12. Effect of MeHg and L-Glu on intracellular ROS level measured with DCFH dye	78
13. Effect of MeHg and L-Glu on intracellular GSH level	80
14. Effect of N-acetylcysteine (NAC) on the cytotoxicity induced by co-treatment of MeHg and L-Glu	81
15. Effect of MeHg and L-Glu on xCT mRNA expression level	83
16. [ $^{14}\text{C}$ ]L-cystine uptake by HeLa S3 cells and the enhancement by treatment with MeHg and L-Glu	85
17. Inhibitory effect of L-cystine (L-Cyst.), L-glutamate (L-Glu), L- $\alpha$ -aminoadipate (L-AAD) and L-aspartate (L-Asp) on [ $^{14}\text{C}$ ]L-cystine uptake in HeLa S3 cells	86
18. Concentration-dependent effect of MeHg cytotoxicity in neuroblastoma cell lines	89
19. Effect of L-Glu on MeHg-induced cytotoxicity in neuroblastoma cells	90

## LIST OF ABBREVIATIONS

$\alpha$	alpha
$\beta$	beta
$^{\circ}\text{C}$	degree Celsius
%	percent
$\Delta\Psi_{\text{m}}$	mitochondrial membrane potential
$\mu\text{M}$	micromolar
$\mu\text{l}$	microliter
AMPA	a-amino-3-hydroxy-5-methyl-4-isoxazolepropionic acid
ANOVA	analysis of variance
BCA	bicinchoninic acid
BSO	buthione-L-sulfoxamine
$\text{CaCl}_2$	calcium chloride
CCCP	carbonyl cyanide 3-chlorophenylhydrazone
$^{14}\text{C}$	carbon-14
cDNA	complementary deoxyribonucleic acid
Ci	Curie
cRNA	complementary ribonucleic acid
D-Asp	D-aspartate
D-Glu	D-glutamate
DCFH-DA	2', 7'-dichlorofluorescein diacetate
DCF	dichlorofluorescein
$\text{DiIc1(5)}$	1,1',3,3,3',3' hexamethylindodicarbocyanine iodide
DMEM	Dulbecco's Modified Eagle's Medium
DPBS	Dulbecco's Phosphate Buffered Saline (DPBS)
EDTA	ethylenediaminetetraacetic acid
<i>et al</i>	and colleagues
FACS	Fluorescence Activated Cell Sorter
FCM	Flow cytometry
FBS	fetal bovine serum
FITC	fluorescein isothiocyanate

## LIST OF ABBREVIATIONS (Cont.)

GSH	glutathione (reduced form)
g	gram
h	hour
H <sub>2</sub> O <sub>2</sub>	hydrogen peroxide
HBSS(-)	Na <sup>+</sup> -free Hanks's balanced salt solution
HCl	hydrochloric acid
HEPES	4-(2-hydroxyethyl)-1-piperazineethanesulfonic acid
KA	kainic acid
KCl	potassium chloride
KH <sub>2</sub> PO <sub>4</sub>	potassium diphosphate
L-AAD	L- $\alpha$ -aminoadipate
L-Asp	L-aspartate
M	molar
MeHg	methylmercury
MeHgCl	methylmercury chloride
MeHg-Cys	methylmercury-cysteine conjugate
MgSO <sub>4</sub>	magnesium sulphate
mM	milimolar
ml	mililiter
MEM	Minimum Essential Medium Eagle
mRNA	messenger ribonucleic acid
MTT	[3-(4,5-dimethylthiazol-2-yl)-2,5-diphenyl tetrazolium bromide]
NAC	N-acetylcysteine
NaCl	sodium chloride
NaOH	sodium hydroxide
Na <sup>+</sup>	sodium ionized form
nM	nanomolar
nm	nanometer
NMDA	N-methyl-D-aspartate
OD	Optical Density
PBS	phosphate buffered saline

**LIST OF ABBREVIATIONS (Cont.)**

PCR	Polymerase Chain Reaction
pH	log concentration of $H^+$
PI	propidium iodide
PS	phosphatidylserine
ROS	Reactive oxygen species
rpm	revolution per minute
RT-PCR	Reverse Transcriptase Polymerase Chain Reaction
SEM	standard error of mean
-SH	sulfhydryl group
U	Unit
UV	ultraviolet
$x_c^-$	cystine/glutamate exchanger
xCT	light subunit of cystine/glutamate exchanger

## CHAPTER I

### INTRODUCTION

Methylmercury (MeHg) is a well-known environmental toxic pollutant that continues to pose great risks to human health. It is a highly lipophilic molecule which facilitate its penetration and distribution, causing pathological damage to several organs system in the body. Intracellularly, MeHg binds to sulfhydryl (–SH)-containing molecule and may bind to a variety of enzymes including those of microsomes and mitochondria causing cells injury and cell death (Gerhardsson, 1996). Several mechanisms have been proposed for MeHg toxicity such as alterations in calcium homeostasis (Marty & Atchison, 1997), facilitation of apoptosis/necrosis (Kunimoto, 1994), change in neurotransmitter system (Aschner *et al.*, 2000). However, the formation of reactive oxygen species (ROS) with the disruption of mitochondrial function is suggested to be the major mechanism of cell damage (Limke & Atchison, 2002; Yee & Choi, 1996). Increased ROS production by MeHg has been reported both in vitro and in vivo including in cultured neuron (Mundy & Freudenrich, 2000), glial cells (Shanker *et al.*, 2003), and brain synaptosomes prepared from animals injected with MeHg (Ali *et al.*, 1992). Mitochondria is the major source of ROS formation, it is likely to be the primary target of the MeHg-mediated oxidative stress (Limke & Atchison, 2002). Exposure to MeHg causes the disturbance of the mitochondrial functions, e.g., the disruption of electron transport chain and  $\text{Ca}^{2+}$  regulation. It also leads to the loss of mitochondrial membrane potential ( $\Delta\Psi_m$ ) and the leakage of hydrogen peroxide (InSug *et al.*, 1997; Marty & Atchison, 1998). Due to its extremely high affinity for thiol groups, MeHg binds to GSH leading to the depletion of GSH (Choi *et al.*, 1996; Gatti *et al.*, 2004; Yee & Choi, 1994). GSH is the major intracellular antioxidant which plays a role in maintaining cellular redox status and protecting against oxidative stress (Meister, 1995). GSH depletion leads to accumulation of ROS and thus exposes cells to free-radical mediated damage (Ou *et al.*, 1999). The capability of antioxidant such as vitamin E, GSH, selenium, catalase as

well as the lipid peroxidation inhibitor  $\alpha$ -lipoic acid in prevention of toxicity has suggested that the oxidative stress plays a key role in the process. (Anuradha & Varalakshmi, 1999; Gasso *et al.*, 2001; Sanfeliu *et al.*, 2001). MeHg-poisoning is characterized by damage of discrete anatomical areas of the brain, such as the visual cortex and the granule layers of the cerebellum (Nagashima, 1997). However, the mechanism underlying the selective toxicity of MeHg in the central nervous system has not been understood.

L-Glutamate (L-Glu) is known as a major excitatory neurotransmitter in the central nervous system (CNS). Besides its role as the neurotransmitter in the brain, several lines of emerging evidence have suggested that Glu also acts as the extracellular signal mediator in the peripheral tissues including bone, testis, pancreas, lung, hepatocyte, and heart (Hinoi *et al.*, 2004; Skerry & Genever, 2001). In these tissues, the similar releasing process and receptor-mediated response as existed at synapses in the CNS are observed (Skerry & Genever, 2001). Glu is the intermediary molecule which contributes to the production of several other important molecules in the metabolism process such as glutathione, polyamines and urea as well as GABA (gamma-aminobutyric acid (Nedergaard *et al.*, 2002). The cytotoxicity property of L-Glu is mediated by two primary mechanisms. The first is mediated by glutamate receptors. Overstimulation of glutamate receptors causes injury or death of neurons by a mechanism termed excitotoxicity (Lipton & Rosenberg, 1994; Namiki *et al.*, 2005). ROS production, as well as mitochondrial  $\text{Ca}^{2+}$  overload, mitochondrial depolarization and ATP depletion, is one of the important mechanisms underlying the excitotoxic damage of neurons (Kao *et al.*, 2007; Reynolds & Hastings, 1995). The second mechanism of L-Glu-induced ROS production is via the inhibition of system  $\text{x}_c^-$ . System  $\text{x}_c^-$  is the cystine/glutamate exchanger that mediates the uptake of cystine in exchange for L-Glu. It provides cells with cystine/cysteine for glutathione (GSH) synthesis (Bannai & Tateishi, 1986). L-Glu inhibits cystine uptake of the cells by the inhibition of system  $\text{x}_c^-$  in a competitive manner leading to a decrease in intracellular GSH level and, in turn, increases ROS (Christensen, 1990; Kanai & Endou, 2001). Beside its permeation through plasma membrane by simple diffusion, MeHg is transported into cells by system L amino acid transporters when it is conjugated with

cysteine (MeHg-Cys) (Kanai & Endou, 2003). In the earlier study on the transporter-mediated MeHg toxicity, the effect of amino acids on the inhibition of MeHg-Cys uptake by the competition at system L were examined in HeLa S3 cell. Surprisingly, L-Glu greatly enhanced the toxicity of MeHg in HeLa S3 cells. Therefore, the present study aims to explore the underlying mechanisms of L-Glu enhancing MeHg toxicity. In addition, there is no direct experimental evidence on the effect of a co-exposure of MeHg and L-Glu. Part I of the study, the specificity of L-Glu on the enhancement of MeHg toxicity was studied. The effect of twenty naturally occurring L-amino acids and the Glu-related acidic amino acids including D-Glu, L-Asp, D-Asp and L- $\alpha$ -aminoadipate (L-AAD) on the MeHg-induced cytotoxicity were examined using MTT assay. In Part II, the mechanism underlying the enhancing effect of L-Glu on the MeHg-induced toxicity were investigated by examining the candidate of primary response genes, apoptotic-mediated process, the role of oxidative stress and the involvement of system  $x_C^-$ . Finally, in Part III, the effect of L-Glu on the MeHg-induced toxicity was examined in neuroblastoma cell lines to partly support that the enhancing toxic effect of L-Glu obtained from the present study was also applicable to neurotoxicity.

**Objectives:**

The present study aimed to investigate the effect and underlying mechanisms by which L-glutamate (L-Glu) enhanced methylmercury (MeHg) toxicity.

The following were specific objectives:

1. To determine the effect of L-Glu on MeHg-induced toxicity.
  - 1.1 The concentration and time-course effects of MeHg and L-Glu were evaluated to obtain the optimal conditions by using the cell viability MTT assay.
  - 1.2 The specificity of L-Glu on the enhancement of MeHg toxicity was investigated by determining the effect of twenty L-amino acids and Glu-related acidic amino acid on the MeHg toxicity.



2. To investigate genes and molecular processes those might be associated with the enhanced toxic effect of L-Glu by using DNA-microarray analysis and followed by Gene Ontology (GO) analysis.
3. To investigate the effect of MeHg and L-Glu on the apoptosis by examining the loss of mitochondrial membrane potential ( $\Delta\Psi_m$ ), the externalization of phosphatidylserine (PS) and the caspase-3 activation.
4. To investigate whether the exacerbation of oxidative stress process was related to the enhanced toxic effect of L-Glu by examining the intracellular reactive oxygen species (ROS) level in parallel to the level of reduced glutathione (GSH). In addition, the protective effect of anti-oxidant, *N*-acetylcysteine (NAC), was investigated to support that oxidative stress-mediated L-Glu did enhance the MeHg toxicity.
5. To investigate the involvement of transport system  $x^-_C$  on mediating L-Glu enhanced the MeHg toxicity by determining the expression level of light subunit of system  $x^-_C$  (xCT) and the transport of [ $^{14}$ C]L-cystine and inhibitory effect of competitive inhibitor of transport system  $x^-_C$ .
6. To investigate the role of glutamate receptor-mediated excitotoxicity in the enhancing effect of L-Glu on the MeHg toxicity by using the agonist of ionotropic glutamate receptors (iGluR).
7. To examine whether the enhanced MeHg toxicity by L-Glu was applicable to neural cells. The cytotoxicities in three neuroblastoma cell lines including Neuro2A, NIE115 and NG108-15 were investigated using MTT assay.

## CHAPTER II

### LITERATURE REVIEW

#### I. Mercury

Mercury is an environmental harmful chemical that bioaccumulates through the food chain and leads to increase in human risk of poisoning (Debes *et al.*, 2006). Within the environment, it exists in three forms which include elemental Hg ( $\text{Hg}^0$ ), inorganic Hg ( $\text{Hg}^+$  and  $\text{Hg}^{2+}$ ), and organic Hg such as methylmercury (MeHg) (Clarkson & Magos, 2006) (Figure A). The release of elemental and mercuric mercury into the environment resulted primarily from the burning of fossil fuels. Elemental Hg is oxidized to mercuric mercury ( $\text{Hg}^{2+}$ ), which can be further methylated by microorganisms to MeHg in aquatic environment, resulting in MeHg accumulation in the sea food-chain and representing the most prevalent source for human consumption of mercury. MeHg is the form of mercury with the highest impact due to its contamination in the environment which continues to pose great risks to human health (Clarkson *et al.*, 2003). Moreover, Several catastrophic epidemics resulting from consumption of MeHg-contaminated food in Iraq (Bakir *et al.*, 1973), and contamination in Japan (Harada, 1995) have led to its recognition as a ubiquitous environmental toxicant (Clarkson, 2002).

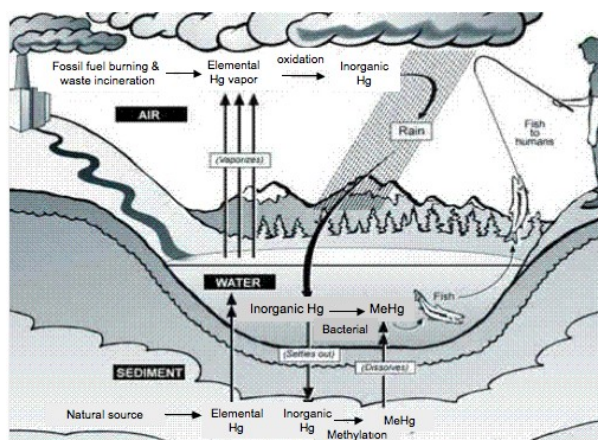


**Figure A.** Mercury cycle in biological system (Clarkson & Magos, 2006)

## 1. Methylmercury (MeHg)

### Absorption, distribution, biotransformation and excretion

All forms of mercury cause toxic effects in a number of tissues and organs, depending on its chemical form, the level and duration of exposure, and the route of exposure. MeHg is a highly lipophilic molecule, following ingestion of MeHg, approximately 90% is absorbed by the gastrointestinal tract (Kershaw *et al.*, 1980). In addition, the lipophilic nature of MeHg facilitates it to readily penetrate membrane resulting in widespread distribution and accumulation throughout our body, thereby induces pathological changes in several organs including brain, kidney and liver (Crespo-Lopez *et al.*, 2007; Zalups, 2000) as well as immune system (Stejskal *et al.*, 1996). MeHg has a high association constant ( $15 < \text{pK}_a < 23$ ) for sulfhydryl (–SH) groups (Carty & Malone, 1979). Therefore, in the systemic circulation, MeHg can bind to numerous nucleophilic groups on molecules especially, it has a high affinity to sulfhydryl (–SH) group-containing molecule such as glutathione (GSH), cysteine, N-acetylcysteine, metallothionein, and albumin, which represent the main chemical target of mercury conjugation in biological system (Mullaney *et al.*, 1994). For example, the binding of MeHg to –SH group of an enzyme leads to alteration in its conformation and as a consequence causing enzyme functional inhibition. Since –SH groups are ubiquitous within cells, the variation in the distribution and many different functions are altered by the binding of MeHg (Mullaney *et al.*, 1994).

In addition, previous study reported that the complex of MeHg and L-cysteine has structurally similar to L-methionine, therefore, it has been proposed that this MeHg-L-cysteine conjugate was transported via amino acid transport system L, which transports large neutral amino acids (Aschner & Aschner, 1990). The binding of MeHg with –SH facilitates its distribution throughout the body. This is also the basis of MeHg transport, binding, distribution, metabolism and detoxification in biological system (Zalups, 2000).

Following MeHg exposure, mercury compounds are excreted mainly via the kidney and the gastrointestinal tract in the bile and feces. Demethylation of methylmercury and the inorganic mercury formed in the liver are excreted in the bile conjugated with glutathione and related compound (WHO, 1990). However, MeHg

undergoes enterohepatic recirculation where it is secreted into bile, and then partly reabsorbed and returned to the liver. Most MeHg is eliminated by demethylation and then excretion of the ionic form in the feces (~90% in feces as mercuric Hg). The excretion rate of MeHg is species dependent, resulting in a different body burden in animals exposed to the same level of MeHg. However, the rate of excretion is directly proportional to the body burden in both human and experimental animals. The range of half-life excretion varies in different species which has been estimated to be around 45-90 days (Clarkson, 1972).

## **2. Toxicity of MeHg**

Severe MeHg poison is known to reveal typical neurological symptoms as the Minamata disease and also accumulation in the kidney and the liver as well, thereby induces pathological changes in these organs (Eto *et al.*, 1992; Zalups, 2000). Although, MeHg has a high affinity for binding to all thiol groups (Hughes, 1957) but numerous biochemical, physiological and morphological investigations on the neurotoxic effects of MeHg have demonstrated that the damage is remarkably selective, being limited to specific areas of the brain, such as the granule layer of cerebellum and the visual cortex of the cerebrum (Eto, 1997; Nagashima, 1997). These data have suggested that there is more than one mechanism that may contribute to the expression of MeHg-induced neurotoxicity. And this selectivity effect of MeHg has not fully explained.

### **2.1 Mechanism of MeHg cytotoxicity**

MeHg exerts its toxic effect via two major mechanisms i) the induction of oxidative stress and ii) the perturbation of intracellular  $\text{Ca}^{2+}$  levels.

#### **2.1.1 Oxidative stress mediated MeHg-induced toxicity**

One of the main mechanisms of MeHg-induced toxicity involves the induction of oxidative stress. Oxidative stress is the result of an imbalance between pro-oxidant and antioxidant homeostasis (Castoldi *et al.*, 2001). If the oxidative persists, oxidative damage to critical biomolecules accumulates and eventually results in several

biological effects such as alterations in signaling transduction and gene expression for mitogenesis, mutagenesis as well as cell death (Ermak & Davies, 2002).

### **1) Accumulation of Reactive oxygen species (ROS)**

Oxidative stress is a deleterious imbalance between the production and removal of reactive radicals resulting in the accumulation of high levels the reactive oxygen species (ROS), including oxygen radical such as superoxide radical ( $\cdot\text{O}_2^-$ ), hydroxyl radical ( $\cdot\text{OH}$ ), as well as non-radical derivatives of oxygen including hydrogen peroxide ( $\text{H}_2\text{O}_2$ ). These toxic reactive species are thought to cause oxidative damage, they are highly oxidizing and potently damaging to cellular-redox-sensitive protein, enzyme and DNA, and also induce lipid peroxidation. In addition, oxidative stress is one of triggers of apoptosis in a variety of cells and is also thought to be involved as a component of the common pathway in execution of apoptosis (Fabisiak *et al.*, 1998; Sandstrom *et al.*, 1994).

Several studies have revealed the important of oxidative stress in MeHg-induced toxicity in multiple experimental models. For example, MeHg induced ROS production in cultured neurons (Mundy & Freudenrich, 2000), glial cells (Shanker & Aschner, 2003) as well as cerebellum synaptosome obtained from MeHg treated rats and mice (LeBel *et al.*, 1990). Yee demonstrated that upon treating the mouse brain with MeHg, there were the increased levels of  $\cdot\text{O}_2^-$  and  $\text{H}_2\text{O}_2$  in various fractions of the brain which was accompanied by significant reductions in the levels of superoxide dismutase (SOD) and glutathione (GSH). It was also shown that the susceptibility of MeHg toxicity was decreased in HeLa cells which overexpressed Mn-SOD, suggesting mitochondrial-mediated  $\cdot\text{O}_2^-$  production that leads to MeHg-induced toxicity (Naganuma *et al.*, 1998). Moreover in astrocyte culture, MeHg also caused a significant increase in the  $\text{F}_2$ -isoprostanes ( $\text{F}_2$ -IsoPs), prostaglandin-like molecules, which act as lipid peroxidation biomarker for oxidative damage (Yin *et al.*, 2007). On the other hand, it has been shown that vitamin E, GSH, selenium, catalase as well as the lipid peroxidation inhibitor  $\alpha$ -lipoic acid antagonize the deleterious effects of MeHg (Anuradha & Varalakshmi, 1999; Gasso *et al.*, 2001; Sanfeliu *et al.*, 2001). Several mechanisms underlying the induction of ROS production by MeHg have been proposed. Ganther (1978) suggested that MeHg itself could generate MeHg radicals

via the homolytic breakdown (Ganther, 1978). Approximately 2% of oxygen radicals are constantly produced in the mitochondria through incomplete reduction of oxygen. Therefore, the alterations of electron transport system can increase the level of ROS (Turrens & Boveris, 1980). Recently, it has been reported that  $\cdot\text{O}_2^-$  and  $\text{H}_2\text{O}_2$  production might occur at complex II in the electron transport chain (Senoo-Matsuda *et al.*, 2001). It has been demonstrated that MeHg-induced ROS production selectively caused by the functional modification in the constituents of complex II-III of the mitochondria by which MeHg-induced increases in the  $\cdot\text{O}_2^-$  and  $\text{H}_2\text{O}_2$  generation rates (Mori *et al.*, 2007).

## **2) Depletion of glutathione (GSH) by MeHg**

Several studies have reported the relationship between glutathione (GSH) and MeHg-induced toxicity and showed the responses of mammalian cells to oxidative stress which occur through several antioxidant systems, including enzymes and nonenzymatic molecules. Among them, glutathione ( $\gamma$ -glutamylcysteinylglycine, GSH) which is the most abundant non-protein thiol that present in mammalian cells and it plays an important role in maintaining cellular redox status and protecting cells against oxidative stress. It is a tripeptide composed of L-glutamate, L-cysteine and glycine and is synthesized in the cytosol by the action of  $\gamma$ -glutamylcysteine synthetase to form  $\gamma$ -glutamylcysteine from cysteine and glutamate, followed by the addition of glycine by glutathione synthetase (Meister, 1995; Wu *et al.*, 2004) (Figure B).

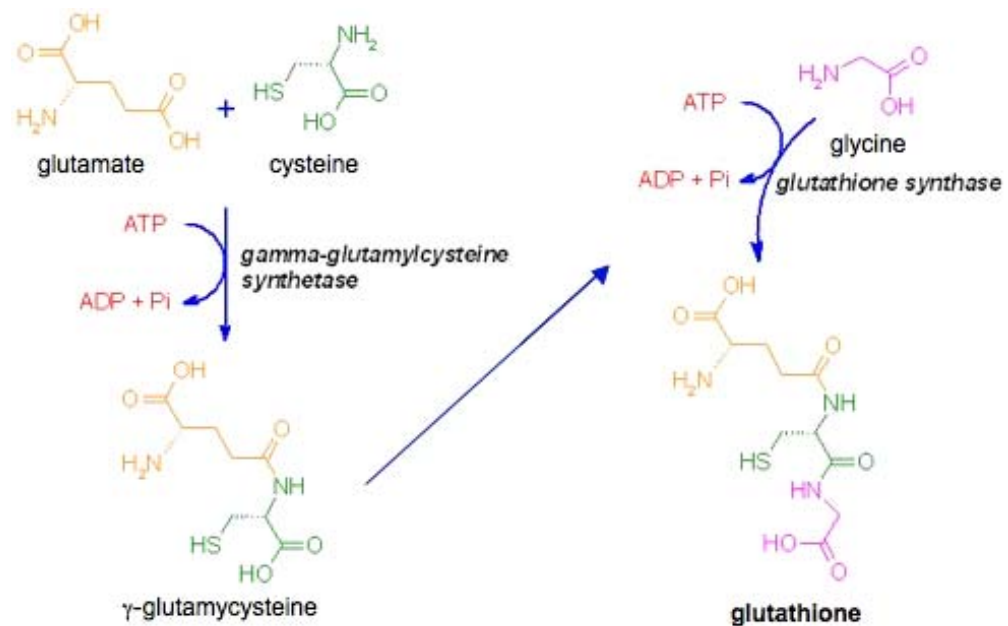


**Figure B.** Glutathione synthesis

Glutathione exists in two forms, the antioxidant “reduced glutathione” (GSH) and the oxidized form which is a sulfur-sulfur linked compound, known as glutathione disulfide of GSSG. GSH serves as the major cytosolic antioxidant by scavenging ROS via the enzymes glutathione peroxidase (GPx) and glutathione reductase (GR), and it also plays a role in maintaining the intracellular redox status (Sarafian *et al.*, 1996) (Figure C).

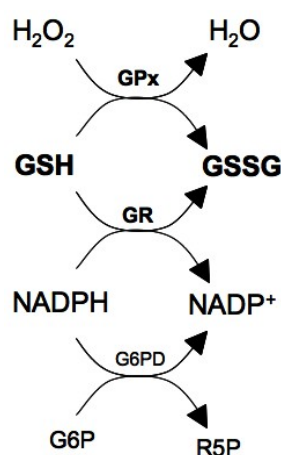


**Figure C.** GSH redox cycling

When GSH is reduced to about 20 to 30% of normal levels, the cell's ability to defend itself will be impaired, and this may eventually lead to cell injury and death (Reed, 1990). GSH depletion also caused by MeHg, that has extremely high affinity for thiol group, binds to GSH and hence exposing the cells to free-radical mediated damage (Gatti *et al.*, 2004; Yee & Choi, 1994). It was demonstrated that the non-toxic low dose of MeHg has shown to increase GSH while the toxic high dose of GSH tended to diminish (Zalups, 2000). It was also shown that the activity of metabolizing enzyme including glutathione reductase (GR),  $\gamma$ -glutamyl transpeptidase (GGT), and glutathione peroxidase (GPx) were decreased in mice treated with MeHg for 7 days (Vijayalakshmi & Sood, 1994). While in the presence of extracellular GSH, the neurotoxicity of MeHg have been decreased in neuroblastoma and cerebral neuronal cell line (Park *et al.*, 1996). Moreover, the administration of antioxidant GSH decreased MeHg-induced ROS formation (Shanker & Aschner, 2003). Similarly, an intracellular GSH-MeHg complex may protect cells by preventing organometallic molecules from attacking essential intracellular thiols (Alexander & Aaseth, 1982). In addition, GSH conjugation appears to be the major pathway for MeHg efflux from the cells and results in protection from MeHg toxicity (Fujiyama *et al.*, 1994).

In addition to its effects on GSH metabolizing enzyme, MeHg has selectively inhibited transport systems for cystine and cysteine, thus decreasing intracellular GSH content and compromising the redox potential (Shanker & Aschner, 2001). In addition, it has been reported that MeHg inhibits uptake system for glutamate and cysteine transport, both of which will compromise glutathione synthesis and redox status in the cell (Shanker *et al.*, 2001). These studies suggested that the oxidative stress appears to play a significant role in cell damage and death following MeHg exposure.

### **2.1.2 Alteration of $\text{Ca}^{2+}$ homeostasis**

Normally, intracellular  $\text{Ca}^{2+}$  concentration in the cytosol is tightly regulated in the range between 10-100 nM, whereas extracellular  $\text{Ca}^{2+}$  is 1-2 mM (Berridge *et al.*, 2000). Both concentrations are maintained by interplay between pump and transporter located in plasma membranes and organelles, and  $\text{Ca}^{2+}$  binding protein (Berridge *et al.*, 2003). In normal cells, intracellular  $\text{Ca}^{2+}$  is stored inside the endoplasmic reticulum



(ER) upon stimulation, intracellular  $\text{Ca}^{2+}$  is changed rapidly, indicated  $\text{Ca}^{2+}$  have important role in signaling process, whereas sustained elevation of intracellular  $\text{Ca}^{2+}$  can activate various signal transduction cascades such as loss of mitochondrial membrane potential, decreased ATP production, increased ROS level, leading to cell damage and cell death (Dong *et al.*, 2006; Duchen, 2000) (Figure D).

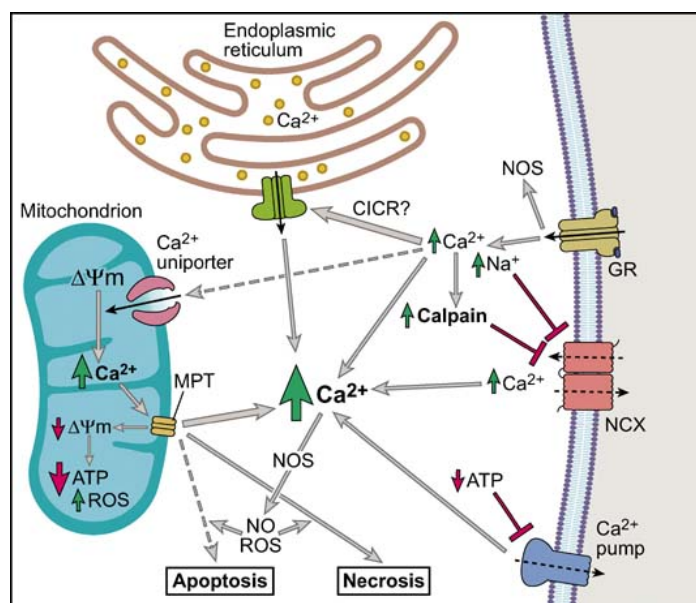


**Figure D.** Dysregulation of intracellular  $\text{Ca}^{2+}$  leads to mitochondrial dysfunction and ultimately cytotoxicity (Dong *et al.*, 2006).

There are several studies reported the evidence of MeHg on the disturbance of  $\text{Ca}^{2+}$  homeostasis. MeHg has been shown to disrupt  $\text{Ca}^{2+}$  homeostasis in several cell types such as neuronal cells (Denny *et al.*, 1993), cerebellar granule cells (Marty & Atchison, 1997), rat brain synaptosome (Denny *et al.*, 1993) and NG108-15 neuroblastoma cell (Denny *et al.*, 1993). In cerebellar cells, MeHg at low concentration (0.2-2  $\mu\text{M}$ ), causing a biphasic increase in intracellular  $\text{Ca}^{2+}$  followed by the influx of extracellular  $\text{Ca}^{2+}$  (Marty & Atchison, 1997). The elevated levels of  $\text{Ca}^{2+}$  have been implicated in the induction of apoptosis cell death. For example, the administration of agent that can buffer the intracellular  $\text{Ca}^{2+}$  as well as both  $\text{Ca}^{2+}$ -chelator and  $\text{Ca}^{2+}$ -channel block protect against MeHg cytotoxicity (Gasso *et al.*, 2001; Marty & Atchison, 1998; Sakamoto *et al.*, 1996).

Mitochondria have been thought to be one possible source of the early onset of  $\text{Ca}^{2+}$  elevation during MeHg exposure (Limke *et al.*, 2003). The elevation of  $\text{Ca}^{2+}$  release from mitochondria has been reported to occur via the induction of oxidative stress (Duchen, 2000). MeHg exposure increased the formation of intracellular superoxide anion, hydrogen peroxide and hydroxyl radicals, indicating that the mitochondrial electron transport chain is an early primary site of ROS formation (Shanker *et al.*, 2005). The consequence of oxidative stress is the induction of the mitochondrial permeability transition (MPT), a megapore formed on the inner mitochondrial membrane in response to adverse conditions, including oxidative stress, elevation of mitochondrial matrix  $\text{Ca}^{2+}$ , and anoxia (Bernardi *et al.*, 1993). Normally, mitochondria accumulate  $\text{Ca}^{2+}$  based on the extremely negative membrane potential within the inner mitochondrial membrane (140-180 mV, negative inside), making  $\text{Ca}^{2+}$  buffering an energetically favorable process (Gunter & Gunter, 1994). Once open, MTP caused the passage of proton, ions and other solutes  $\leq 1.5$  kDa, including  $\text{Ca}^{2+}$  (Zoratti & Szabo, 1995), leading to a collapse of the mitochondrial membrane potential ( $\Delta\Psi_m$ ). Therefore, the induction of MPT may relate to the alteration of intracellular  $\text{Ca}^{2+}$  as well as be a critical factor in determining cell survival following MeHg exposure.

## 2.2 Cell death induced by MeHg

Cell death can occur by one of two distinct mechanisms: apoptosis and necrosis which depend on many factors such as the intensity and duration of the stimulus, the extent of ATP depletion and the availability of caspase (Zeiss, 2003).

### 2.2.1 Apoptosis

Apoptosis, or programmed cell death (PCD), is ATP-dependent and tightly control mode of cell death characterized by morphological changes, including cell shrinkage, cytoplasmic membrane blebbing, lobing of nucleus, nuclear DNA fragmentation, and disassembly into apoptotic bodies. This apoptotic bodies are further engulfed by macrophages and thus without causing the inflammatory response. Conversely, necrosis cell death is occurred when cells are exposed to extreme variances from physiological condition (e.g. hypothermia, hypoxemia, ischemia, etc.), which result in the loss of membrane integrity. Serious physical or chemical insult may result in an impairment of the cell's ability to maintain homeostasis, and an influx of water and extracellular ions which lead to cell/organelle swelling and complete lysis, causing release of cellular content which further results in damage of surrounding cells and a strong inflammatory response in the corresponding tissue (Leist & Jaattela, 2001). This is the ATP-independent process, which requires no energy investment by the cell and it is (Figure E).

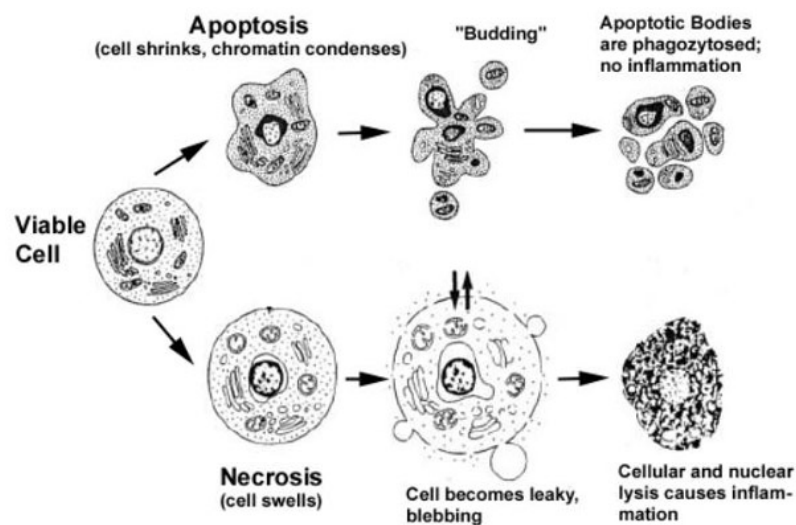


**Figure E.** Morphological changes of the apoptotic and necrotic cell death processes (Van Cruchten & Van Den Broeck, 2002).

## 2.2.2 Apoptosis signaling pathway

Apoptosis can occur via two major biochemical pathways including the receptor pathway (extrinsic), and the mitochondrial pathway (intrinsic) (Figure E). However, there are evidence that these two pathways are linked together and molecules in one pathway can influence the other (Igney & Krammer, 2002) by which they converge on the same terminal, or execution pathway. Apoptosis is initiated by the cleavage of caspase-3 which results in DNA fragmentation, degradation of cytoskeletal and nuclear protein, cross-linking of proteins, formation of apoptotic bodies, expression of ligands for phagocytic cell receptors and finally the apoptotic cell is removed by phagocytic cell.

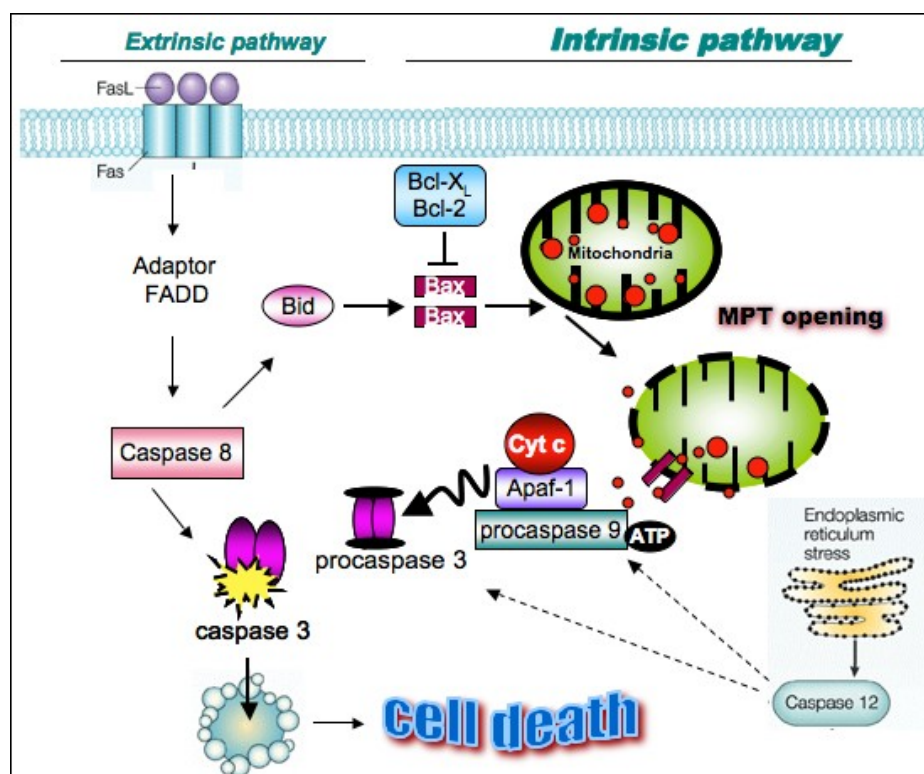


**Figure F.** Extrinsic and Intrinsic apoptotic pathway

### 1. Extrinsic or Death receptor-mediated pathway

Extrinsic pathway is mediated by the activation of death receptor. Stimulation of death receptors of the tumor necrosis factor (TNF) receptor superfamily such as CD95 (APO-1/Fas) or TNF-related apoptosis-inducing ligand (TRAIL) receptors, in

turn, recruits caspase-8, initiator caspase, to form the death-inducing signaling complex (DISC) is the critical event that transmits the death signal by activating caspase-8, and the subsequent activation of the effector caspase-3, which is the central caspase responsible for the proteolytic cascade leading to cell death.

## **2. Intrinsic or Mitochondrial-mediated pathway**

The intrinsic pathway is mediated by mitochondria, and, in response to apoptotic stimulus to trigger the release of apoptogenic factors, such as cytochrome c, from the mitochondrial intermembrane space to the cytosol (Wang, 2001). Besides the release of cytochrome c from the intramembrane space, another intramembrane contents that are consequently released contain apoptosis inducing factor (AIF) to facilitate DNA fragmentation, and Smac/Diablo proteins to inhibit the inhibitor of apoptosis (IAP) (Walczak & Krammer, 2000). Once in the cytosol, cytochrome c binds to Apaf-1 (apoptosis protease-activating factor 1) in the presence of dATP, and to form apoptosome complex, which further binds and activates procaspase-9 (Cain *et al.*, 2000). Caspase-9 activates the executioner caspase-3, then cleaves key substrates in the cell to produce many of the cellular and biochemical events of apoptosis (Bratton *et al.*, 2001).

The linkage between extrinsic and intrinsic apoptosis pathway has been revealed at different levels. However, both of them end at the point of the execution phase, which is the activation of execution caspase. The activation of caspase-8 after death receptor activation may result in cleavage of Bid, a Bcl-2 family protein with a BH3 domain only, which in turn translocates to mitochondria, causing the release of cytochrome c thereby initiating a mitochondrial-mediated apoptotic pathway (Cory & Adams, 2002). In addition, the cleavage of caspase-6 downstream of mitochondria may feed back to the receptor pathway by cleaving caspase-8 (Cowling & Downward, 2002). The morphological changes are a consequence of characteristic molecular and biochemical processes occurring in apoptotic cells such as protein cleavage, protein cross-linking, DNA breakdown, and phagocytic recognition that together result in the distinctive structural pathology were described previously (Hengartner, 2000).

### 2.2.3 Biochemical feature of apoptosis

Biochemical changes characteristic of apoptosis include alteration in mitochondrial membrane permeability, activation of intracellular cysteine protease (caspase), internucleosome fragmentation of the genomic DNA and externalization of membrane phosphatidylserine (PS) etc.

#### 1) Loss of mitochondrial membrane potential ( $\Delta\Psi_m$ )

The mitochondrial transmembrane potential ( $\Delta\Psi_m$ ) is often used as an indicator of cellular commitment to death and/or cellular viability, as the proton gradient across the inner membrane enables the energetically unfavorable production of ATP, the cellular energy source. Thus, the disruptions to this transmembrane potential have severe consequences in mitochondrial respiration, energy production, and, accordingly, cell survival. Most apoptosis-inducing conditions involve the disruption of the mitochondrial inner transmembrane potential ( $\Delta\Psi_m$ ) as well as the mitochondrial permeability transition pore (MTP). The alteration in  $\Delta\Psi_m$  resulting in the opening of MTP and that are thought to be regulated by the Bcl-2 family of pro- and antiapoptotic proteins (Kroemer *et al.*, 1997). MTP is the process of sudden increase of the inner mitochondrial membrane permeability to solutes with a molecular mass below 1.5 kDa. As MTP opens, solute ( $K^+$ ,  $Mg^{2+}$  and  $Ca^{2+}$ ) and water enter, leading to mitochondrial swelling which eventually causes the rupture of the outer mitochondrial membrane, resulting in the release of proapoptotic proteins from the mitochondrial membrane space into the cytoplasm (Bernardi *et al.*, 1999; Loeffler & Kroemer, 2000). Importantly, the release of mitochondrial factors, the dissipation of  $\Delta\Psi_m$  and MPT also lead to inhibition of ATP synthesis and further an increase in reactive oxygen species (ROS) are increased (Kroemer & Reed, 2000).

#### 2) Caspase activation

Caspases belong to the family of cysteine protease that are synthesized as inactive proforms and upon activation, the protein at aspartate residue is cleaved out (Alnemri *et al.*, 1996; Degterev *et al.*, 2003). They are categorized into two classes: the initiator caspases (caspase-2, -8, -9 and -10) and the effector caspases (caspase-3, -6 and -7). Caspases can activate each other by which the activation of an initiator

caspase can further activate the downstream caspase through a protease cascade of activation. Caspase-3 is considered to be the most important of the executioner caspases.

A number of different substrates both functional and structural protein in cytoplasm or nucleus are cleaved by caspase-3, leading to many of the morphological changes of apoptotic cell (Degterev *et al.*, 2003). For example, caspase-3 specifically activates the endonuclease CAD (caspase-activated DNase) results in the polynucleosomal DNA fragmentation within nuclei and causes chromatic condensation (Nagata, 2000). Caspase-3 also induces the degradation of several cytoskeletal proteins such as actin or fodrin which will lead to loss of cell shape, whereas proteolysis of lamin results in nuclear shrinking (Degterev *et al.*, 2003).

### **3) DNA fragmentation**

During apoptosis, the cell nucleus undergoes chromatin condensation, margination, and finally fragmentation. The fragmentation of DNA into oligonucleosomal ladders (180 to 200 base pair) by  $\text{Ca}^{2+}$  and  $\text{Mg}^{2+}$ -dependent endonucleases is characteristic of early event in apoptosis (Bortner *et al.*, 1995).

### **4) Externalization of phosphatidylserine**

Phosphatidylserine (PS) is a phospholipid that is normally limited to the inner leaflet of the plasma membrane. The externalization of phosphatidylserine (PS) has been identified as one of the early and prominent features of apoptosis (Bratton *et al.*, 1997; Martin *et al.*, 1995). Exposure of PS on the outer leaflet of the plasma membrane serves as an important signal for the recognition and removal of the apoptotic cell by phagocytes, allowing quick phagocytosis with minimal effect to the surrounding cells (Fadok *et al.*, 1992).

## **2.3 MeHg-induced apoptosis**

Exposure of MeHg causes apoptosis in various cell types such as neural cell (Wilke *et al.*, 2003), glial (Belletti *et al.*, 2002), myogenic (Usuki & Ishiura, 1998) and lymphoid cells (Usuki & Ishiura, 1998). MeHg-treated cells exhibit a decrease in the adenine nucleotide energy charge ratio, an elevation in  $[\text{Ca}^{2+}]_i$ , and alteration in the

membrane function including altered phospholipid synthesis, loss of normal lipid packing, and the translocation of phosphatidylserine from the inner to the outer membrane. Although several studies have been revealed the mechanism underlying MeHg-induced apoptosis, mitochondria are believed to be a primary target of MeHg and are an important site of ROS formation (Limke & Atchison, 2002). The elevation of ROS levels directly caused the oxidation of lipids, proteins, and DNAs, thereby enhancing the disruption of mitochondrial membrane potential ( $\Delta\Psi_m$ ) as a part of a positive feed back (Marchetti *et al.*, 1997). Changes in  $\Delta\Psi_m$  have been originally postulated to be early and obligate events in the apoptotic signaling pathway (Cohen, 1997). Shenker demonstrated that exposure of human T-cells to MeHg for 1 h resulted in a profound decrease in the  $\Delta\Psi_m$  (Shenker *et al.*, 2002). They have shown that low-level mercury exposure causes functional and morphological alteration in mitochondria consistent with the activation of the apoptotic cascade (Shenker *et al.*, 1998). MeHg can cause the disruption of electron transport chain, leading to loss of the mitochondrial membrane potential and also the leakage of hydrogen peroxide (InSug *et al.*, 1997; Lund *et al.*, 1993). Mitochondrial stress was also recognized at the early stage of MeHg cytotoxicity (Belletti *et al.*, 2002). This effect can impair the function of mitochondria through elevation of intracellular  $\text{Ca}^{2+}$  levels (Marty & Atchison, 1998). MeHg exposure disrupts  $\text{Ca}^{2+}$  regulation in mitochondria by decreasing  $\text{Ca}^{2+}$  uptake and inducing  $\text{Ca}^{2+}$  release (Levesque & Atchison, 1991).

The involvement of ROS at different phases of apoptosis, such as induction of mitochondrial permeability transition (MPT), release of mitochondrial death amplification factors, activation of intracellular caspases and DNA damage has been clearly established (Le Bras *et al.*, 2005). Change in the  $\Delta\Psi_m$  leading to the development of the permeability transition which in turn results in the opening of the transmembrane megapore channels that are thought to be regulated by Bcl-2 family of pro- and anti-apoptotic protein (Kroemer *et al.*, 1997). Once open, a number of mitochondrial-associated proteins are released into the cytoplasm, these proteins include cytochrome c, Apaf-1 and apoptosis-inducing factor (Golstein, 1997) formed a complex that activate the caspase cascade. The cytochrome c and Apaf-1 oligomerize to form the apoptosome complex that recruits and binds caspase-9. The apoptosome is



then able to activate, by autocatalytic cleavage, and then cleaves and activates the executioner caspases 3, 6, and 7 (Bossy-Wetzel & Green, 1999).

## II. Glutamate (Glu)

Glutamate is an acidic amino acid, consists of a side chain  $\text{CH}_2\text{CH}_2\text{COO}^-$  attached to the  $\alpha$ -carbon (Figure G). It is one of the most abundant amino acids in several organs such as liver, kidney, skeletal muscle and brain (Brosnan *et al.*, 1983). In most of the cells, the intracellular concentration of Glu is maintained at quite high concentrations compared with its extracellular fluid concentration. Typically, intracellular concentrations of 2-5 mM are common, compared with extracellular concentration of  $\sim 0.05$  mM. The high concentrations of glutamate point to the important roles of glutamate in all tissues. Glutamate is not metabolized by extracellular enzymes, but is removed from the extracellular fluid by cellular uptake. In order to regulate its concentration, most of the organs in the body express highly efficient glutamate-transport system (Howell *et al.*, 2001).

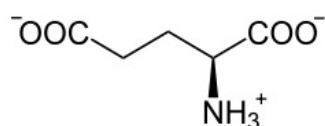


**Figure G.** Chemical structure of glutamate

### 1. Functional role of Glutamate

#### 1.2 Glutamate as the Neurotransmitter

Glutamate is the major excitatory neurotransmitter in the central nervous system (CNS). There are reports that its action is mediated through two major types of membrane proteins which are glutamate receptors (GluRs) for the signal input and glutamate transport system for the signal termination. Glutamate receptors (GluRs) are composed of two superfamilies including ionotropic glutamate receptors (iGluRs) and metabotropic receptors (mGluRs) according to their differential intracellular signal transduction mechanism and molecular homologies (Figure H) (Hollmann *et al.*, 1989).

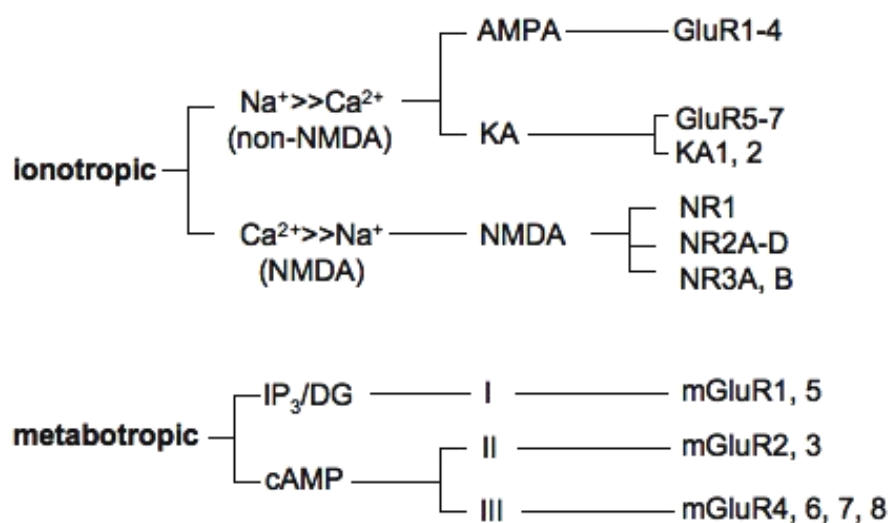


**Figure H.** Classification of glutamate receptors (Hinoi *et al.*, 2004)

iGluR are linked directly to cationic channels with ligand binding sites and they are known to mediate fast excitatory glutamate response. There are further classified into 3 major subtypes; DL- $\alpha$ -amino-3-hydroxy-5-methylisoxazole-4-propionate (AMPA), kainic acid (KA), and N-methyl-D-aspartate (NMDA) (Hollmann *et al.*, 1989). In contrast to iGluR, the mGluRs are G-protein-coupled membrane and regulate the synthesis of different intracellular second messengers (Schoepp, 1994). As with iGluR, the mGluRs are also classified into 3 functional groups. Group I (mGluR1 and mGluR5) subtype stimulates formation of inositol 1,4,5-triphosphate ( $IP_3$ ) and diacylglycerol (DG), while group II (mGluR2 and mGluR3), and group III (mGluR4, mGluR6, mGluR7, and mGluR8) induce reduction of intracellular cyclic AMP (cAMP) (Tanabe *et al.*, 1992). In addition, glutamate mediated signaling are regulated by glutamate transporter by either releasing or uptaking glutamate. There are two main category of glutamate transporter have been described,  $Na^+$ -independent, chloride-dependent high affinity Glu uptake system term cystine/glutamate exchanger ( $x_C^-$ ) (Sato *et al.*, 1999) and high-affinity  $Na^+$ -dependent glutamate transport system ( $x_{AG}$ ) (Bender *et al.*, 2000).

## 1.2 Glutamate as an intermediary molecule

It has been suggested that glutamate and its metabolites provide a metabolic fuel in the body, by which, dietary proteins are broken down by digestion into amino acids (Christensen, 1990). A key process in amino acid degradation is transamination of amino acid group to  $\alpha$ -keto acid, which finally produces glutamate. In addition to its role as a key transamination partner, glutamate is also required for the synthesis of several key molecules in the body such as glutathione, polyamines and amino acids as well as GABA;  $\gamma$ -aminobutyric acid neurotransmitter (Nedergaard *et al.*, 2002). Finally, Glu, by virtue of being readily convertible to  $\alpha$ -ketoglutarate by means of a variety of reversible transaminases, can serve as an anaplerotic function for the Krebs's cycle (Figure I).

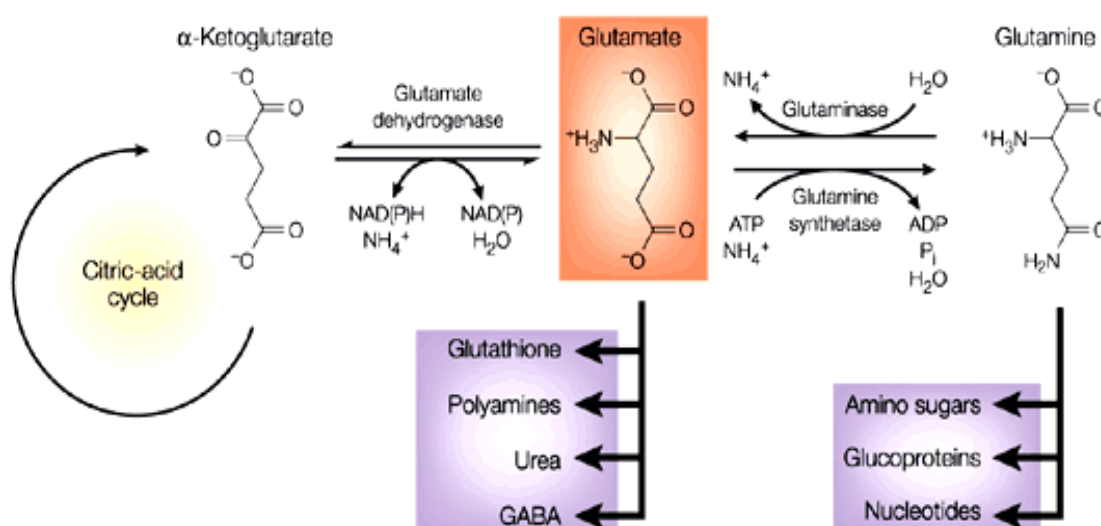


**Figure I.** Glutamate is the intermediary molecule contributed to produce several other important molecules in the metabolism process

Glu is also involved in the glutamate/aspartate shuttle, which affects the oxidation of cytoplasmically produced NADH in many cells (Ralphe *et al.*, 2005). Taken together, there are no other amino acids displayed such remarkable metabolic versatility as glutamate.

## **2. Functional roles of glutamate in the peripheral tissue**

Glutamate-mediated signaling has not only been described to act as the excitatory neurotransmitter in the CNS, there are emerging evidence for a role of glutamate as an extracellular signal mediator in the autocrine and/or paracrine system in several tissues in the body (Skerry & Genever, 2001), these data have derived from studies of the distribution of glutamate receptor and transporter both in several tumor cells and peripheral tissues (Takano *et al.*, 2001). The level of glutamate in blood and other fluids are also tightly controlled at around 30-80  $\mu\text{M}$  (Meldrum, 2000). The expression of glutamate receptor in peripheral tissues indicated that in addition to CNS, they are also a potential target effector sites for neurotransmission and excitotoxicity. Most organs, including kidneys, intestines, lungs, muscles and liver, express highly efficient glutamate-transport systems which demonstrated by the intravenous infusion of glutamate causes only a transient elevation of the plasma concentration of the amino acid (Gill & Pulido, 2001; Hanley & Varelas, 1999). However, there are a variety of the effects of Glu in different organ system. For example, NMDA receptors are expressed in osteoblasts and osteoclast, suggesting that Glu may be one of the endogenous paracrine factors used for intercellular communication in bone cell (Chenu *et al.*, 1998). It has been reported that islet of Langerhans cells express Glu receptor and the activation of receptor positively modulate the secretion of both glucagons and insulin (Brice *et al.*, 2002; Gonoï *et al.*, 1994). Testis tissue expressed both glutamate receptor (mGluR1 and mGluR5, but not for mGluR2 and mGluR3) and also glutamate transporter (Danbolt, 2001; Tong *et al.*, 2002). Moreover, many evidences have demonstrated the role of Glu as a signaling molecule in several other tissues (e.g. lung, liver, heart, kidney, stomach and intestine) as well.

## **3. Mechanism of glutamate-induced toxicity**

Glutamate appears to exert the toxicity when its extracellular concentration is high therefore, the regulation of the glutamate concentration is necessary to keep low by glutamate transport system (Trotti *et al.*, 1998). There are two mechanisms that have been reported as being implicated in the cytotoxic effect of glutamate including excitotoxicity and oxidative glutamate toxicity.

### 3.1 Excitotoxicity

The extracellular glutamate induces excitotoxicity via the activation of *N*-methyl-D-aspartate (NMDA) receptors (Figure J). The mechanism for the toxicity is thought to be due to membrane depolarization (excitation), which can also activate voltage-dependent calcium channels then accompanying the influx of calcium ion ( $\text{Ca}^{2+}$ ) (Choi, 1988). Excessive accumulation of intracellular  $\text{Ca}^{2+}$  is the key observed process leading to neuronal death or injury by excitotoxicity.  $\text{Ca}^{2+}$  influx leads to generation of nitric oxide (NO) and other free radicals, which may cause lipid peroxidation (Beal *et al.*, 1995). Mitochondria have been known to regulate the level of intracellular  $\text{Ca}^{2+}$ , therefore the disturbance of intracellular  $\text{Ca}^{2+}$  level may cause mitochondrial dysfunction, resulting in local free radical formation in mitochondria, an inability to handle free  $\text{Ca}^{2+}$  and decreased energy production (Dugan *et al.*, 1995). The elevation of intracellular  $\text{Ca}^{2+}$  is crucial to determination of injury and  $\text{Ca}^{2+}$  also initiates a cascade-like effect leading to cell death (Atlante *et al.*, 2001). This high concentration of  $\text{Ca}^{2+}$  triggers the activation of several enzymes and signaling cascades including phospholipase, protein kinase C, protease, protein phosphatase, nitric acid synthases and the generation of free radicals (Choi, 1992; Lipton & Rosenberg, 1994). For example,  $\text{Ca}^{2+}$  activates the enzyme phospholipase A2 (PLA2), which leads to the production of arachidonic acid, which in turn, is transformed by cyclooxygenase, causes the increasing formation of superoxide anion.  $\text{Ca}^{2+}$  also activates NO-synthase, increasing the presence of nitric oxide, which can react with superoxide anion to form the highly toxic compound peroxynitrite ( $\text{ONOO}^-$ ). These toxic oxidizing agents that cause the oxidation of lipids, proteins and DNAs leading to a form of cell death that has the characteristics of apoptosis.

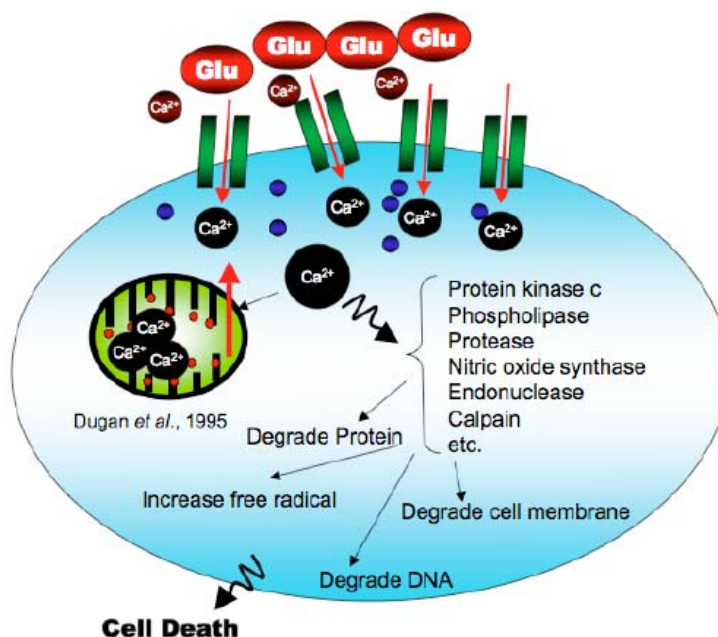


**Figure J.** Overstimulation of glutamate receptor leads to excitotoxicity (Choi, 1988)

### 3.2 Oxidative glutamate toxicity

In addition to induce the excitotoxicity, which is the rapid process, increased extracellular glutamate also leads to a more prolonged cell death by oxidative stress called “oxidative glutamate toxicity” (Tan *et al.*, 2001) (Figure K). Oxidative stress is thought to play a role in this pathway by Glu mediated by inhibiting the uptake of cystine into the cell via the cystine/glutamate transporter system ( $x_c^-$ ), leading to a depletion of cellular glutathione synthesis and level (Murphy *et al.*, 1990). Because GSH plays an important role in the defense against oxidative stress, therefore the depletion of GSH by extracellular glutamate lead to cell death (Tan *et al.*, 1998). This mode of glutamate-induced toxicity has previously described in both neuronal and non-neuronal cells (Cho & Bannai, 1990; Piani & Fontana, 1994). Concentration of extracellular glutamate as low as 100  $\mu$ M inhibits the import of cystine and ultimately causing the depletion of GSH (Sagara & Schubert, 1998).

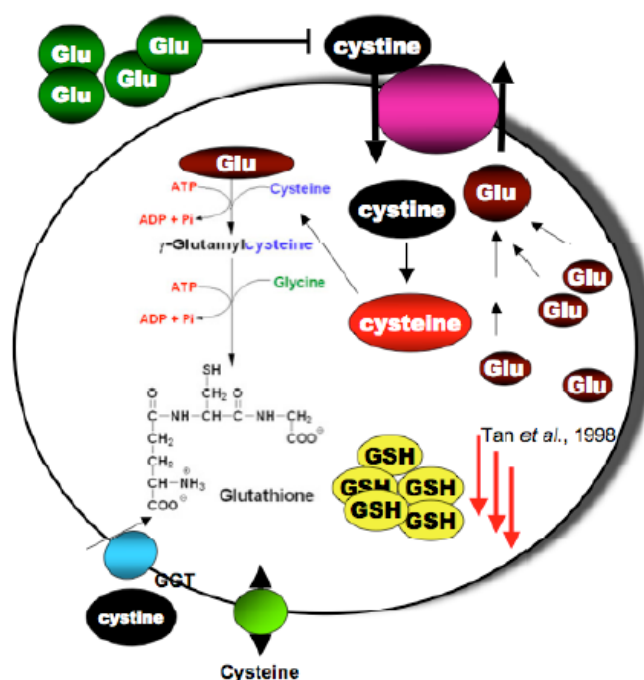


**Figure K.** Oxidative glutamate toxicity (Tan *et al.*, 2001)

### Transport of cystine

Cystine is required for the synthesis of glutathione (GSH), which is a major intracellular-reducing agent and antioxidant that functions in protecting cells from free radicals, reactive oxygen species, and many toxic substances. Because glutamate and glycine occur at relatively high intracellular concentrations, therefore, the synthesis of GSH is largely dependent on the intracellular level of cysteine. Even though, cysteine is directly transported with high capacity into the cell by the  $\text{Na}^+$ -dependent amino acid transport system called the ASC system (Knickelbein *et al.*, 1997). However, the extracellular cysteine concentration is quite low because it is easily oxidized extracellularly to form cystine, cystine levels are generally higher than cysteine levels in extracellular fluid. Therefore, the adequate transport of cystine into the cells is essential for the maintenance of intracellular cysteine levels and is thought to be a rate-limiting process in GSH synthesis (Bannai & Tateishi, 1986).

There are at least two transporter systems that have been shown to transport cystine, including  $\text{x}_c^-$  transport system (Bannai, 1986) and  $\text{X}_{AG}^-$  family of  $\text{Na}^+$ -

dependent high affinity glutamate transporters (Kanai & Endou, 2003; Kanai & Hediger, 1992). They are acidic amino acid transporters and characterized by their unique substrate specificity, dependence on (or lack of dependence) an inwardly directed  $\text{Na}^+$  gradient as a driving force, and selective inhibition by amino acids or amino acid analogs (Table 1).

**Table 1.**Transporter systems for cystine and/or glutamate

Transport system		Substrate	Inhibitor	Family
$\text{Na}^+$ -dependent	$\text{Na}^+$ -independent			
$\text{X}_{\text{AG}}^-$			$\text{A}\beta\text{H}$	
		L-cyst., L-Glu, L-/D-Asp	THA	SLC1
			<i>trans</i> -PDC	
	$\text{x}_{\text{C}}^-$		HCA	
		L-cyst., L-Glu	AAA	SLC7
			Quisqualate	

$\text{A}\beta\text{H}$ , L-aspartic acid- $\beta$ -hydroxamate; THA, threo- $\beta$ -hydroxy-aspartate; L-trans-pyrrolidine-2,4-dicarboxylic acid, *trans*-PDC; HCA, L-homocysteic acid;  $\alpha$ -aminoadipic acid (AAA); SLC, solute carrier family is a naming of transporter families by Human Gene Nomenclature Committee.

#### $\text{x}_{\text{C}}^-$ transport system

$\text{x}_{\text{C}}^-$  is the  $\text{Na}^+$ -independent transporter system, consists of two subunits, the specific subunit xCT and the 4F2 heavy chain (Sato *et al.*, 1999). xCT is a member of the CD98 light chain family, consisting of 12 putative transmembrane domains and associated with a single 4F2 heavy chain through an extracellular disulfide bond (Verrey *et al.*, 1999) (Figure L). The transport activity is thought to be mediated by the light chain subunit, xCT, while the heavy chain is found in a variety of amino acid transporter systems (Sato *et al.*, 1999). The  $\text{x}_{\text{C}}^-$  system transports cystine (L-cystine) inward and glutamate (L-Glu) outward with the glutamate gradient provides the



driving force for cystine uptake. It is inhibited by quisqualate or elevated extracellular levels of glutamate which are its related substrate (Bannai, 1984). In addition, the  $x_c^-$  system-mediated transport may be inhibited by L-homocystein acid (HCA) and  $\alpha$ -aminoadipic acid (AAA) (Pacheco *et al.*, 2006).

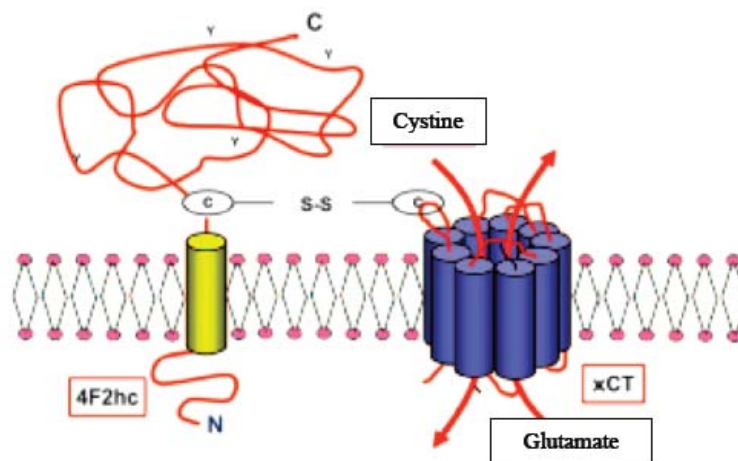


**Figure L.** Structure of cystine/glutamate exchanger  $x_c^-$  (Takarada & Yoneda, 2008)

Studies on the transport activity of system  $x_c^-$  transporter xCT in *Xenopus* oocytes with 4F2hc revealed that it prefers L-cystine and L-glutamate as the substrate whereas L-aspartate is not a good substrate (Kim *et al.*, 2001). Therefore, it is proposed that the substrate binding site of xCT possesses a negative charge recognition site which is possibly composed of positively charged amino acid residues to interact with the negative charge of the acidic amino acid side chains so that xCT recognizes amino acids as anions (Matsuo *et al.*, 2002). Because those amino acid residues proposed to be situated at the certain distance from the  $\alpha$ -carbon and the negative charge on the side chain, therefore it would be an important determinant to be accepted by the substrate-binding site of xCT. Thus, it is understandable that glutamate and homocysteate are well accepted by xCT whereas aspartate with a shorter side chain is not. Due to the widespread expression and regulation by oxidative stress, the  $\text{Na}^+$ -independent,  $x_c^-$  transport system is believed to be the primary transport system related to uptake of cystine into the mammalian cell (Bertran *et al.*, 1992; Christensen, 1990).

### **$X_{AG}^-$ transporter**

$X_{AG}^-$  is the  $Na^+$ -dependent high affinity glutamate transporter, comprising of five transporter members (EAAT1-5), that is potently inhibited by the competitive inhibitors DL-theo- $\beta$ -hydroxy-aspartate (THA), L-aspartate- $\beta$ -hydroxamate ( $A\beta H$ ) or L-trans-pyrrolidine-2,4-dicarboxylic acid (*trans*-PDC). It transports L-glutamate and D-or L-aspartate by coupling the electrochemical gradient of three co-transported sodium ions ( $Na^+$ ) and one counter-transported potassium ion ( $K^+$ ) with that of the amino acids (McBean, 2002; Zerangue *et al.*, 1995).  $X_{AG}^-$  is the  $Na^+$ -dependent transport system, meaning that it relies on a  $Na^+$  gradient maintained by  $Na^+$ - $K^+$  ATPase. During oxidative stress, the levels of intracellular ATP decreased, these would negatively influence  $Na^+$ -dependent transport systems. Conversely, the expression of  $x_C^-$  transport is upregulated by oxidative stress in several cell types (Bannai *et al.*, 1989; Li *et al.*, 1999; Sato *et al.*, 1995).

When cystine uptake is blocked lead to the depletion of GSH pools, the consequent reduction in intracellular GSH levels may then render the cell susceptible to reactive oxygen species (ROS)-induced damage, ultimately leading to oxidative cell death. However, Tan has reported that GSH depletion is not sufficient to cause the maximal mitochondrial ROS production. Indeed, there is an early requirement for protease activation, changes in gene expression, and a late requirement for  $Ca^{2+}$  mobilization (Tan *et al.*, 1998). In addition, the glutamate toxicity mediated through this process requires a higher concentration (10-100 fold) and a longer exposure (12-24 h) of glutamate in comparison with that of the NMDA receptor-mediated mechanism (Murphy *et al.*, 1989).

### **4. Effect of oxidative stress on $x_C^-$ transport system**

Initially, it was described that  $x_C^-$  transport system, mediating cystine uptake is inhibited by glutamate, resulting in lowered glutathione levels, which may lead to oxidative stress (Murphy *et al.*, 1989). Recently, it has been described that various stress stimuli including electrophilic agent such as diethyl maleate (DEM) and  $H_2O_2$  (Sasaki *et al.*, 2002), oxygen (Sato *et al.*, 2001), lipopolysaccharide (LPS) (Sato *et al.*,

1995), as well as the nitric oxide donor 3-nitroso-N-acetylpenicillamine (Bridges *et al.*, 2001) promote the up-regulation of xCT expression, thus increasing the  $x_C^-$  transport activity. In addition, it has been reported that xCT is upregulated on the GSH depletion by treatment with diethyl maleate (Ishii *et al.*, 1991). Moreover, it has been revealed that up-regulate expression of the  $x_C^-$  transporter by inducing xCT subunit expression, resulting in a corresponding increase in GSH synthesis. For example, treatment with diethyl maleate (DEM) increased GSH levels with a corresponding increase in xCT mRNA expression in blood brain barrier cell line (Hosoya *et al.*, 2002). Since, the widespread expression and regulation by oxidative stress, the system  $x_C^-$  is believed to be the primary transport system related to the uptake of cystine into the cells. The  $x_C^-$  activity correlated with the cellular GSH levels in a variety of cell types, for example treatment with DEM increased GSH levels with a corresponding increase in xCT mRNA expression in blood brain barrier cell line (Hosoya *et al.*, 2002).

## CHAPTER III

### MATERIALS AND METHODS

#### 3.1 Chemicals

Minimum essential with Earle's salts (MEM), fetal bovine serum (FBS), streptomycin, penicillin, Dulbecco's Modified Eagle's Medium (DMEM), Dulbecco's Phosphate Buffered Saline (DPBS), *N*-acetylcysteine (NAC), 3-(4,5-dimethylthiazol-2-yl)-2,5-diphenyltetrazolium bromide (MTT), Dimethyl sulfoxide (DMSO), mannitol and all L-amino acid were purchased from Sigma Aldrich Chem. Co. (St. Louis, MO, USA). Methylmercury chloride (MeHgCl) was purchased from WAKO Pure Chemical Ind. Ltd. (Osaka, Japan). BCA Protein assay reagent kit was purchased from PIERCE. RNeasy<sup>®</sup> mini kit was purchased from QIAGEN. Superscript<sup>™</sup> III First-Strand Synthesis System for RT-PCR was purchased from Invitrogen (Invitrogen, Carlsbad, CA). Annexin V-FITC apoptosis detection kit was purchased from BD Biosciences (San Jose, CA, USA).

Cyanine dye (1,1',3,3',3' hexamethylindodicarbocyanine iodide) [DiI(1)] and fluorescent probe [2',7'-dichlorofluorescein diacetate (DCFH-DA) was purchased from Molecular Probes, Inc (Leiden, Netherlands). Caspase-3 colorimetric activity assay kit was purchased from Chemicon International, Inc (Temecula, California, USA). Glutathione assay kit was from Bioassay System (Hayward, CA, USA). Bicinchoninic acid (BCA) Protein assay was from Pierce Biotechnology (Rockford, USA). CodeLink Human Whole Genome Bioarray was purchased from Applied Microarrays (Arizona, USA). CodeLink expression assay reagent kit (GE Health Care, NJ, USA). [<sup>14</sup>C]L-cystine was purchased from Perkin Elmer Life Sciences Inc. (Boston, MA, USA). All chemicals were commercially obtained and were of analytical grade.

## 3.2 Experimental Procedures

### 3.2.1 Cell culture

HeLa S3 (human cervix adenocarcinoma) cells were maintained in Minimal Essential growth medium (MEM, Appendix A) supplemented with 10% heat-inactivated fetal bovine serum, 100 µg/ml streptomycin and 100 U/ml penicillin at 37°C in a humidified 5% CO<sub>2</sub> incubator and cells were sub-cultured every 3-4 days. Neuro2A (mouse neuroblastoma), NIE115 (mouse neuroblastoma), and NG108-15 (mouse neuroblastoma x rat glioma hybrid) cells were maintained in Dulbecco's Modified Eagle's Medium (DMEM) with the similar supplements and conditions. Cells were seeded onto 24-well plates or 15 cm plate at density of  $1 \times 10^4$  cells/ml, however, in transport study HeLa S3 cells were seeded on 24-well plates at density  $1 \times 10^5$  cells/well. All experiments were performed at 48 h after seeding.

### 3.2.2 RNA preparation

Total cellular RNA were isolated and purified from the treated cells using RNeasy Mini Kit according to the manufacturer's instruction (Qiagen Sciences, Maryland, USA). Aliquots of the total RNA sample were prepared for quality control, RT-PCR and microarray experiment. Quality of the RNA for RT-PCR was assessed by OD<sub>260/280</sub> in an UV/visible spectrophotometer (Ultrospec 2100, Amersham Pharmacia Biotech, NJ, USA). For microarray experiment, RNA samples were quality-checked by RNA 6000 Nanochip using the 2100 BioAnalyzer (Agilent Technologies Inc., Palo Alto, CA, USA). Only very high quality RNA (RNA Integrity Number; RIN  $\geq 7$ ) preparation was considered for microarray screening.

### 3.2.3 Cytotoxicity study

Cytotoxicity was determined by MTT quantitative colorimetric assay, which is capable of detecting cell viability. The principle of this assay is based on the change in the yellow MTT 3-(4,5-Dimethylthiazol-2-yl)-2,5-diphenyltetrazolium bromide to purple formazan using mitochondrial dehydrogenase in the mitochondria of living cells. The amount of water-insoluble formazan crystal is directly proportional to number of living cells in the system. Stock MTT solution 5 mg/ml were prepared in

distilled water and filter through a 0.22  $\mu$ M filter (Millipore, MA, USA) to sterile and remove small and insoluble residues. This solution was protected from light and kept at room temperature. At the end of incubation time, cell samples were incubated with 10% (v/v) stock MTT solution (5 mg/ml) for 4 h at 37°C. After incubation, a blue formazan crystal was solubilized with 0.04 M HCl in absolute isopropanol, and plate was shook on a plate shaker (Taiyo Micro Mixer, Taitee Co., Saitama, Japan) at maximum speed for at least 30 min. Aliquots were quantitated spectrophotometrically at 570 nm using UV/visible spectrophotometer, using the solubilisation buffer. Relative number of viable cells in each treatment condition to untreated control (=100%) will be calculated as follows: % cell viability =  $[(OD - OD_0)/(OD_c - OD_0)] \times 100$ , where  $OD_c$  is the mean of the control cell and  $OD_0$  is the mean of the control cell without added MTT.

### **3.2.4 Flow Cytometric (FCM) Analysis**

Fluorescence Activated Cell Sorter (FACS Calibur) (Becton-Dickinson, Immunofluorometry systems, CA, USA) was used for all flow cytometric analysis. Cells were passed at a rate of about 200 per second, using PBS (Appendix A) as the sheath fluid. A 488 (blue) or 635 (red) nm laser beam was used for excitation and the emission signal was selected according to the fluorescence dye used in each parameter (Fibach, 1998). A two-parameter dot-plot of the side light scatter (SSC) and forward light scatter (FSC) of the population was first analyzed. A gate was set to include the group cell, which had the highest population and to exclude the cell debris. Flow cytometry data was done with CellQuest<sup>®</sup> software.  $1 \times 10^4$  events per sample were acquired to ensure adequate mean fluorescence levels.

### **3.2.5 Staining cell for the externalization of phosphatidylserine (PS) analysis using FCM**

Exposed phosphatidylserine (PS) during apoptosis was evaluated by fluorescein isothiocyanate (FITC)-conjugated Annexin V and propidium iodide (PI) staining using Annexin V-FITC Apoptosis Detection Kit (Vermes *et al.*, 1995). At the indicated time of exposure, the culture medium containing test condition was removed from the treated cells. The remaining monolayer cells were detached using trypsin-

EDTA for 3 minutes at 37°C in a humidified 5% CO<sub>2</sub> incubator, resuspended in MEM, and centrifuged at 1,500 rpm for 5 min to obtain cell pellet (Kubota 5910, Kubota Co., Osaka, Japan). Cell pellets were washed twice with cold phosphate-buffer saline (PBS) and centrifuged. Cell pellets were stained with FITC-labeled Annexin V and PI according to manufacture's instruction. A minimum of 10,000 cells were collected and analyzed immediately with FACS Calibur. Fluorescence Annexin V/FITC and PI were detected at 488/530 nm and 488/600 nm of excitation and emission, respectively. The different staining pattern reflects the different mode/stages of cell death: healthy cell (FITC<sup>-</sup>/PI<sup>-</sup>), early apoptotic cells (FITC<sup>+</sup>/PI<sup>-</sup>), late apoptotic (FITC<sup>+</sup>/PI<sup>+</sup>), and necrotic cells (FITC<sup>-</sup>/PI<sup>+</sup>) were obtained by CellQuest<sup>®</sup> software.

### 3.2.6 Determination of Membrane potential ( $\Delta\Psi_m$ ) using FCM analysis

Cells were stained with MitoProbe<sup>™</sup> DiIC1 (5), a mitochondrial specific dye according to the manufacturer's instruction (Molecular Probe, Leiden, Netherland). The fluorescence intensity from the dye is reduced when mitochondrial membrane potential is disrupted (Lu *et al.*, 2004). As a positive control, cells were treated with 50  $\mu$ M of the protonophore uncoupling agent, carbonyl cyanide 3-chlorophenylhydrazone (CCCP). Cells were harvested at  $2.5 \times 10^5$  cells from the experimental sample, bring total volume up to 1 ml of warm medium. Cell suspensions were then incubated with 50 nM DiIC1 (5) in a dark condition for 30 min at 37°C. Cells were resuspended in PBS, and then the changes in fluorescence intensity were analyzed immediately using FACS Calibur at 488 nm and the emission was detected at 633 nm emission wavelengths.  $1 \times 10^4$  cells were analyzed using CellQuest<sup>®</sup> software.

### 3.2.7 Detection of caspase-3 activity

Caspase-3 activity was determined using the caspase-3 Colorimetric Activity Assay Kit (Chemicon, Temecula, USA). The assay is based on spectrophotometric detection of the chromophore *para*-nitroaniline (pNA) after cleavage from the labeled substrate DEVD-pNA. The assay procedures were done according to the kit instructions. Enzyme-catalyzed release of pNA was monitored using a spectrophotometer at 405 nm and compared to a standard curve obtained by serial

dilutions of the pNA standard provided in the kit. Protein concentration was determined using bicinchoninic acid (BCA) Protein assay (Pierce Biotechnology, Rockford, USA) (Smith *et al.*, 1985) (Appendix B).

### **3.2.8 Measurement of intracellular ROS level using FCM analysis**

The level of intracellular ROS was monitored by using the peroxide-sensitive fluorescence probe, 2',7'-dichlorofluorescein diacetate (DCFH-DA) (Molecular Probes, Leiden, Netherland). DCFH-DA solution was obtained by diluting stock solution (5 mM) in DMSO to make 20  $\mu$ M working solution and was then stored at -20°C in the dark. The principle of this study is that the fluorescent dye DCFH-DA passes through the cell membrane and undergoes deacetylation by intracellular esterases to produce the non-fluorescent compound DCFH that is trapped inside the cells. Oxidation of DCFH by ROS produces the highly fluorescent DCF. By quantifying fluorescence, the attached cells were preloaded with 20  $\mu$ M DCFH-DA for 15 min at 37°C in the dark before treatment. After pre-incubation with DCFH-DA dye, monolayer cells were washed twice with warm D-PBS, then cells were exposed to the test condition as previous mentioned. Hydrogen peroxide (250  $\mu$ M) was used as a positive control for this measurement. At the end of incubation, cells were washed with warm PBS and trypsinized with 0.25% trypsin EDTA, and then cells ( $1 \times 10^5$ ) were prepared and resuspended in cold PBS. Intracellular ROS levels were measured using FACS Calibur. The labeled cells were excited at 488 nm and the emission was detected at 520 nm.  $1 \times 10^4$  cells were analyzed using CellQuest<sup>®</sup> software.

### **3.2.9 Intracellular glutathione (GSH) assay**

GSH was quantified by using QuantiChrom<sup>™</sup> Glutathione Assay Kit (Bioassay, Hayward, CA, USA). Buthionine-L-sulfoxamine (BSO), a specific inhibitor of  $\gamma$ -glutamylcysteine synthetase was used as a positive control of the reaction. The assay was performed according to the manufacturer's instruction. Protein concentration was determined using bicinchoninic acid (BCA) assay (Appendix B).



### 3.2.10 Gene expression and Gene ontology (GO) analysis

Twelve biotin-cRNA samples were prepared by the CodeLink method using the CodeLink expression assay reagent kit (GE Health Care, NJ, USA). All reagents used were from this kit unless otherwise specified. One  $\mu\text{g}$  of total RNA in 8  $\mu\text{l}$  of nuclease-free water was spiked with 1  $\mu\text{l}$  of working solution of bacterial control mRNAs and 2  $\mu\text{l}$  of diluted poly (A) RNA control, then incubated with 1  $\mu\text{l}$  of T7-oligo (dT) primer at 70°C for 10 min and cooled on ice. First-strand cDNA was synthesized by adding 2  $\mu\text{l}$  of 10x first-strand buffer, 4  $\mu\text{l}$  of 5 mmol/L dNTP mix, 1  $\mu\text{l}$  of RNase inhibitor, 1  $\mu\text{l}$  of reverse transcriptase and then incubating at 42°C for 2 h. Second-strand cDNA was synthesized in a 100  $\mu\text{l}$  reaction volume by adding 63  $\mu\text{l}$  of nuclease-free water, 10  $\mu\text{l}$  of 10x second-strand buffer, 4  $\mu\text{l}$  of 5 mmol/L dNTP mix, 2  $\mu\text{l}$  of DNA polymerase mix, 1  $\mu\text{l}$  of RNase H, and then incubating at 16°C for 2 h. Double-stranded DNA was purified using the QIAquick PCR purification kit (Qiagen). Double-stranded complementary DNA (cDNA) was synthesized from 5  $\mu\text{g}$  total RNA using the Superscript Choice System (Invitrogen, Carlsbad, CA, USA). Then the complementary DNA (cDNA) was synthesized and used as template for transcription in vitro of biotinylated complementary (cRNA). Fragmented biotin-labeled cRNA was hybridized with Codelink Human Whole Genome Bioarray with 55,000 human gene targets and expressed sequence tags (ESTs), including some 45,00 well-characterized human gene and transcript targets. After hybridization, signal was developed using streptavidin-Cy5 and reading was carried out on the Applied Biosystems 1700 Chemiluminescent Microarray Analyzer. IVT reaction was performed by mixing purified double-stranded DNA with 4  $\mu\text{l}$  of 10x T7 reaction buffer, 4  $\mu\text{l}$  of T7 ATP solution, 4  $\mu\text{l}$  of T7 GTP solution, 4  $\mu\text{l}$  of T7 CTP solution, 3  $\mu\text{l}$  of T7 UTP solution, 7.5  $\mu\text{l}$  of 10 mmol/L biotin-11-UTP (Perkin-Elmer Corp., MA, USA), and 4  $\mu\text{l}$  of 10x T7 enzyme mix and then incubating for 14 h at 37°C; final reaction volume was 40  $\mu\text{l}$ . Biotin-labeled cRNA products were purified with the RNeasy mini kit (Qiagen, Maryland, USA). Fifteen  $\mu\text{g}$  of cRNA from each sample were fragmented following the recommended procedures in the CodeLink target preparation manual.

Raw Codelink data output was imported into GeneSpring GX 7.1 (Agilent Technologies, California, USA) according to the manual. Briefly, the data was normalized by setting all measurement  $<0.01$  to 0.01, normalizing each array to the

50<sup>th</sup> percentile of all measurements taken for that array, and normalizing each gene to the median measurement for that gene across all arrays. Analysis of data was carried out using the following criteria (1) probes set with “absent” flag in arrays of all experimental groups (Control, MeHg alone, MeHg plus L-Glu and L-Glu alone) were excluded; (2) probes set with no change call between MeHg and MeHg plus L-Glu arrays were excluded; (3) probes set showed “present” flag in all 4 different experiments (4) a threshold of two-fold change in the levels of mRNAs in MeHg plus L-Glu to MeHg array was included.

### **3.2.11 Semiquantitative analysis of xCT transporter mRNA expression**

The first-strand complementary DNA (cDNA) was synthesized using SuperScript III Reverse Transcriptase (Invitrogen, CA, USA). Reverse-transcriptase polymerase chain reaction (RT-PCR) was used to analyze the expression of mRNA for xCT and  $\beta$ -actin (internal control). Primer sequences were given below. PCR was performed using GeneAmp (PCR system 9700; Applied Biosystem, CA, USA) for 25 and 15 cycles with specific primers for human xCT (Kim *et al.*, 2001) and human  $\beta$ -actin (Fuchs *et al.*, 1983). The sense and antisense primers for human xCT were 5'-GTC AGA AAG CCT GTT GTG TCC ACC A-3' and 5'-TAA GAA AAT CTG GAT CCG GGC G-3' corresponding to nucleotides 139-163 and 696-717 of human xCT (GenBank accession no. AB040875). The sense and antisense primers for human  $\beta$ -actin were 5'-CAA GAG ATG GCC ACG GCT GCT-3' and 5'-TCC TTC TGC ATC CTG TCG GCA-3' corresponding to nucleotides 2181-2202 and 2434-2455 of human  $\beta$ -actin (GenBank accession no. NM001101). PCR products were separated by electrophoresis on 2% agarose gels and visualized under UV light using 0.1% (v/v) ethidium bromide. The amount of PCR products were quantified by densitometric analysis and normalized in relation to the amount of  $\beta$ -actin mRNA. Visualization and densitometric analysis of band intensity of each sample was performed using LAS-4000 digital imaging system (mini version 2.0) with Multi Gauge (version 3.1) software (Fuji Photo Film Co., Tokyo, Japan).

### 3.2.12 Cytine uptake and Inhibition studies

HeLa S3 cells were seeded on 24-well plates ( $10^5$  cells/well) and cultured at 37°C with 5% CO<sub>2</sub> and humidity for 48 h until the confluent was about 80%. Cells were treated with MEM containing 10 mM L-Glu alone, 8 µM MeHg alone or MeHg plus L-Glu for 10 h. At the end of incubation, cells were washed three times with Na<sup>+</sup>-free Hank's balance salt solution (HBSS) containing 125 mM choline-Cl, 25 mM HEPES, 4.8 mM KCl, 1.2 mM MgSO<sub>4</sub>, 1.2 mM KH<sub>2</sub>PO<sub>4</sub>, 1.3 mM CaCl<sub>2</sub> and 5.6 mM glucose (pH 7.4) (Appendix A) and pre-incubated in the same solution at 37°C for 10 min. Cystine uptake by HeLa S3 cells were initiated by incubation in Na<sup>+</sup>-free HBSS containing 5 µM [<sup>14</sup>C]L-Cystine (25 mCi/mmol; PerkinElmer Life & Analytical Science, MA, USA) at 37 °C for 5 min. Uptake was terminated by washing three times with ice-cold Na<sup>+</sup>-free HBSS. After that, cells were lysed with 0.5 ml of 0.1 N NaOH for 1 h. To determine intracellular [<sup>14</sup>C]L-Cystine uptake, 0.5 ml of cell lysate was mixed with 3.5 ml of Emulsifier-Safe scintillation solution (PerkinElmer Life Science, Boston, USA), and the radio activity was measured using Aloka LSC-5100 β-scintillation counter (Aloka, Tokyo, Japan). A 20 µl aliquot of cell lysate was used to determine protein concentration by BCA protein assay (Pierce Biotechnology, Rockford, USA). The values were expressed as a percentage of the control cystine uptake in untreated control.

To examine the inhibitory effect of the L-cystine, L-Glu, L-α-amino adipate (L-AAD) and L-Asp on cystine transport, the uptake of [<sup>14</sup>C]L-cystine (5 µM) by HeLa S3 cells were measured in the presence of 1 mM unlabeled L-cystine, L-Glu, L-α-amino adipate or L-Asp. Briefly, the treated HeLa S3 cells were washed and pre-incubated in Na<sup>+</sup>-free HBSS containing 5 µM [<sup>14</sup>C]L-Cystine in the presence or absence of 1 mM unlabeled amino acid inhibitor (L-Cyst., L-Glu, L-AAD and L-Asp) at 37°C for 5 min. The cystine uptake in the presence of the inhibitors was expressed as percentage of control cystine uptake measured in the absence of inhibitors for each corresponding treatment condition.

### 3.3 Statistical analysis

Data were expressed as mean  $\pm$  S.E.M of three independent experiments. Statistical significance was assessed by one-way analysis of variance (one-way ANOVA) with Tukey's post hoc analysis for multiple comparisons.  $P < 0.05$  was considered statistically significant.

### 3.4 Experimental Protocols

In the present study, human cervical carcinoma cell line (HeLa S3) was used as a model to study the enhancing effect of L-Glu on MeHg-induced toxicity in Part I and Part II. In addition, three neuroblastoma cell lines including mouse neuroblastoma (Neuro2A and NIE115) and mouse neuroblastoma x rat glioma hybrid (NG108-15) were used to examine whether the enhanced MeHg toxicity by L-Glu was also applicable to neural cell line in Part III.

#### **Part I: Effect of L-glutamate (L-Glu) on methylmercury (MeHg)-induced cytotoxicity**

##### **Experiment 1.1 Concentration and time-course effect of MeHg-induced cytotoxicity**

This experiment was aimed to determine the optimal concentration and time-course of MeHg-induced toxicity. At each period of exposure, there were divided into 5 groups of cells as follows:

- |          |                                |
|----------|--------------------------------|
| Group 1) | Control                        |
| Group 2) | Treatment with MeHg 2 $\mu$ M  |
| Group 3) | Treatment with MeHg 4 $\mu$ M  |
| Group 4) | Treatment with MeHg 8 $\mu$ M  |
| Group 5) | Treatment with MeHg 16 $\mu$ M |

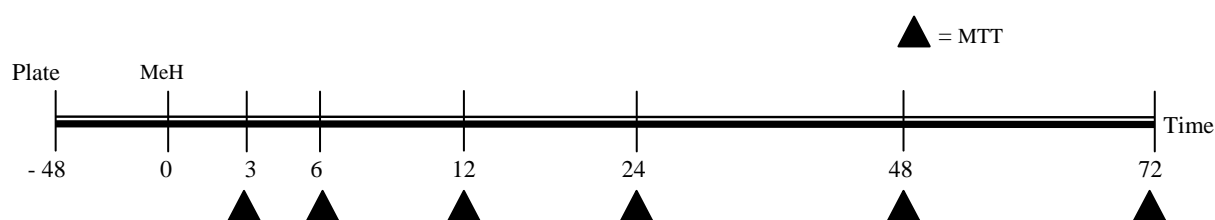


**Figure M1.** Schematic diagram showing time course of treatment and sample collection

The effect of MeHg toxicity was evaluated in HeLa S3 cells. Cells were seeded onto 24-well plates at density of  $1 \times 10^4$  cells/ml and cultured for 48 h in MEM supplemented with 10% FBS before starting the experiment. After seeding, the cultured media were removed and cells were exposed to 250  $\mu$ l of regular media or media containing various concentration of MeHg (2, 4, 8, and 16  $\mu$ M) for 3, 6, 12, 24, 48 and 72 h. At the end of incubation period, cell viability was assessed using MTT assay. Briefly, 25  $\mu$ l of stock MTT solution (5 mg/ml) were added into each well, and continuously incubated at 37°C for 4 h. The assay was conducted as described in the experimental procedure (3.2.3).

After the optimal range of MeHg concentration and time of exposure were established, the experiment was conducted to further screen the optimal condition of MeHg. In this study, cells were treated with MeHg alone (2 to 8  $\mu$ M), MeHg plus 10 mM L-Glu or 10 mM L-Glu alone for 3 to 12 h. At the end of incubation, cell viability was determined by MTT assay. The optimal concentration and time of MeHg was chosen for studying the effect of L-Glu on MeHg toxicity in the subsequent experiment.

### Experiment 1.2 Effect of L-Glu on MeHg-induced toxicity

The objective was to determine the optimal concentration of L-Glu on the MeHg-induced toxicity. Similar to the experiment 1.1, cells were treated with the optimal concentration of MeHg alone (8  $\mu$ M), MeHg plus various concentrations of L-Glu and L-Glu alone for 12 h. Since, some concentrations of L-Glu for cells treatment were relatively high, cells were treated with mannitol in the separate experiment in order to exclude the possibility of osmolality-induced cell damage. Cell viability was

determined at the end of incubation period as described in experimental procedure (3.2.3.). In this experiment, cells were divided into 13 groups as follows:

- Group 1) Control (MEM containing 10% FBS)
- Group 2) MeHg 8  $\mu$ M alone
- Group 3)-6) MeHg+L-Glu at 1, 5, 10 and 20 mM, respectively
- Group 8)-10) L-Glu at 1, 5, 10 and 20 mM, respectively

The optimal concentration of L-Glu was chosen for evaluating the enhanced effect of L-Glu on MeHg-induced toxicity in the subsequent experiment.

### Experiment 1.3 Specific effect of L-Glu on MeHg-induced toxicity

#### Experiment 1.3.1 Comparative effect of various L-amino acids on MeHg-induced toxicity

In order to investigate whether the enhancement of MeHg toxicity was specific to L-Glu, twenty naturally occurring L-amino acids in Table M1 were examined on MeHg-induced cytotoxicity. Cells were seeded into 24-well plated and cultured for 48 h before treatment. After seeding, cells were treated with 8  $\mu$ M of MeHg, MeHg plus 10 mM of each amino acid or amino acid alone. At 12 h of incubation, cell viability was measured by MTT assay.

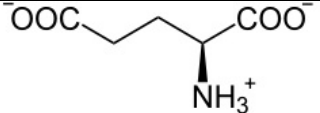
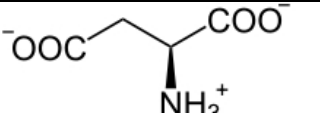
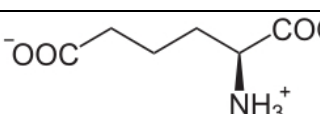
**Table M1.** List of 20 amino acids used in this experiment

L-amino acids	Abbreviation	L-amino acid	Abbreviation
1. Alanine	Ala	11. Glycine	Gly
2. Valine	Vla	12. Serine	Ser
3. Leucine	Leu	13. Threonine	Thr
4. Isoleucine	Ile	14. Cysteine	Cys
5. Phenylalanine	Phe	15. Tyrosine	Tyr
6. Tryptophan	Trp	16. Asparagine	Asn
7. Methionine	Met	17. Glutamine	Gln
8. Proline	Pro	18. Lysine	Lys
9. Aspartate	Asp	19. Arginine	Arg
10. Glutamate	Glu	20. Histidine	His

### Experiment 1.3.2 Effect of Glu-related amino acid on the enhancement of MeHg toxicity

This experiment was aimed to further investigate the specificity of L-Glu on the enhancement effect of MeHg-induced toxicity. Amino acids which are structurally similar to that of glutamate (Glu) and/or their side chain are shorter than Glu (Table M2) were used to examine the potential enhancement of MeHg toxicity. The experiment was conducted similar to that in experiment 1.3.1 excepted that cells were treated with 8  $\mu$ M MeHg plus 10 mM D-Glu, L-Asp, D-Asp or L- $\alpha$ -aminoadipate (L-AAD) or 10 mM each Glu-related amino acid for 12 h. At the end of incubation period, cell viability was determined using MTT assay.

**Table M2.** Chemical structure of Glu-related acidic amino acids

Chemical Structure	Acidic amino acid
	L-glutamate (L-Glu)
	L-aspartate (L-Asp)
	L- $\alpha$ -aminoadipate (L-AAD)

## Part II: Study the molecular mechanism underlying the enhancing toxic effect of MeHg by L-Glu

This study was aimed to examine the possible mechanism underlying L-Glu enhanced MeHg toxicity.

### Experiment 2.1 Gene expression profile and Gene Ontology (GO) analysis

Based on the reason that co-treatment of MeHg and L-Glu might induce the set of early response genes, which would initiate apoptotic cell death. Other genes might be activated later in response to the cellular changes, which brought about by the cell death program. In the present experiment, microarray-based gene expression profiling was used to elucidate the patterns of gene expression throughout the time course of L-Glu enhanced MeHg toxicity at 3, 6, and 12 h of exposure. The gene expression profiles in the MeHg treated cell were compared to those in co-treatment with MeHg and L-Glu. Additionally, the biological functions of differentially expressed genes between the two treatments were explored (Figure M2).

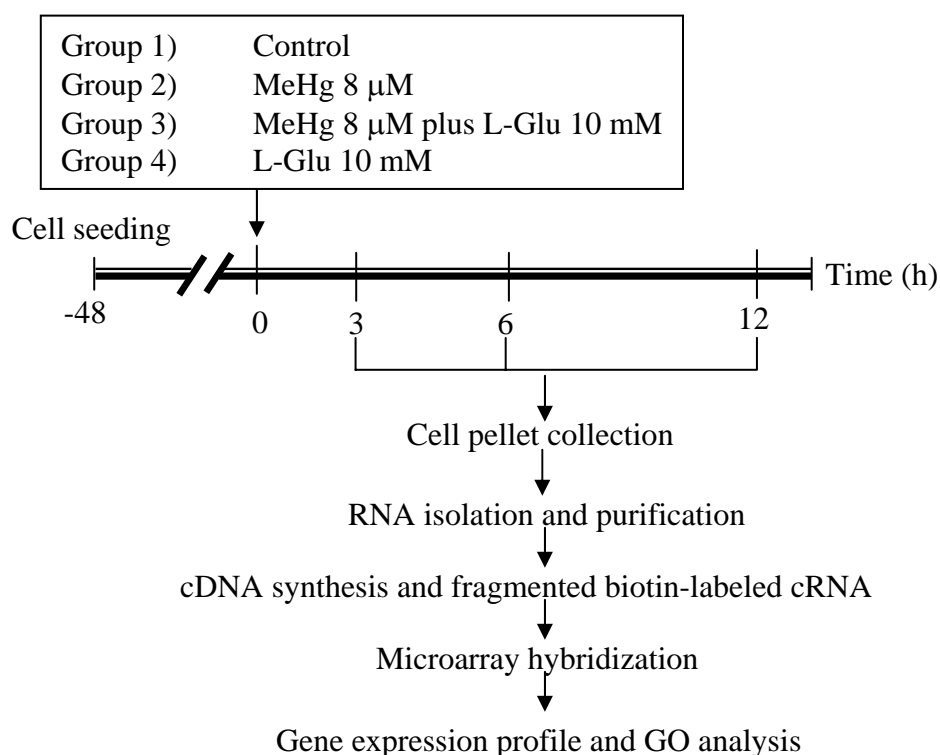


**Figure M2.** Schematic diagrams showing the step of sample collection for microarray experiment



Briefly, cells were seeded into 15 cm dish and cultured for 48 h before treatment with 8  $\mu$ M MeHg alone, MeHg plus 10 mM L-Glu, or 10 mM L-Glu. After treatment for 3, 6 and 12 h, cells were harvested by scraping, and then total RNA were extracted and purified. The cell pellets were kept at -80°C until used. For gene expression analysis, the RNA samples of fragmented biotinylated cRNA were prepared for hybridization to the Codelink<sup>TM</sup> Human Whole Genome bioarray. The list of differentially expressed genes (at least 2-fold difference) in MeHg plus L-Glu compare to MeHg alone was divided into an upregulated and downregulated list for the presentation and further analysis.

To gain an understanding of the biological processes affected by the changes of gene expression, the functional annotation of differentially expressed genes was performed using the gene ontology (GO) software GStat (Beissbarth & Speed, 2004) as well as Pubmed literature <http://www.pubmed.com>. Ultimately, the obtained results facilitated the understanding of the mode of action and toxicity of this enhancing on cytotoxicity.

## **Experiment 2.2 Effect of L-Glu on MeHg-induced apoptosis**

There was a possibility that apoptosis might mediate the cellular destruction induce by co-treatment of L-Glu and MeHg. This study was designed in order to investigated whether L-Glu enhanced the MeHg-induced apoptosis. The experimental groups were designed similar to that of Experiment 2.1

### **Experiment 2.2.1 Effect of L-Glu and MeHg on the mitochondrial membrane potential ( $\Delta\Psi_m$ )**

To determine whether the mitochondrial dysfunction contributes to L-Glu enhanced the MeHg-induced apoptosis, the alteration of the mitochondrial membrane potential ( $\Delta\Psi_m$ ) was evaluated. At the end of treatment, cells pellet were prepared and stained with MitoProbe<sup>TM</sup>DilC1 (5), a mitochondrial specific dye and then the fluorescence intensity was determined using flow cytometer as described in the materials and methods. As a positive control, cells were treated with 50  $\mu$ M of the protonophore uncoupling agent, CCCP for 30 min at 37°C before staining with DilC1

dye. Data were presented as percentage of cells with lowered membrane potential ( $\Delta\Psi_m$ ).

**Experiment 2.2.2** Effect of L-Glu on MeHg-induced the externalization of phosphatidylserine (PS)

The experimental protocol was similar to that of Experiment 2.2.1. At the end of incubation, cell death was determined by staining cells with FITC conjugated Annexin-V, and counterstaining with propidium iodide (PI) (BD Bioscience, CA, USA). Annexin-V/FITC was used in order to detect the phosphatidylserine (PS), a phospholipid only present in the outer membrane of cells undergoing apoptosis. For PI, it is excluded from cells with intact membrane. By flow cytometry analysis, the different in cell staining (Annexin V/FITC, PI) allowed us to differentiate the cells according to healthy cell (FITC<sup>-</sup>/PI<sup>-</sup>), early apoptotic cells (FITC<sup>+</sup>/PI<sup>-</sup>), late apoptotic/necrotic cells (FITC<sup>+</sup>/PI<sup>+</sup>), and necrotic cells (FITC<sup>-</sup>/PI<sup>+</sup>).

**Experiment 2.2.3** Effect of L-Glu on MeHg-induced caspase 3 activity

As caspases are activated during apoptosis by proteolytic process at specific aspartate cleavage sites (Thornberry & Lazebnik, 1998), they are important mediators of apoptosis caused by various apoptotic stimuli (Desagher *et al.*, 1999).

This experiment was conducted to determine whether the activation of caspase 3 is involved in the apoptosis mediated L-Glu that ultimately lead to enhance MeHg toxicity. The activity of caspase 3 was measured using Colorimetric Activity Assay Kit from Chemicon International (California, USA). Briefly, cell pellets were collected at the end of incubation period, and then the cell lysates were prepared using lysis buffer provided in the assay kit. DEVD-*p*NA substrate was added and the released *p*NA was determined spectrophotometrically at 405 nm. A *p*NA calibration curve was plotted from a *p*NA stock solution and the caspase 3 activity was measured relative to this curve.

**Experiment 2.3 Effect of L-Glu on MeHg-induced oxidative stress**

The aim of this study was to examine whether the exacerbation of oxidative stress process was related to the enhancing affect of L-Glu on MeHg-induced toxicity. In these experiments the level of ROS, GSH and  $x_c^-$  expression were evaluated as described below.

**Experiment 2.3.1 Effect of L-Glu and MeHg on the level of intracellular ROS**

Intracellular ROS was determined overtime by staining the cell with ROS sensitive dye DCFH. However, cells were preloaded with the DCFH before treatment with the treatment condition. Hydrogen peroxide (250  $\mu$ M) was used as a positive control for this measurement. The DCF fluorescence intensity was measured using flow cytometer as described in the materials and methods (3.2.8).

**Experiment 2.3.2 Effect of L-Glu and MeHg on the intracellular GSH level**

This experiment was designed to determine whether the oxidative stress following L-Glu and MeHg treatment is mediated by the disturbance of intracellular antioxidant. The experimental group was similar to the previous experiment (Exp. 2.1). At the end of incubation period, the level of reduced glutathione (GSH) was measured using QuantiChrom™ Glutathione Assay Kit according to the manufacturer's instruction. Buthionine-L-sulfoxamine (BSO), a specific inhibitor of  $\gamma$ -glutamylcysteine synthetase, was used as a positive control of the reaction.

**Experiment 2.3.3 Protective effect of NAC against the enhancement effect of L-Glu on MeHg toxicity**

To further confirm the participation of oxidative stress in the enhancement of MeHg by L-Glu, this experiment was performed to investigate the effect of N-acetylcystein on L-Glu enhanced MeHg-induced toxicity (Figure 3M). N-acetylcystein (NAC) is the source of thiol groups and scavenger of free radicals such as  $H_2O_2$  and  $\cdot OH$  (Aruma *et al.*, 1989). Cells were seeded into 24-well plates and cultured for 48 h. After seeding, cells were pre-incubated with 1 mM NAC 12 h, and the cells were washed three times with D-PBS, and then medium containing MeHg alone, MeHg plus L-Glu and L-Glu alone was added to the cell and continued culturing for 12 h

after treatment. At the end of incubation, the cell viability was determined using MTT assay.

### Experimental protocol

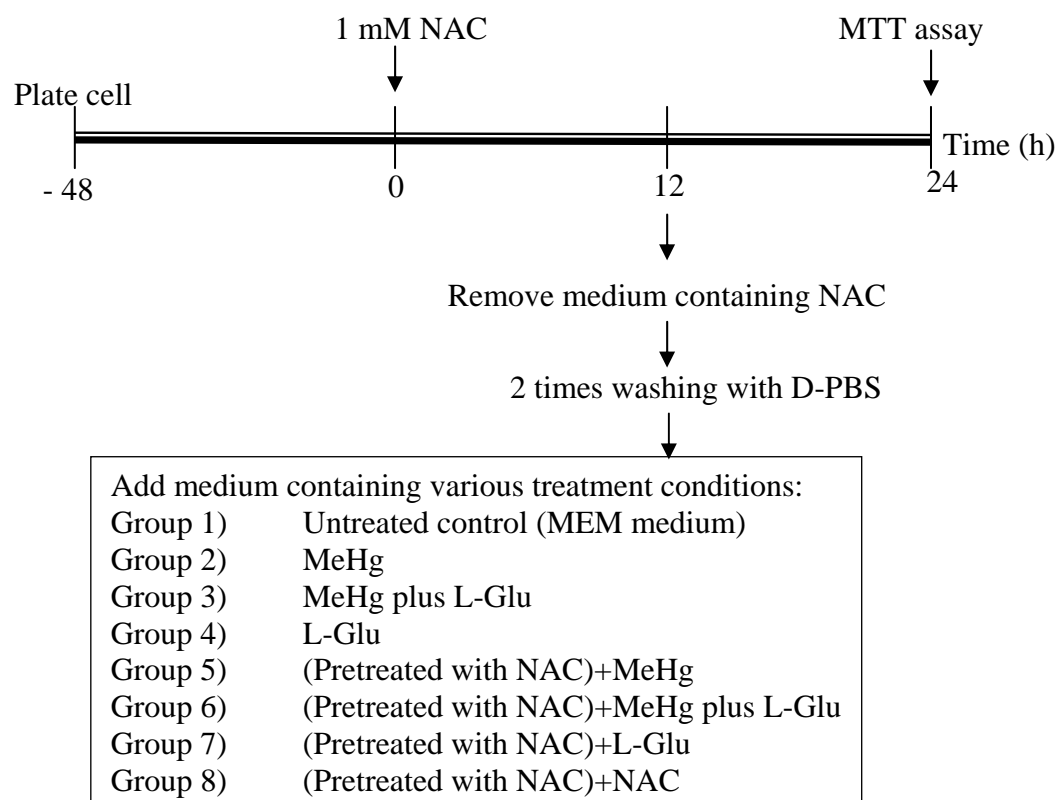


**Figure M3.** Schematic diagrams showing the period of NAC pretreatment and experimental treatment group

#### **Experiment 2.3.4** Effect of L-Glu and MeHg on the expression of system $x_c^-$ (cystine/glutamate exchanger)

It has been shown that xCT is upregulated upon the oxidative stress induction and plays an essential role to protect the cell against oxidative stress (Kato *et al.*, 1993). This experiment was aimed to examine whether L-Glu enhanced MeHg toxicity related to the induction of xCT expression. The experimental group was similar to those describe in Exp. 2.1. At the end of incubation period, cell pellets were collected, and then the total RNA was isolated. The level of cystine/glutamate exchanger subunit (xCT) was assessed by semiquantitative RT-PCR analysis with

specific primer designed base on the mRNA sequences from the Genbank database. Densitometric analysis of band intensities in treatment condition was determined and normalized with  $\beta$ -actin as described in the materials and method (3.2.11).

## **Experiment 2.4** Effect of L-Glu and MeHg on the transport activity of cystine/glutamate transporter ( $x_c^-$ )

### **Experiment 2.4.1** Effect of L-Glu and MeHg on cystine uptake.

$x_c^-$  is the  $Na^+$ -independent transporter system, consists of two subunits, the specific subunit xCT and the 4F2 heavy chain. The transport activity is thought to be mediated by the light chain subunit, xCT (Sato *et al.*, 1999). To evaluate the effect of Glu on the transport activity of  $x_c^-$ , the uptake of [ $^{14}C$ ]L-Cystine was determined in HeLa S3 cells treated with MeHg alone, MeHg plus L-Glu or L-Glu alone for 10 h. Briefly, cells were seeded on 24-well plates ( $10^5$  cells/well) and cultured at 37°C with 5%  $CO_2$  and humidity for 48 h before treating with above mentioned group. At the end of incubation, the transport activity was determined by measuring the uptake of [ $^{14}C$ ]L-Cystine as described in the materials and methods (3.2.12). Values were expressed as a percentage of the control cystine uptake in untreated control.

### **Experiment 2.4.2** Inhibitory effect of cystine uptake via cystine/glutamate transporter

To examine the inhibitory effect of L-cystine, L-Glu, L-AAD and L-Asp on cystine transport, the uptake of [ $^{14}C$ ]L-cystine (5  $\mu$ M) by HeLa S3 cells was also measured in the presence of 1 mM unlabeled amino acid above after cells were exposed to MeHg and/or L-Glu for 10 h. The uptake was determined as described in the materials and methods (3.2.12). The experimental groups were divided into 20 groups as follows:

- Group 1) Untreated control (no inhibitor)
- Group 2) MeHg treated cell (no inhibitor)
- Group 3) L-Glu treated cell (no inhibitor)
- Group 4) MeHg plus L-Glu (no inhibitor)
- Group 5)-8) Similar to Group 1)-4), 1 mM L-cystine was used the inhibitor

Group 9)-12) “-----” 1 mM L-Glu was used as the inhibitor

Group 13-16) “-----” 1 mM L-AAD was used as the inhibitor

Group 17-20) “-----” 1 mM L-Asp was used as the inhibitor

The cystine uptake was expressed as percentage of control cystine uptake measured in the absence of inhibitors.

### **Experiment 2.5** Effect of the excitotoxicity-mediated L-Glu enhanced MeHg toxicity

The objective of this study was to examine whether glutamate receptor-mediated the enhancement of MeHg cytotoxicity in HeLa S3 cells. Three agonist of glutamate receptor including  $\alpha$ -amino-3-hydroxy-5-methyl-4-isoxazolepropionic acid (AMPA), kainic acid (KA) and N-methyl-D-aspartate (NMDA) were used in this study. At the end of incubation with following treatment, the viability of cell was determined by using MTT assay. The experimental groups were divided into 20 groups as follows:

Group 1)	Untreated control (MEM with 10% FBS)
Group 2)	8 $\mu$ M MeHg alone
Group 3)-5)	MeHg + 10 $\mu$ M, +100 $\mu$ M, +10 mM L-Glu, respectively
Group 6)-7)	MeHg + 10 $\mu$ M, +100 $\mu$ M AMPA, respectively
Group 8)-9)	MeHg + 10 $\mu$ M, +100 $\mu$ M KA, respectively
Group 10)-11)	MeHg + 10 $\mu$ M, +100 $\mu$ M NMDA, respectively
Group 12)-14)	L-Glu at 10 $\mu$ M, 100 $\mu$ M and 10 mM alone, respectively
Group 15)-16)	AMPA at 10 $\mu$ M and 100 $\mu$ M alone, respectively
Group 17)-18)	KA at 10 $\mu$ M and 100 $\mu$ M alone, respectively
Group 19)-20)	NMDA at 10 $\mu$ M and 100 $\mu$ M alone, respectively

**Part III:** Investigate the effect of L-Glu on MeHg-induced toxicity in neuroblastoma cell line.

The aim of this study was to examine whether the enhanced MeHg toxicity by L-Glu is also applicable to neural cell.

**Experiment 3.1** Concentration-response effect of MeHg toxicity in neuroblastoma cell lines

This experiment was conducted to obtain the optimal concentration of MeHg in three different neuroblastoma cell lines.

Briefly, three neuroblastoma cells (Neuro2A, NIE115 and NG108) were plated in poly-D-lysine coated 24-well plates at the density of  $1 \times 10^4$  cells/ml in Dulbecco's Modified Eagle's Medium (DMEM) containing 10% FBS. Cells were cultured at 37°C in a humidified 5% CO<sub>2</sub> for 48 h before treatment with DMEM containing different concentrations of MeHg. After 12 h of incubation, the viability of cell was determined by using MTT assay.

**Experiment 3.2** Enhancement effect of MeHg cytotoxicity by L-Glu in neuroblastoma cell lines

The objective of this study was to investigate whether the enhancing effect of L-Glu on MeHg-induced toxicity also occurred in neuronal cell lines. Three neuroblastoma cell lines were treated with the optimal concentration of MeHg alone, MeHg plus 10 mM L-Glu or L-Glu alone for 12 h. At the end of incubation, the viability of cell was determined by using MTT assay.

## CHAPTER IV

### RESULTS

#### **Part I: Effect of L-glutamate (L-Glu) on methylmercury (MeHg)-induced cytotoxicity**

##### **Experiment 1.1 Concentration- and time-course effect of MeHg toxicity**

This experiment was conducted to determine the optimal concentration and time of exposure to MeHg to induce toxicity in HeLa S3 cells. Cell viability was determined after exposure to various concentrations of MeHg (2 to 16  $\mu$ M) for 3 to 72 h by using MTT assay. As shown in Figure 1, treatments with MeHg at 2 to 8  $\mu$ M for 3 to 12 h slightly induce cytotoxic effect while longer exposure times (for 24 to 72 h) further elicit the toxic effect. The highest concentration of MeHg used for treatment was 16  $\mu$ M. At 6 and 12 h after exposure, the viabilities of cells were decreased to  $63 \pm 0.7\%$  and  $50 \pm 1.1\%$  as compared to the untreated control, respectively. HeLa S3 cells employed in the present study were relatively resistant to MeHg toxicity which would allow us to observe the enhancing toxic effect by L-Glu. To further examine the potential enhancing effect of L-Glu on the MeHg toxicity and investigate the determining pathway for the fate of cell death after cell damage, less toxic concentrations of MeHg at 2 to 8  $\mu$ M and the optimal time of exposure for 3 to 12 h were chosen for following experiments. To determine the optimal concentration of MeHg in the presence of L-Glu, HeLa S3 cells were treated with 2  $\mu$ M to 8  $\mu$ M MeHg alone and with those of MeHg plus 10 mM L-Glu for 3, 6 and 12 h. This concentration of L-Glu was obtained from the earlier study on LAT1 transporter-mediated MeHg toxicity. As shown in Figure 2, the viability of cell slightly decreases in the MeHg-treated group (8  $\mu$ M) for 12 h as compared to the untreated control ( $P < 0.05$ ). No significant toxic effect was observed in the cells treated with lower concentrations of MeHg at all time points analyzed ( $P > 0.05$ ). However, treatment with MeHg at 4 or 8



$\mu\text{M}$  together with L-Glu at 10 mM markedly decreased the viability of cells as compared to that of MeHg alone ( $P<0.05$ ). The viability of cells treated with 8  $\mu\text{M}$  MeHg together with L-Glu for 6 and 12 h were decreased to  $65 \pm 4\%$  and  $45 \pm 5\%$ , respectively ( $P<0.01$ ) as compared to MeHg alone.

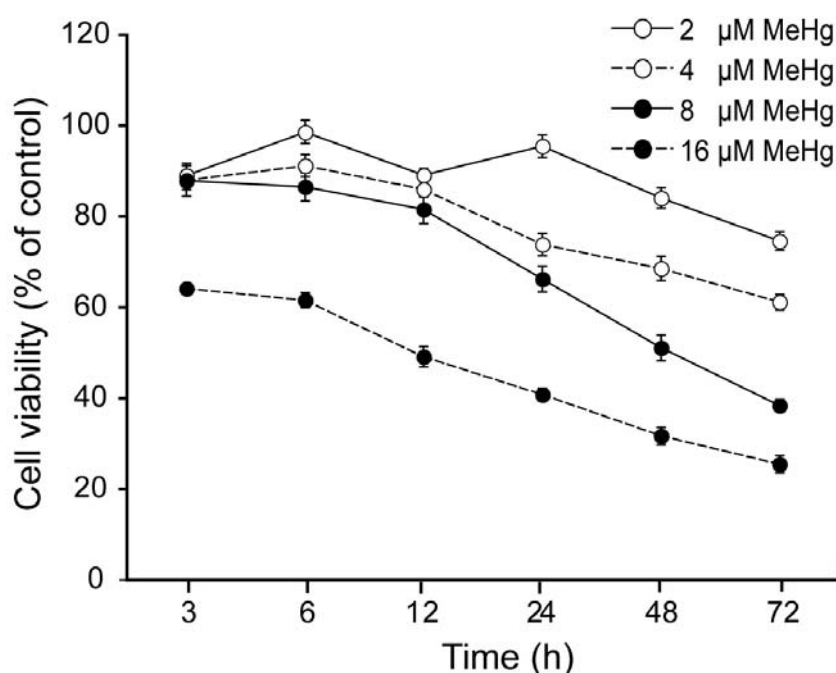


**Figure 1.** Concentration- and time-course effect of MeHg cytotoxicity in HeLa S3 cells. Cells were treated with various concentrations of MeHg (2 to 16  $\mu\text{M}$ ) for 3, 6, 12, 24, 48, and 72 h. At the end of incubation, cell viability was determined using MTT assay. Values are expressed as percentage of untreated control (100%).

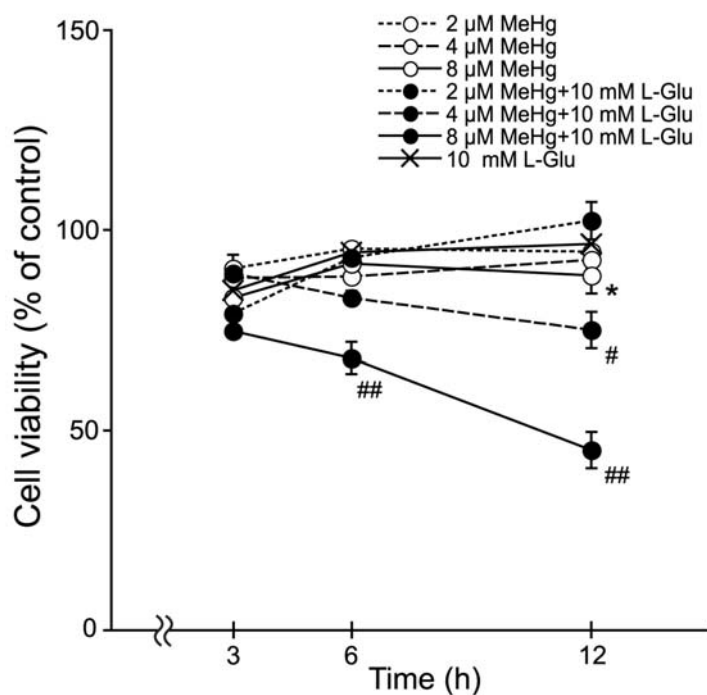


**Figure 2.** Effect of L-Glu on MeHg cytotoxicity in HeLa S3 cells. Cells were exposed to MeHg (2, 4 and 8  $\mu$ M) or MeHg plus 10 mM L-Glu for 3, 6 and 12 h. At the end of incubation, cell viability was determined using MTT assay. The values are expressed as percentage of the untreated control.

\* $P < 0.05$  as compared to the untreated control

# $P < 0.05$  as compared to 4  $\mu$ M MeHg alone

## $P < 0.01$  as compared to 8  $\mu$ M MeHg alone

### **Experiment 1.2 Effect of L-Glu on MeHg-induced toxicity**

The optimal concentration of L-Glu for enhancing MeHg toxicity was determined using MTT assay. HeLa S3 cells were treated with MeHg (8  $\mu$ M) alone, MeHg plus various concentrations of L-Glu (1, 5, 10 and 20 mM) and L-Glu alone for 12 h. As shown in Figure 3, the increase in cytotoxicity is dependent on the concentration of L-Glu between 1 to 10 mM while L-Glu at 20 mM alone induced the toxicity to the cell (data not shown). By treatment with MeHg (8  $\mu$ M) plus L-Glu (1, 5 and 10 mM), the cell viability was significantly decreased when compared with MeHg alone, whereas L-Glu alone had no effect on the cell viability at these concentrations. Treatment with MeHg plus 1 and 5 mM L-Glu, the cell viability was decreased to  $83 \pm 1.5\%$  and  $76 \pm 1.5\%$ , respectively ( $P < 0.05$  and  $P < 0.01$  compared to those with MeHg alone). The maximum toxic effect was detected in the treatment with 8  $\mu$ M MeHg plus 10 mM L-Glu, the cell viability was reduced to  $45 \pm 0.9\%$  as compared to that with MeHg alone ( $P < 0.01$ ). Therefore, 8  $\mu$ M of MeHg and 10 mM of L-Glu were chosen for further experiments.

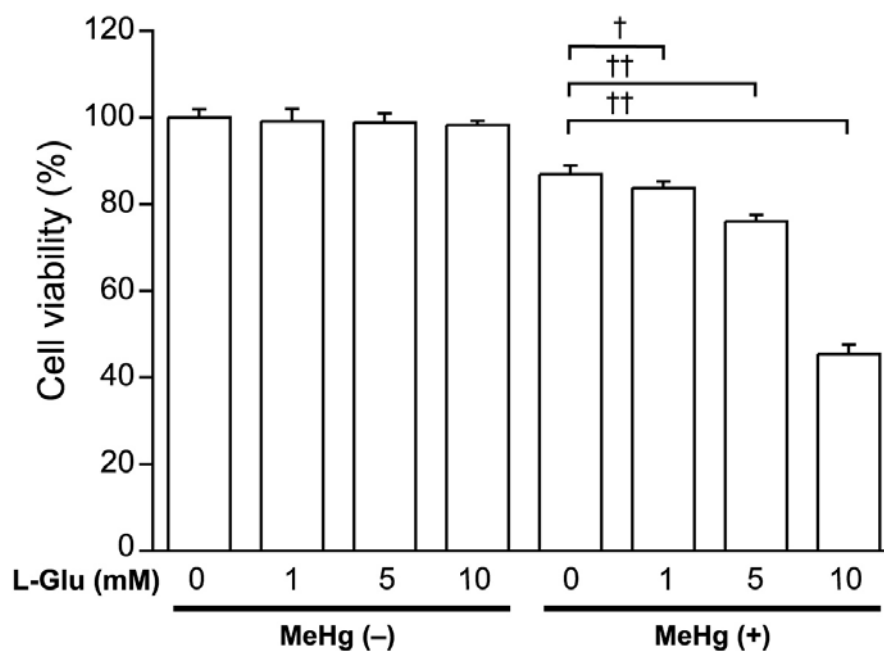


**Figure 3.** Concentration-dependent effect of L-Glu to enhance cytotoxicity of MeHg (8  $\mu$ M) for 12 h. Cell viability was measured in the presence of MeHg [MeHg(+)] or without MeHg [MeHg(-)] at varying concentrations of L-Glu (1-10 mM). Values are expressed as percentage of untreated control [MeHg(-), L-Glu 0 mM].


† $P < 0.05$  and †† $P < 0.01$  as compared to MeHg alone.

### **Experiment 1.3 Specific effect of L-Glu on MeHg-induced toxicity**

#### **1.3.1 Comparative effect of various L-amino acids on MeHg-induced toxicity**

To investigate whether the enhancement of MeHg toxicity was specific to L-Glu, the effects of 20 naturally occurring L-amino acids (10 mM) were examined on the MeHg-induced cytotoxicity using MTT assay. As shown in Table 1, only L-Glu significantly decreases the viability of cell in the presence of 8  $\mu$ M MeHg ( $P < 0.01$  compared to MeHg alone). The cell viability was decreased to about  $44 \pm 1.7\%$  as compared to that with MeHg alone ( $P < 0.01$ ). No significant difference in cell viability was observed when cells were treated with MeHg plus the others amino acids. MeHg plus Asp ( $81 \pm 5.61\%$ ), Cys ( $82 \pm 3.44\%$ ), and Gly ( $83 \pm 1.77\%$ ) caused slightly toxic but no statistical difference in the cell viability as compared to that with MeHg alone was observed. No toxic effect was observed in cells treated with each individual amino acid (data not shown).

**Table 1.** Comparison of the effect of various L-amino acids on MeHg-induced toxicity in HeLa S3 cells.

Group		% of Control (Mean $\pm$ SEM)
MeHg	L-amino acid	
	(-)	89.46 $\pm$ 3.98
	Glu	44.04 $\pm$ 1.67*
	Asp	81.35 $\pm$ 5.61
	Cys	81.94 $\pm$ 3.44
	Gly	83.05 $\pm$ 1.77
	Gln	84.49 $\pm$ 2.76
	Phe	85.93 $\pm$ 4.78
	His	88.15 $\pm$ 1.68
	Arg	88.22 $\pm$ 6.21
	Trp	88.81 $\pm$ 1.75
	Asn	90.38 $\pm$ 2.86
	Pro	90.45 $\pm$ 1.40
	Tyr	91.82 $\pm$ 6.67
	Lys	93.26 $\pm$ 4.17
	Ile	93.98 $\pm$ 6.39
	Val	94.18 $\pm$ 3.31
	Leu	95.62 $\pm$ 4.17
	Ser	96.47 $\pm$ 1.11
	Met	96.47 $\pm$ 6.08
	Ala	98.77 $\pm$ 7.16
	Thr	101.70 $\pm$ 0.24

Cells were treated with MeHg with and without L-amino acid for 12 h, and cell viability was determined using MTT assay. Values are the percentage of untreated control.  $P^* < 0.01$  as compared to MeHg alone.

### **1.3.2 Effect of Glu-related amino acid on the enhancement of MeHg toxicity**

In addition to L-amino acid, in order to confirm whether MeHg toxicity was very specifically enhanced by L-Glu, the Glu-related acidic amino acids including D-Glu, L-Asp, D-Asp and L- $\alpha$ -aminoadipate (L-AAD) were examined. As shown in Figure 4, L-AAD is as effective as that of L-Glu whereas D-Glu, L-Asp and D-Asp do not alter MeHg toxicity. No toxic effect was observed in cells treated with amino acid alone.

Therefore, the results of this part indicated that the cytotoxicity of MeHg at 8  $\mu$ M was clearly evident and specifically increased by co-exposure with L-Glu at 10 mM. The molecular mechanism underlying this phenomenon was further examined in the subsequent experiments.

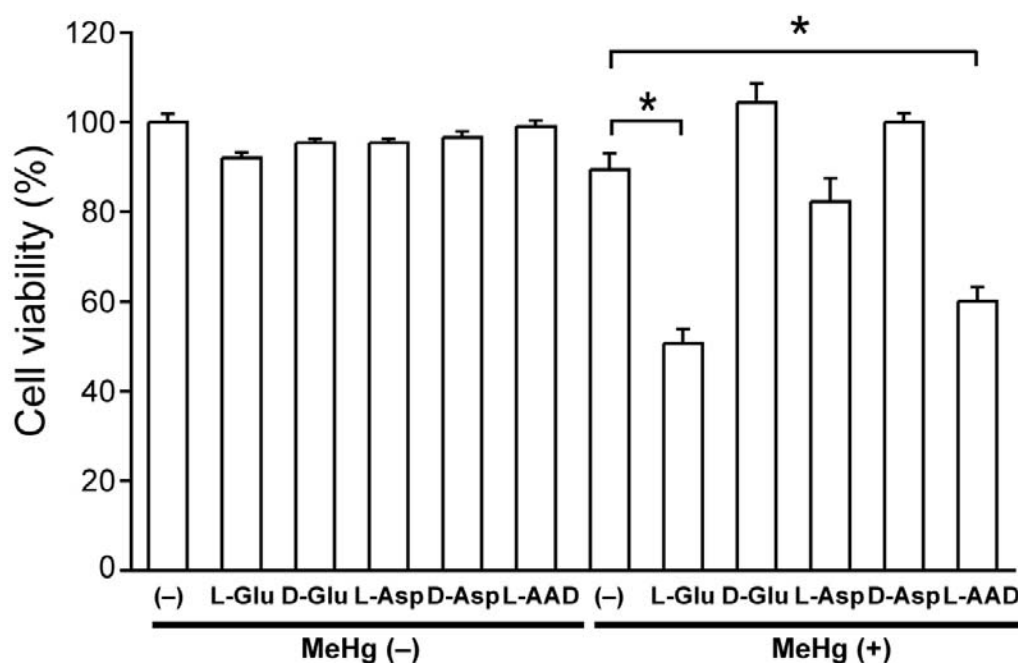


**Figure 4.** Effect of Glu-related amino acids on MeHg cytotoxicity. Cell viability was measured with 8  $\mu$ M MeHg [MeHg(+)] with or without amino acids and L-AAD (L- $\alpha$ -amino adipate). Values are expressed as percentage of untreated control

\* $P < 0.01$  as compared to MeHg alone.



## **Part II: Molecular mechanisms underlying the enhancing toxic effect of MeHg by L-Glu**

### **Experiment 2.1 Gene expression profile and Gene Ontology (GO) analysis**

#### **2.1.1 Effect of MeHg and L-Glu treatment on gene expression profile**

As the MeHg cytotoxicity is specifically enhanced by L-Glu, it is interesting to investigate how L-Glu modulates genes to give the responses. Microarray analysis was conducted to identify candidate primary response genes that may mediate the enhancement of MeHg toxicity by L-Glu throughout the time-course of exposure (3, 6, and 12 h). Figure 5 shows the scatter plot comparing the hybridization signal intensities of MeHg alone and co-treatment of MeHg and L-Glu at each time analyzed. For comparison, the mean signal intensities for the effect of MeHg alone on gene expression were plotted against those for the co-treatment of MeHg and L-Glu. Only genes whose expression levels changed by 2.0 folds or greater in either direction (fold change  $\geq 2.0$  or  $\leq 0.5$ ) at all time points were included in the subsequent analysis. Total of 71, 1491 and 401 genes were differentially expressed between MeHg alone and MeHg plus L-Glu treatment for 3, 6 and 12 h, respectively.

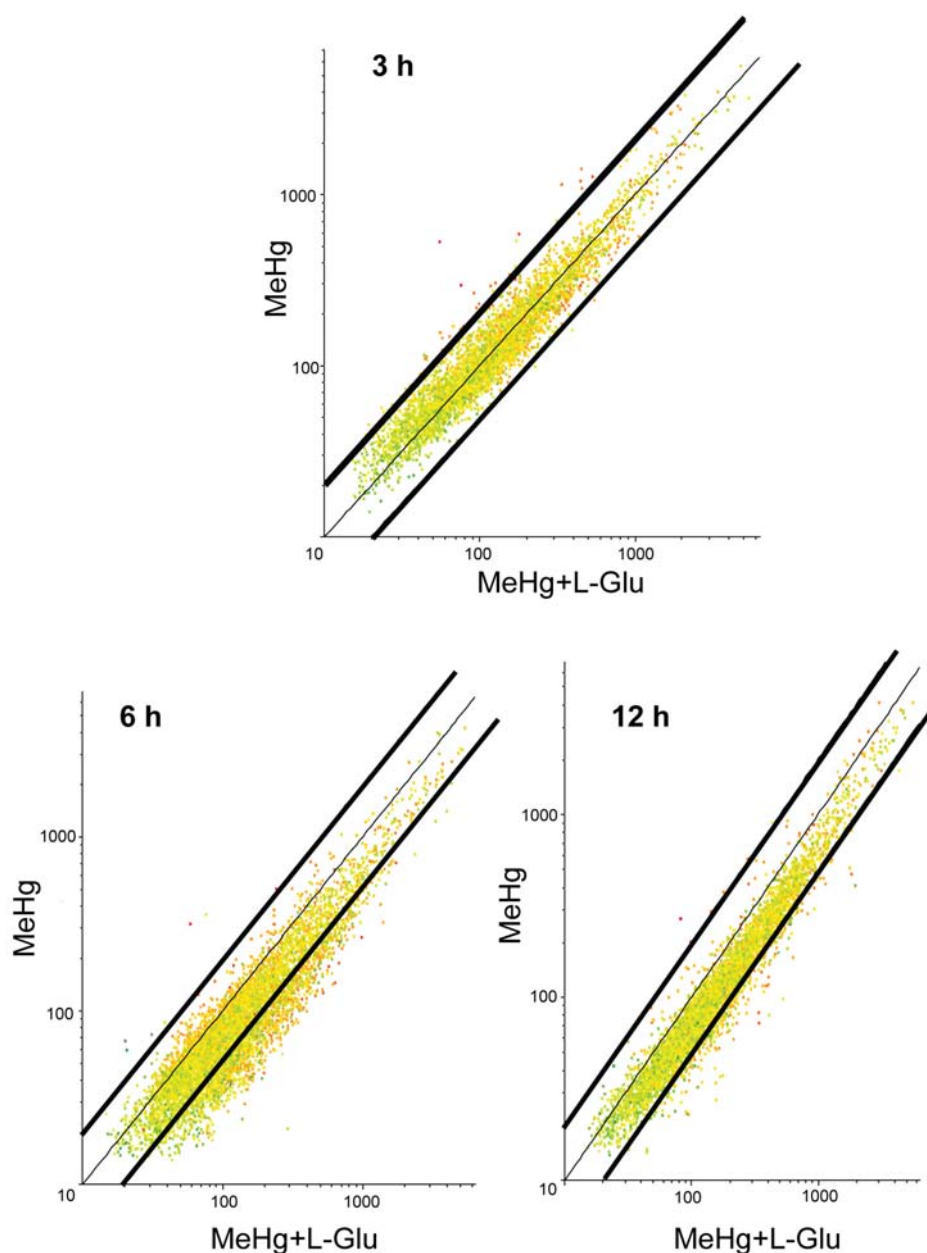


**Figure 5.** Scatter plot analysis comparing the hybridization signals of MeHg alone and MeHg plus L-Glu at various time points. Cells were harvested and gene expressions were analyzed on DNA microarray. Changes in gene expression were quantified by comparing fluorescent intensity in control and MeHg and/or L-Glu treated and analyzed by Genespring software. The majority of genes fall on the diagonal line and changes as result of toxicity at the time point analyzed; thick black lines indicate a 2-fold change.

The result of gene expression profile showed the total of 67, 9, and 6 of genes were increased (Figure 6A) and 4, 1482, and 395 genes were decreased after 3, 6, and 12 h exposure to MeHg plus L-Glu as compared to MeHg alone at corresponding time (Figure 6B). These genes were categorized into moderate ( $>2.0$  to  $3.5$  and  $>0.2$  to  $0.4$  fold) and strong ( $>3.5$  and  $>0.4$  fold) expressed genes based on the extent of relative differential expression. The distribution of the fold changes within the entire set of both up- and down-regulated genes were composed of both known and unknown genes. For the up-regulated genes, the highest numbers of gene (67 genes) were found in the early time point of exposure (3 h), and then the number of up-regulated genes were decreased to 9 and 6 genes at 6 and 12 h of exposure, respectively (Figure 6A). In addition, the majority of the up-regulated genes at 3 h displayed moderate induction and 2 genes were strongly induced. With regard to down-regulated gene, the highest number of down regulated genes were presented in mid-period of incubation (6 h) and the number of genes were decreased according to the degree of down regulation from strong to moderate level, respectively (Figure 6B). The expression of several genes were down-regulated at 6 and 12 h compared to 3 h of exposure, suggesting that cells may be undergoing an adaptive response and switching-off non-essential functions after exposure to MeHg and L-Glu.

In the previous cytotoxicity result, it demonstrated that in the first 3 h of co-treatment with MeHg and L-Glu, there was only a small change in the cell viability as compared to 6 and 12 h of exposure. In order to examine which process(s) determine the fate of cells to die after cells were exposed to MeHg and L-Glu at the later time points (6 and 12 h), we, therefore, further analyzed the up-regulation of early response genes at 3 h in the following section.

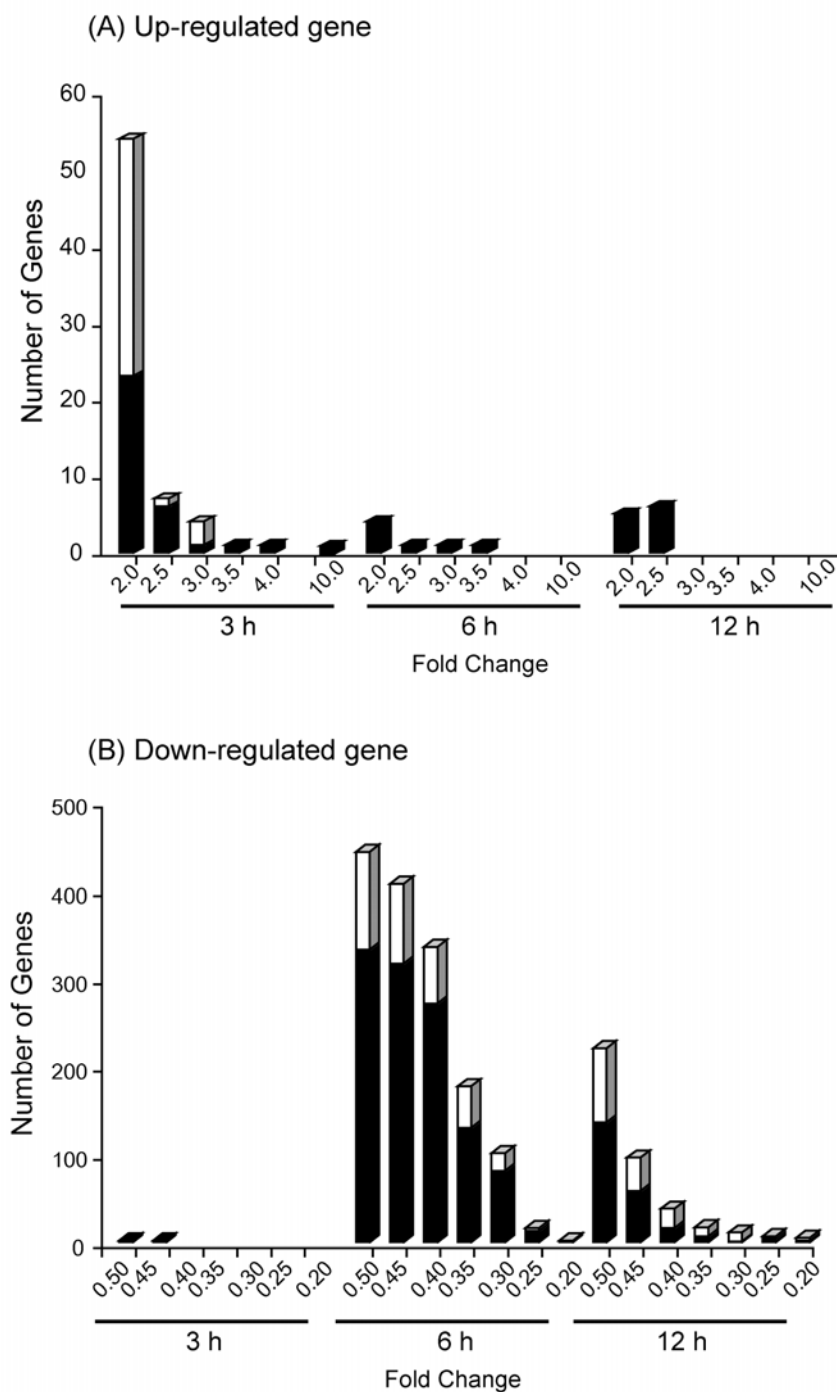


**Figure 6.** Distribution of fold change of the gene in the cells co-treated with MeHg and L-Glu for 3 h using microarray analysis. Solid bars or portion of bars show known genes and open bars or portion of bars show unknown genes.

### **2.1.2 Up-regulated gene by co-treatment with MeHg and L-Glu for 3 h classified into discrete functional groups**

To further investigate the alterations in gene expression those are associated with L-Glu enhanced MeHg toxicity, total 67 of up-regulated genes in MeHg plus L-Glu treatment for 3 h were analyzed using Gene Ontology (GO). Genes were categorized based on their reported or suggested functions and can be placed into six broad functional groups (Table 2). Results demonstrated that co-treatment of MeHg and L-Glu induced several sets of genes which might play roles in L-Glu enhanced MeHg toxicity. Two of six functional processes including stress-response and apoptosis are of particular interested since these processes have been reported as the major mechanism of the MeHg-mediated toxicity (Nagashima, 1997; Yee & Choi, 1996).

**Table 2.** Gene ontology (GO) of up-regulated differentially expressed genes between MeHg alone and MeHg plus L-Glu treated for 3 h

Gene ontologies in MeHg plus L-Glu vs MeHg				Differential expressed gene	
No.	GO term	GO ID	Group count	Total count	p-value Gene Name
1	Response to stress	0006950	9	1222	1.05E-04 hmgbl ctgfhspal a hspal b sod2 il6 thbs1 cfb il8 id3
2	Response to wound healing	0009611	6	423	2.06E-04 ctgf il6 thbs1 cfb il8 id3
3	Apoptosis	0006915	7	855	5.66E-04 nfkbia hmgb1 hspal a hspal b axud1 sod2 il6 id3
4	Response to stimulus	0050896	12	3553	6.95E-04 nfkbia hist1h2bk hspal a il6 hist2h2be cfb il8 id3 hmgb1 ctgfh sod2 thbs1
5	Response to external stimulus	0009605	6	633	6.95E-04 ctgf il6 thbs1 cfb il8 id3
6	Protein binding	0005515	18	9005	9.11E-04 pfdn2 acat2 il6 alcam hist2h2be cfb il8 id3 atp1b3 thbs1 nfkbia hspal a mcm5 hmgb1 ctgfh lsm5 sfrsl1 dnaja4

Group count: number of differentially expressed genes associated to the gene ontology term; total count: number of all genes associated to the gene ontology term

Ten and eight genes were functionally categorized into stress-response (Table 3) and apoptosis (Table 4). In these two categories, six genes were grouped into both processes. This indicated that one gene is also involved in more than one function. Totally of 12 of early response genes were gathered into Table 5. The expression of these genes were taken to compare with the longer time point of exposure to investigate the alteration of gene expression in a delayed response period. As shown in Table 5, several genes were found to be up-regulated at 3 h, however, their level of expressions are decreased at 6 and 12 h of exposure, or no longer differentially express/similar extent between 6 and 12 h of exposure. Among all of these changed genes by co-treatment of MeHg and L-Glu, Hspa1b (heat shock protein 1B) was the highest induced gene (9.8 folds). The heat shock protein (Hsp) is generally induced by oxidative stress such as by ethanol, infection, inhibitors of energy metabolism, and heavy metal (Morimoto *et al.*, 1992). The level of Hsps are known to increase at in the early stage stress-response and it has been shown to suppress apoptosis by several mechanisms including block caspase activity, mitochondrial damage, and nuclear fragmentation (Mosser *et al.*, 1997), inhibition of stress kinase (Gabai *et al.*, 1997), prevention of bax translocation to the mitochondria (Stankiewicz *et al.*, 2005), and antagonism of apoptosis-inducing factor (AIF) (Ravagnan *et al.*, 2001). On the other hand, some studies reported the pro-apoptotic role for Hsp70s (Nakatsu *et al.*, 2005; Ran *et al.*, 2004). However, the stress-related apoptotic mechanism of Hsp70 is still controversial. Indeed, one of gene is ctgf. Its expression was also increased by co-treatment of MeHg and L-Glu. The pattern of ctgf expression at different time analyzed showed that its expression was higher at 6 h than at 3 h and then decreased at 12 h. ctgf has been reported to participate in the induction of apoptosis and activation of caspase-3 (Hishikawa *et al.*, 1999). Together, these gene changes suggested that the cells may be undergoing stress-response process, which may be important in the enhancement of MeHg-induced cell death by L-Glu. This classification revealed that the regulation of stress and apoptosis process might act in a coordinated manner to initiate and propagate apoptotic cell death in the co-exposure of MeHg and L-Glu.

**Table 3.** List of up-regulated genes associated with stress-response in MeHg plus L-Glu for 3 h of exposure in HeLa S3 cell

GenBank ID	Gene Symbol	Gene Name	Fold change
NM_002128	HMGB1	high-mobility group box 1	2.49
NM_001901	CTGF	connective tissue growth	3.96
NM_005345	HSPA1A	heat shock 70kDa protein 1A	2.01
NM_005346	HSPA1B	heat shock 70kDa protein 1B	9.78
NM_000636	SOD2	superoxide dismutase 2	2.32
NM_000600	IL6	interleukin 6	2.20
BU959813	THBS1	thrombospondin 1	2.51
NM_001710	CFB	complement factor B	2.20
NM_000584	IL8	interleukin 8	2.23
AW589426	ID3	inhibitor of DNA binding 3	2.16

**Table 4.** List of up-regulated genes associated with apoptosis in MeHg plus L-Glu for 3 h of exposure in HeLa S3 cell

GenBank ID	Gene Symbol	Gene Name	Fold change
AA595964	NFKBIA	nuclear factor of kappa light polypeptide gene enhance	2.04
NM_002128	HMGB1	high-mobility group box 1	2.49
NM_005345	HSPA1A	heat shock 70kDa protein 1A	2.01
NM_005346	HSPA1B	heat shock 70kDa protein 1B	9.78
NM_033027	AXUD1	AXIN1 up-regulated 1	2.35
NM_000636	SOD2	superoxide dismutase 2	2.32
NM_000600	IL6	interleukin 6	2.20
AW589426	ID3	inhibitor of DNA binding 3	2.16



**Table 5.** Comparison of genes with be classified into both stress-response and apoptosis process in MeHg plus L-Glu treated at various times

No.	Gene symbol	Gene description	GenBank ID	h		
				3	6	12
1	HMGB1	high-mobility group box 1	NM_002128	2.5	0.9	1.1
2	ID3	inhibitor of DNA binding 3n	AW589426	2.2	1.1	1.2
3	IL6	interleukin 6	NM_000600	2.2	1.9	1.3
4	AXUD1	AXIN1 up-regulated 1	NM_033027	2.4	1.0	1.0
5	CTGF	connective tissue growth factor	NM_001901	4.0	5.5	3.3
6	NFKBIA	nuclear factor of kappa light polypeptide gene enhancer in B-cells inhibitor, alpha	AA595964	2.0	0.8	0.6
7	SOD2	superoxide dismutase 2	NM_000636	2.3	1.0	1.2
8	HSPA1A	heat shock 70kDa protein 1A	NM_005345	2.0	1.7	2.1
9	HSPA1B	heat shock 70kDa protein 1B	NM_005346	9.8	2.1	2.1
10	THBS1	thrombospondin 1	BU959813	2.5	1.3	1.5
11	CFB	complement factor B	NM_001710	2.2	0.8	1.2
12	IL8	interleukin 8	NM_000584	2.2	1.4	1.1

## **Experiment 2.2 Effect of L-Glu on MeHg-induced apoptosis**

In the line with the cytotoxicity and the results of microarray analysis, several reports have demonstrated that the mechanism of MeHg toxicity may involve oxidative stress and apoptosis (Belletti *et al.*, 2002; InSug *et al.*, 1997). Therefore, we then investigated the effect of L-Glu on MeHg-induced cytotoxicity in the line of apoptosis pathway. The study included the determination of the mitochondrial membrane potential ( $\Delta\Psi_m$ ), the externalization of phosphatidylserine (PS), and caspase-3 activity.

### **2.2.1 Effect of L-Glu and MeHg on the mitochondrial membrane potential ( $\Delta\Psi_m$ )**

The maintenance of the mitochondrial membrane potential ( $\Delta\Psi_m$ ) is a fundamental for the normal performance and survival of cells. Additionally, it has been reported that the alteration in mitochondrial transmembrane potential is an early marker in the apoptotic process. The alteration of mitochondrial membrane potential ( $\Delta\Psi_m$ ) by L-Glu on MeHg-induced apoptosis was determined by staining cell with 50 nM cyanine dye; DiIc(5). This dye is the lipophilic cationic dye that is driven into the cell, selectively accumulates and aggregates inside the mitochondrial as the result of the negative potential of mitochondria (-150 mV) (Kroemer *et al.*, 1997). Whereas in cells with damaged mitochondria, or altered mitochondrial transmembrane potential, the dye cannot aggregate and remains in the cytoplasm. Figure 7 shows the representative histogram indicating the DiIc1(5) fluorescent intensity in cell treated with MeHg and/or L-Glu at 3, 6 and 12 h of exposure. The number indicated in the area marked indicated the percentage of cell exhibiting loss  $\Delta\Psi_m$ . It was set from the untreated control and the positive control (CCCP; carbonyl cyanide 3-chlorophenylhydrazone treated cell). When the  $\Delta\Psi_m$  is compromised, the histogram peak is shift to the left side, which has lower intensity than the right side. As shown in Figure 8, the mitochondrial membrane is markedly depolarized at 12 h when cells are co-treated with MeHg and L-Glu by about  $23 \pm 2\%$  ( $P < 0.05$  as compare to MeHg alone). However, treatment with MeHg alone and L-Glu alone did not significantly affect the membrane potential at all time analysed.

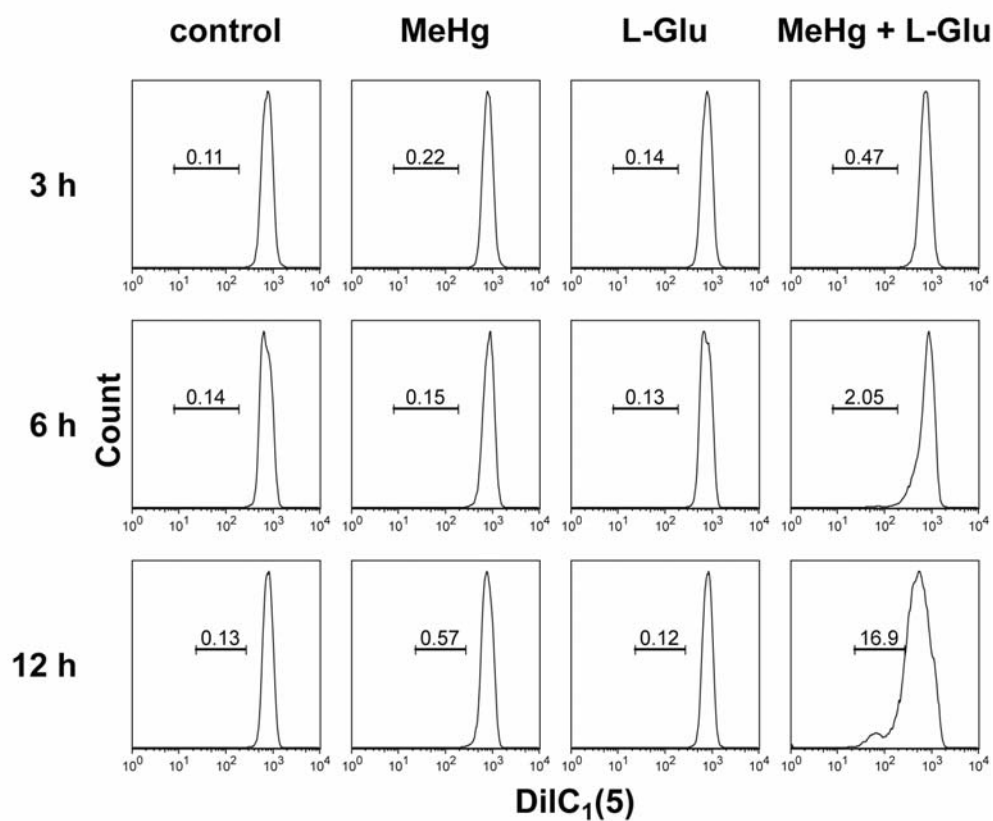


**Figure 7.** Representative histograms of FACS analysis of mitochondrial membrane potential ( $\Delta\Psi_m$ ). Cells were treated with MeHg and/or L-Glu at indicated time. Alteration in  $\Delta\Psi_m$  was measured by flow cytometry using DiIC<sub>1</sub>(5). The decrease in  $\Delta\Psi_m$  was determined by a decrease in the DiIC<sub>1</sub>(5) fluorescent intensities. The number indicated in the region marked is defined as the percentage of cells with decreased  $\Delta\Psi_m$ .

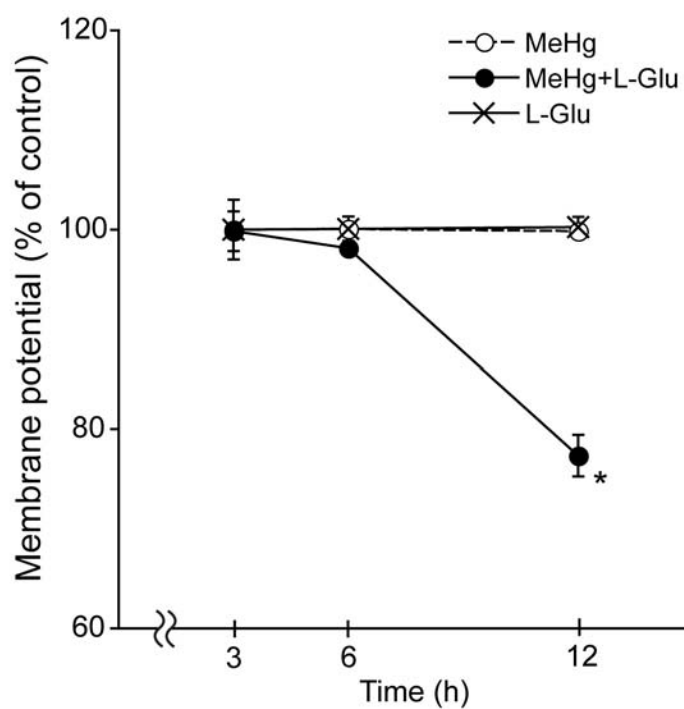


**Figure 8.** Change of mitochondrial membrane potential ( $\Delta\Psi_m$ ) in MeHg and/or L-Glu treatment at with time. Fluorescent intensity was quantitated by FACS analysis. The results are expressed as a percentage of mitochondrial membrane potential compared with untreated control cells.  
\* $P < 0.05$  as compared to MeHg alone.

### **2.2.2 Effect of L-Glu on MeHg-induced the externalization of phosphatidylserine (PS)**

Since the perturbation of lipid organization in the plasma membrane is a common feature of apoptotic cell death (Martin *et al.*, 1995), in this study the effect of MeHg and L-Glu on phosphatidylserine (PS) translocation to the outer layer of the plasma membrane was determined by staining cell with FITC-conjugated Annexin-V (Annexin V/FITC) and propidium iodide (PI). PI, it is usually excluded from cells with intact membrane. The different staining pattern of Annexin V/FITC and PI was used to differentiate the modes/stages of cell death; healthy cell (FITC<sup>-</sup>/PI<sup>-</sup>), early apoptotic cells (FITC<sup>+</sup>/PI<sup>-</sup>), late apoptotic/necrotic cells (FITC<sup>+</sup>/PI<sup>+</sup>), and necrotic cells (FITC<sup>-</sup>/PI<sup>+</sup>).

As shown in Figure 9, treatment with MeHg plus L-Glu causes a gradual increase in the number of early stage of apoptotic cells (FITC<sup>+</sup>/PI<sup>-</sup>) at 3 and 6 h of exposure (1.2% and 2.2%, respectively). However, the percentage of early apoptotic cells was maximally increased after exposure to MeHg plus L-Glu for 12 h (5.5%). The percentage of an early (FITC<sup>+</sup>/PI<sup>-</sup>) and late (FITC<sup>+</sup>/PI<sup>+</sup>) stages of apoptosis was highly increased in MeHg plus L-Glu treated group (5.5% and 15.5% compared to MeHg alone). By analyzing the mode of cell death at 12 h, the result showed that the cause of cell death in cells treated with MeHg plus L-Glu was by apoptosis (FITC<sup>+</sup>/PI<sup>-</sup> and FITC<sup>+</sup>/PI<sup>+</sup>) rather than necrosis (FITC<sup>-</sup>, PI<sup>+</sup>). Thus, co-treatment with MeHg and L-Glu not only resulted in the depolarization of mitochondrial membrane but also causing the translocation of PS to the outer membrane. In addition, as the apoptosis is usually accompanied by the induction of caspase cascade, the caspase-3 activity, the executive caspase was also determined in the next experiment.

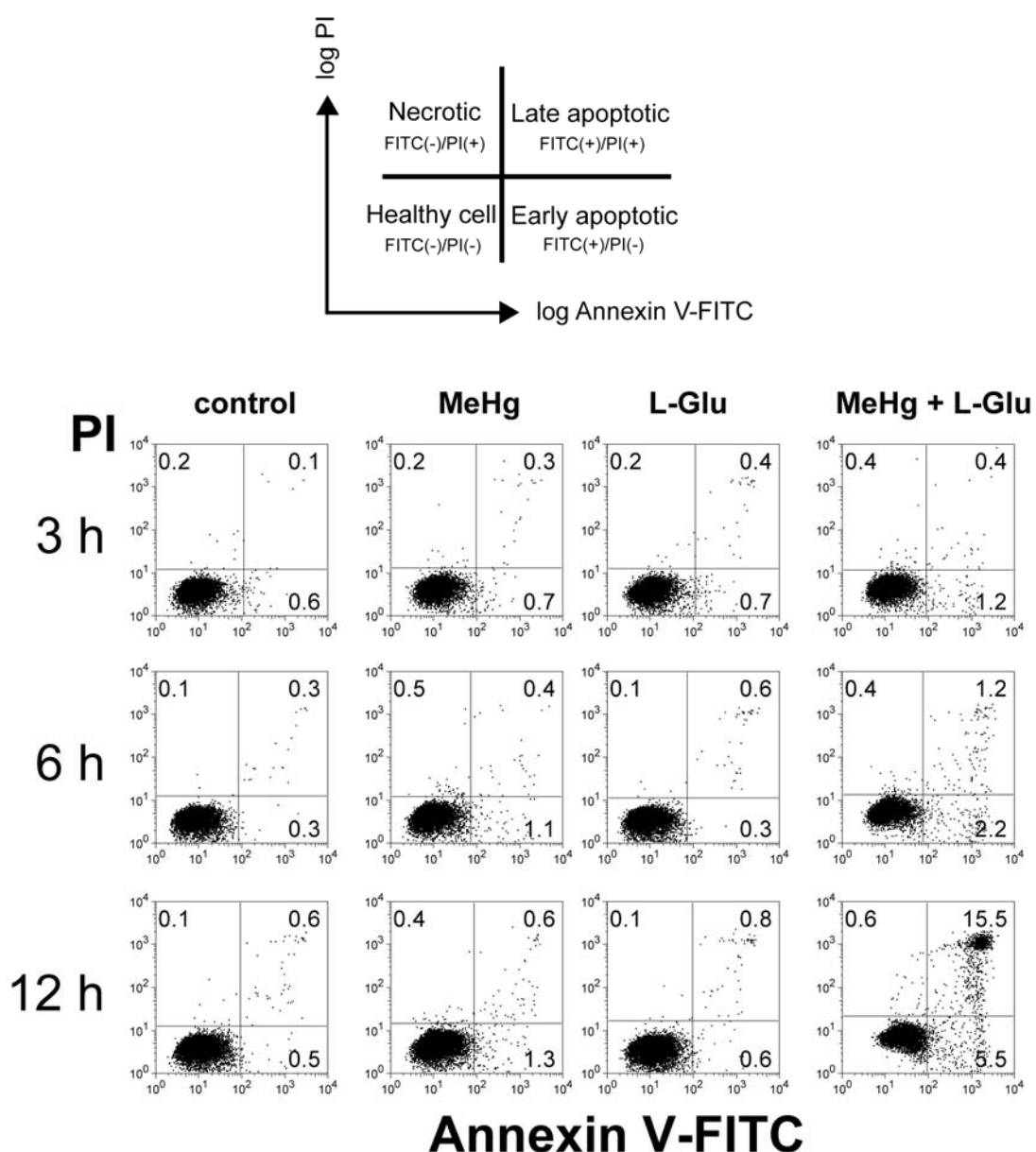


**Figure 9.** Representative dot plot analysis of an Annexin V-FITC staining cell population after MeHg and/or L-Glu treatment. Cells were treated with MeHg and/or L-Glu at time indicated. They were then stained with Annexin V conjugated to FITC/PI and analyzed by using FACS. Lower left, lower right, upper left and upper right quadrants indicate FITC<sup>-</sup>/PI<sup>-</sup> healthy cells, FITC<sup>+</sup>/PI<sup>-</sup> early apoptotic cells, FITC<sup>-</sup>/PI<sup>+</sup> necrotic cells and FITC<sup>+</sup>/PI<sup>+</sup> late apoptotic cells, respectively. The number in each quadrant indicates percentage of cells in the quadrant.

### 2.2.3 Effect of L-Glu on MeHg-induced caspase-3 activity

The results of the previous section revealed that L-Glu enhanced MeHg toxicity occurred via induction of apoptosis by the loss of  $\Delta\Psi_m$  and the externalization of PS on the membrane. In addition, it has been reported that caspases are activated during apoptosis by proteolytic processing at specific aspartate cleavage sites (Thornberry & Lazebnik, 1998), and they are important mediators of apoptosis caused by various apoptotic stimuli (Desagher *et al.*, 1999). The present experiment was conducted to determine whether L-Glu enhanced MeHg-induced apoptosis was related to the caspase activation process. The activity of caspase-3 was measured by the cleavage of the fluorogenic substrate Ac-DEVD-pNA (*p*-nitroaniline) in a flurometric assay. As shown in Figure 10, caspase 3 activity is significantly increased at 6 h of treatment by approximately to  $118 \pm 3.3\%$  and  $162 \pm 1.3\%$  in MeHg alone and MeHg plus L-Glu as compare to untreated control  $P<0.05$  and  $P<0.01$ , respectively. Treatment with MeHg plus L-Glu at 6 h markedly increased the activity of caspase-3 compared to MeHg ( $P<0.01$ ). In contrast, the caspase-3 activity was decreased at 12 h in MeHg alone and MeHg plus L-Glu. L-Glu did not effect caspase-3 activity at all time analyzed.

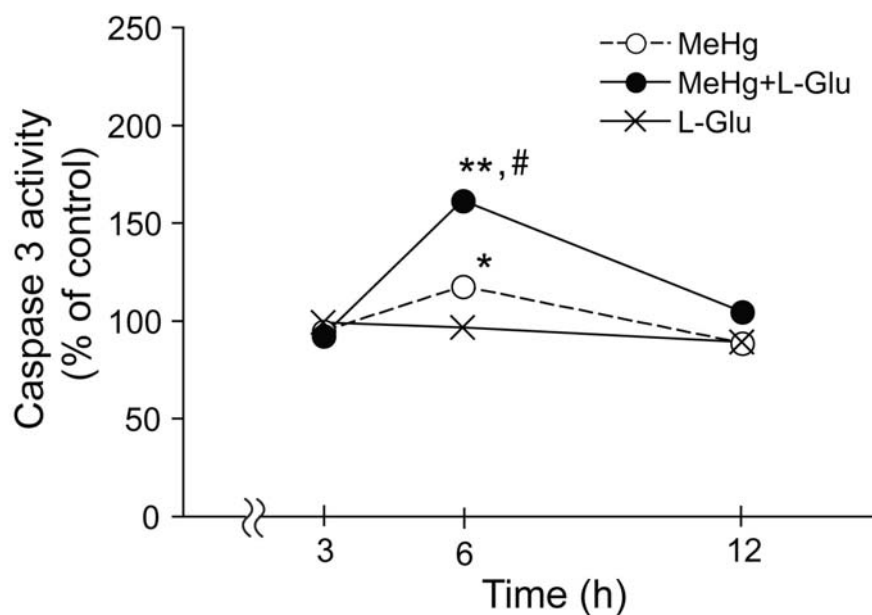


**Figure 10.** Effect of MeHg and L-Glu on caspase-3 activity. Cells were treated with MeHg and/or L-Glu for the indicated time. Caspase-3 activity was determined and expressed as percent of the untreated control cells.

\* $P < 0.05$  and \*\* $P < 0.01$  as compared to untreated control

# $P < 0.05$  as compared to MeHg alone



## **Experiment 2.3 Effect of L-Glu on MeHg-induced oxidative stress**

### **2.3.1 Effect of L-Glu and MeHg on the induction of intracellular reactive oxygen species (ROS)**

To test if oxidative stress process is involved in the enhancing toxic effect of L-Glu on MeHg, level of ROS was determined in cells treated with MeHg (8  $\mu$ M) and/or L-Glu (10 mM) by staining the cells with the ROS sensitive dye DCFH-DA. Figure 11 shows the representative histogram indicating the DCF fluorescent intensity. The number indicated in region mark is set base on the untreated control and positive control (250  $\mu$ M H<sub>2</sub>O<sub>2</sub> treated cell). When the level of intracellular ROS was increased, the peak was shifted to the higher DCF intensity (shift right). The level of ROS increased with time beginning at 3 h after MeHg exposure. Interestingly, co-treatment of MeHg and L-Glu markedly increased ROS level compared to MeHg at all time points. It increased from 0.57% at 3 h to 20.8% at 12 h of exposure. As clearly shown in Figure 12, the percentage of positive cells exhibiting the increased in DCF fluorescent intensity, MeHg alone increase the ROS level from  $1.62 \pm 2 \%$  at 12 h ( $P < 0.01$  as compare to untreated control). However, co-treatment with MeHg and L-Glu had much greater effect on the ROS level than MeHg alone ( $20.8 \pm 2 \%$ ,  $P < 0.01$  compared to MeHg alone at 12 h). No significant effect was detected for L-Glu alone on the ROS level at all times analysed.

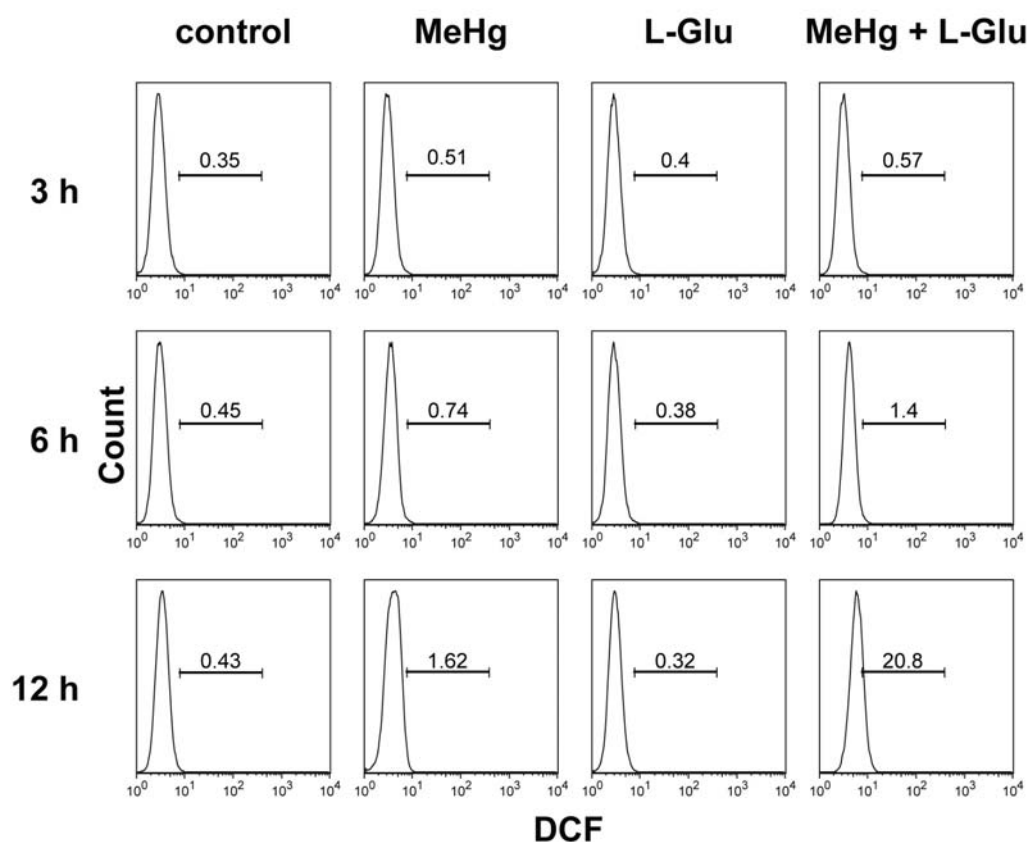


**Figure 11.** Representative histograms showing the level of ROS in MeHg and/or L-Glu treated cell by FACS. Cells at time indicated were pre-loaded with medium containing 20  $\mu$ M DCFH for 15 min at 37°C. After loading fluorescence probe, cells were treated with MeHg and L-Glu at time indicated, cells were washed and then DCF fluorescence was analyzed using FACS. The increase in ROS level was determined by the increase in the DCF fluorescent intensities. The number indicated in region marked is defined as the percentage of cells exhibiting positive DCF fluorescence.

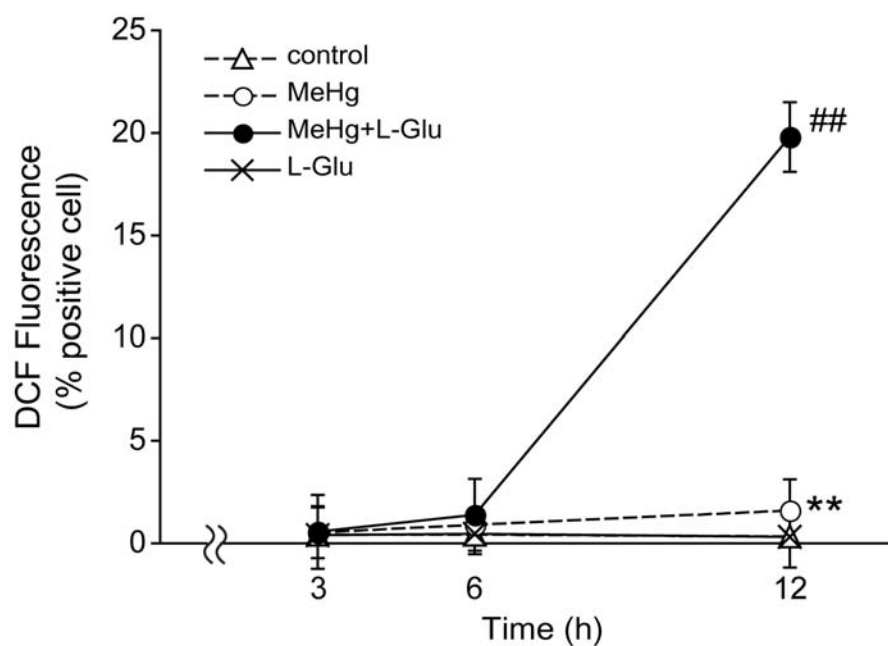


**Figure 12.** Effect of MeHg and L-Glu on intracellular ROS level measured with DCFH dye. The fluorescent intensity of DCF, an oxidized product of DCFH, was assayed by using FACS. Values are expressed as the percentage of DCF positive cell.

\*\* $P < 0.01$  as compared to untreated control

## $P < 0.01$  as compared to MeHg alone

### **2.3.2 Effect of L-Glu and MeHg on the intracellular reduced glutathione (GSH) level**

To determine if the increased ROS level following MeHg and L-Glu treatment was associated with the depletion of intracellular antioxidants, the intracellular reduced glutathione (GSH) level was measured. Treatment of cells with buthionine-L-sulfoxamine (BSO, a glutathione synthesis inhibitor) for 12 h as a positive control for GSH depletion decreased GSH levels to approximately 50% as compared to untreated control (data not shown). As shown in Figure 13, L-Glu does not significantly affect the GSH level whereas MeHg alone significantly decreases GSH level at 12 h to  $82 \pm 4\%$  as compared to untreated control ( $P < 0.05$ ). GSH level was markedly decreased by  $41 \pm 6\%$  in the co-treatment with MeHg and L-Glu at 12 h ( $P < 0.05$  as compared to MeHg alone).

### **2.3.3 Protective effect of NAC against the enhancing effect of L-Glu on MeHg toxicity**

In parallel with determination of GSH level, the effect of 1 mM N-acetylcysteine (NAC) on the enhancing effect of L-Glu was also examined. As shown in Figure 14, the enhancing effect of L-Glu on MeHg toxicity can be inhibited by pretreatment with antioxidant NAC, the viability of cell is increased from  $45 \pm 4.8\%$  to  $83 \pm 1.7\%$  ( $P < 0.01$  as compare to MeHg plus L-Glu without NAC). NAC itself did not affect cell viability.

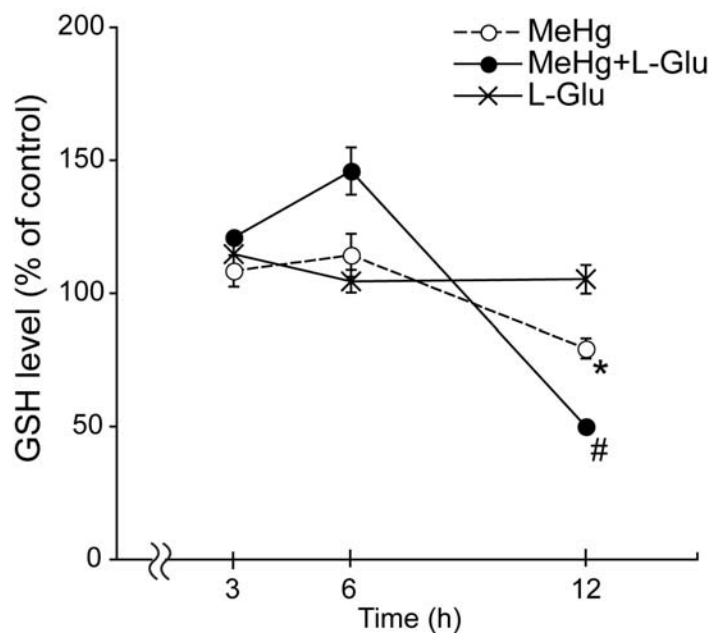


**Figure 13.** Effect of MeHg and L-Glu on intracellular GSH level. Cells were treated with MeHg (8  $\mu$ M) and/or L-Glu (10 mM) for the indicated times, and treated cells were collected and analyzed for GSH level. The values are expressed as percent change from untreated control group.

\* $P < 0.05$  as compared to untreated control

# $P < 0.05$  as compared to MeHg alone

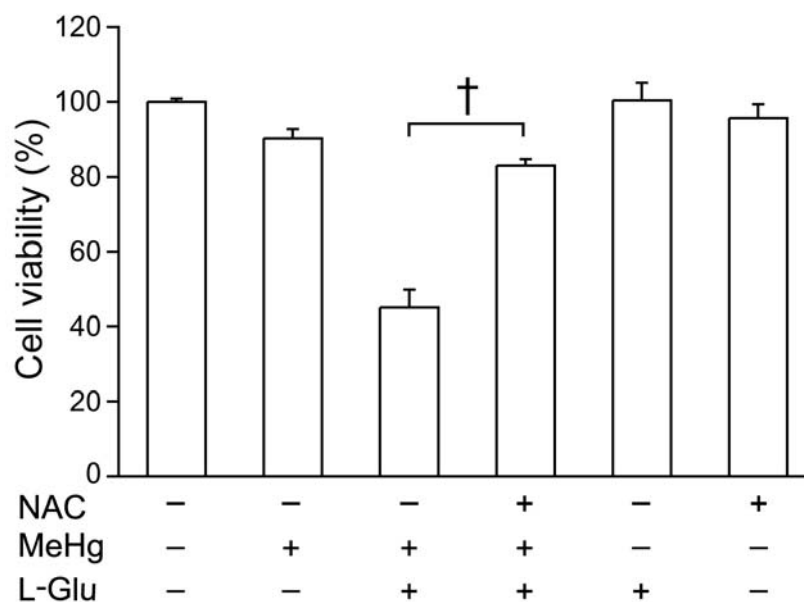


**Figure 14.** Effect of *N*-acetylcysteine (NAC) on the cytotoxicity induced by co-treatment of MeHg and L-Glu. Cells were pre-incubated with 1 mM NAC for 12 h. After removing NAC, the cells were treated with MeHg and/or L-Glu for 12 h. Cell viability was measured at the end of treatment with MeHg and/or L-Glu. The values are expressed as percentage of untreated control.

<sup>†</sup> $P < 0.01$  as compared to MeHg plus L-Glu.

#### **2.3.4 Effect of L-Glu and MeHg on the expression of system $x_c^-$ (cystine/glutamate exchanger)**

The level of light chain subunit of system  $x_c^-$  (xCT), which is one evidence determining the oxidative stress in the cell was assessed by semiquantitative PCR analysis. As shown in Figure 15A, xCT mRNA in the HeLa S3 cells levels are increased in time-dependent manner after exposure to MeHg (8  $\mu$ M), and MeHg (8  $\mu$ M) plus L-Glu (10 mM) for 6 and 12 h. Densitometric analysis of band intensities showed that the treatment with MeHg alone, and MeHg plus L-Glu for 12 h significantly increased the level of xCT mRNA (2.1 and 2.4 folds as compared to untreated control,  $P<0.01$ , respectively) (Figure 15B). L-Glu alone tended to increase xCT mRNA level at 12 h. However, these were not statistically significant compared to the untreated control (Figure 15B).

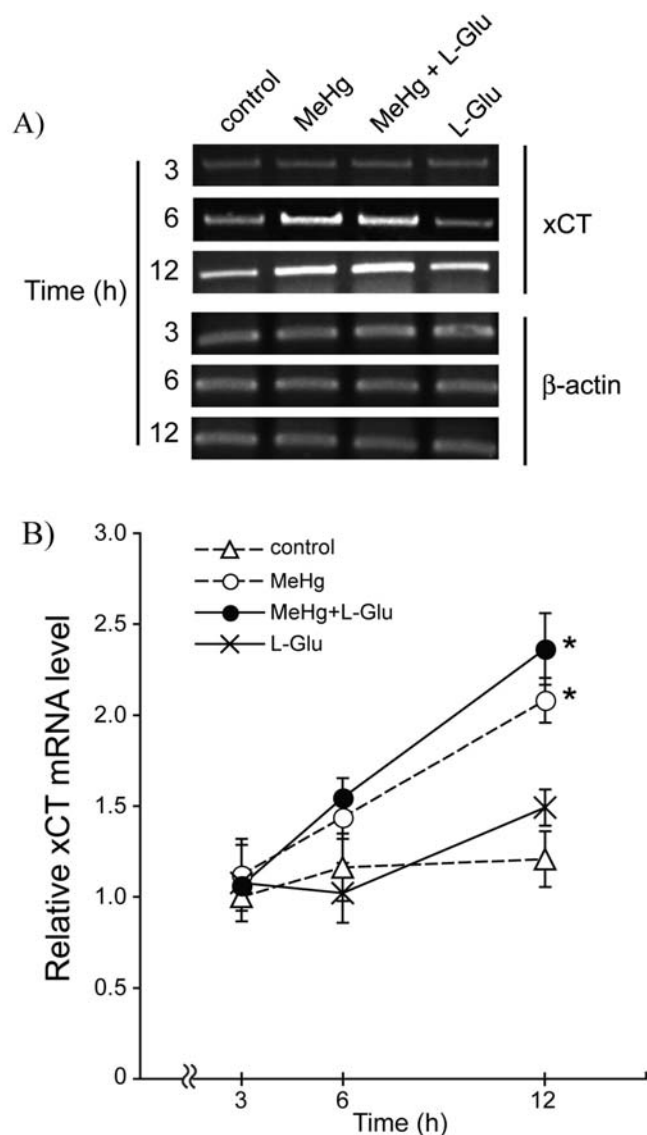


**Figure 15.** Effect of MeHg and L-Glu on xCT mRNA expression level. Cells were treated with MeHg (8  $\mu$ M) and/or L-Glu (10 mM) for 3, 6 and 12 h. The mRNA level of cystine/glutamate exchanger xCT were analyzed by RT-PCR and normalized for  $\beta$ -actin mRNA level based on densitometric analysis of band intensities. A, representative agarose gel electrophoresis of PCR products for xCT and  $\beta$ -actin stained with ethidium bromide. B, relative mRNA level of xCT for each treatment condition compared with that for the untreated control at 3, 6 and 12 h. The values are expressed as ratios to that of untreated control at 3 h.

\* $P < 0.01$  as compared to the untreated control at each time point.



#### **Experiment 2.4 Effect of L-Glu and MeHg on the transport activity of cystine/glutamate transporter ( $x_c^-$ )**

To provide evidence for the expression of system  $x_c^-$  in HeLa S3 cells, the uptake of [ $^{14}\text{C}$ ]L-cystine into these cells were studied in untreated cells or cells treated with MeHg and/or L-Glu (Figure 16) and the substrate specificity of the uptake process in treated cells were also assessed by competitive experiment (Figure 17). In this experiment, the activity of  $x_c^-$  in untreated control, MeHg and/or L-Glu treatment for 10 h in HeLa S3 cell was assessed by measuring [ $^{14}\text{C}$ ]L-cystine uptake. The untreated cell were found to take up the [ $^{14}\text{C}$ ]L-cystine uptake activity and this process was inhibited by unlabeled cystine, L-Glu and L-AAD but not by L-Asp, indicating that HeLa S3 cells possessed endogenous cystine uptake activity mediated by  $x_c^-$  transport system (Figure 16-17). The activity of  $x_c^-$  was slightly increased by the treatment with L-Glu (10 mM) or MeHg (8  $\mu\text{M}$ ) and greatly increased by co-treatment with MeHg (8  $\mu\text{M}$ ) plus L-Glu (10 mM) (Figure 16). Competition experiments revealed that the increased [ $^{14}\text{C}$ ]L-cystine uptake in the cells treated with MeHg and/or L-Glu was inhibited by unlabeled cystine as well as by L-Glu and L-AAD but not by L-Asp, similar to that of untreated HeLa S3 cell (Figure 17). The results from the previous experiment together with this experiment suggested that HeLa S3 cells expressed xCT mRNA, exhibited  $x_c^-$  and its transport activity was enhanced when cells were exposed to MeHg, and MeHg plus L-Glu.

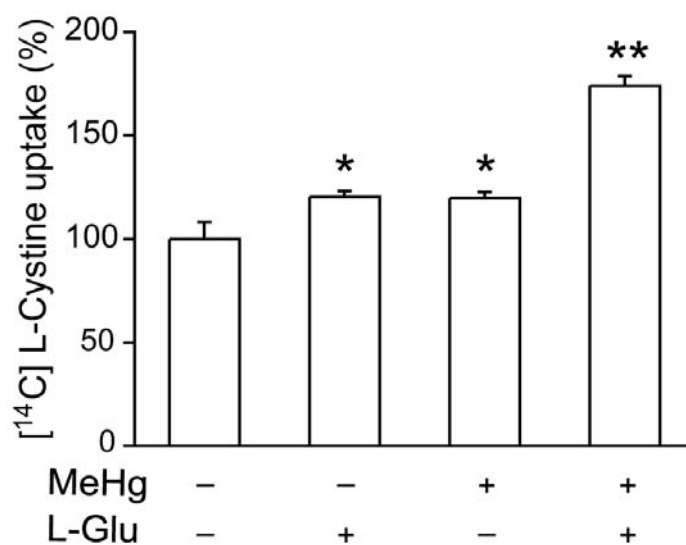


**Figure 16.** [<sup>14</sup>C]L-cystine uptake by HeLa S3 cells and the enhancement by the treatment with MeHg and L-Glu. Cells were treated with 10 mM L-Glu and/or 8 μM MeHg for 10 h and the uptake of [<sup>14</sup>C]L-Cystine (5 μM) was measured for 5 min. Values are expressed as percentage of untreated control.

\**P*<0.05 and \*\**P*<0.01 as compared to untreated control.

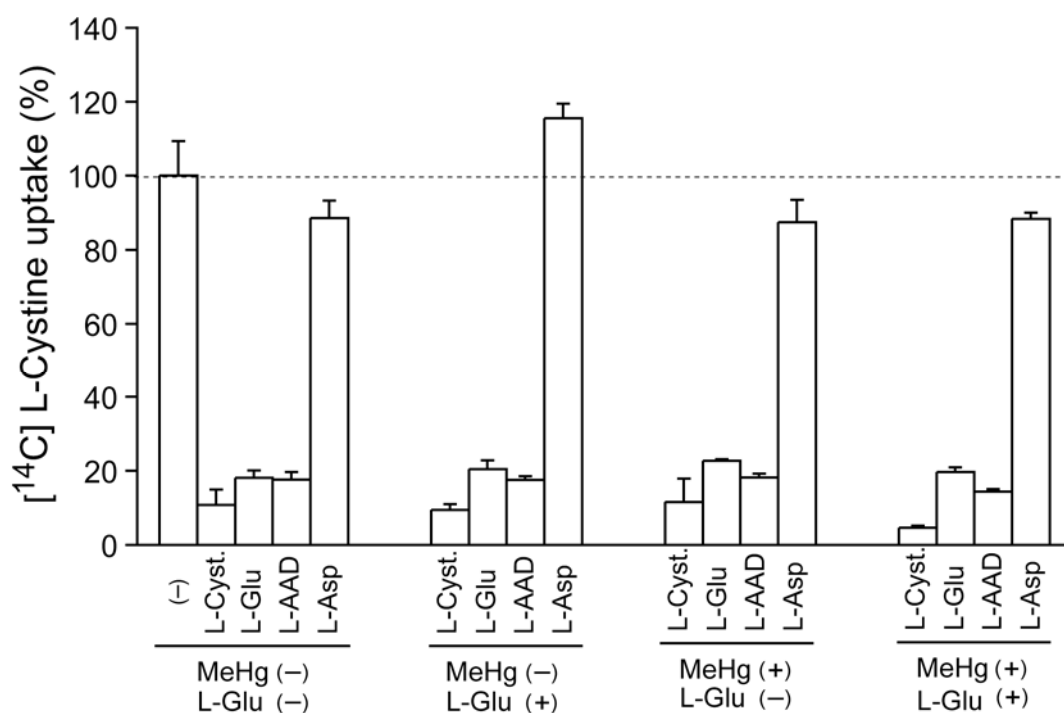


**Figure 17.** Inhibitory effect of L-cystine (L-Cyst.), L-glutamate (L-Glu), L- $\alpha$ -amino adipate (L-AAD) and L-aspartate (L-Asp) on [ $^{14}\text{C}$ ]L-cystine uptake in HeLa S3 cells. Cells were treated with 10 mM L-Glu and/or 8  $\mu\text{M}$  MeHg for 10 h and the uptake of [ $^{14}\text{C}$ ]L-cystine (5  $\mu\text{M}$ ) was measured for 5 min in the presence or absence of indicated amino acids (1 mM). The cystine uptake in the presence of the inhibitors is expressed as percentage of control cystine uptake measured in the absence of inhibitors for each treatment condition (dash line).

To further confirm that L-Glu enhanced MeHg toxicity occurred via oxidative glutamate toxicity by inhibition of  $x_{\text{C}}^{-}$  activity, cells were treated with the agonist of glutamate receptor parallel with L-Glu as in the previous experiment in order to examine whether L-Glu-enhanced MeHg toxicity was related to glutamate receptor-mediated excitotoxicity.

### Experiment 2.5 Effect of the excitotoxicity-mediated L-Glu enhanced MeHg toxicity

The effect of MeHg-induced toxicity was examined after cells were co-treated with MeHg and various agonists of glutamate receptor for 12 h. As shown in

Table 5, the enhancement of MeHg cytotoxicity is unlikely due to the glutamate receptor-mediated excitotoxicity because the agonists of glutamate receptors such as  $\alpha$ -amino-3-hydroxy-5-methyl-4-isoxazolepropionic acid (AMPA), kainic acid and N-methyl-D-aspartate (NMDA) did not enhance the toxicity of 8  $\mu$ M MeHg at the concentrations of 10~100  $\mu$ M at which has been reported to fully activate non-NMDA and NMDA receptors (Sinor *et al.*, 2000; Verdaguer *et al.*, 2002). The result obtained in this experiment was consistent with the previous result on the effect of L-Glu on the expression and activity of system  $x_C^-$ . It is, thus, proposed that the enhanced MeHg cytotoxicity by L-Glu observed in this HeLa S3 cell was resulted from the inhibition of system  $x_C^-$  by L-Glu.

**Table 6.** Effect of glutamate receptor agonist on MeHg cytotoxicity.

Treatment	% of Control (Mean $\pm$ SEM)		
MeHg	87.8 $\pm$ 1.02*		
L-Glu	MeHg (+)		
	10 $\mu$ M	100 $\mu$ M	10 mM
	95.20 $\pm$ 2.19	97.51 $\pm$ 3.57	45.50 $\pm$ 2.06 <sup>#</sup>
Agonist	10 $\mu$ M	100 $\mu$ M	
KA	98.50 $\pm$ 2.11	90.80 $\pm$ 2.55	
AMPA	90.98 $\pm$ 4.41	86.98 $\pm$ 3.46	
NMDA	93.79 $\pm$ 1.86	85.47 $\pm$ 2.11	
L-Glu	MeHg (–)		
	10 $\mu$ M	100 $\mu$ M	10 mM
	98.28 $\pm$ 4.51	96.56 $\pm$ 2.97	95.70 $\pm$ 1.17
Agonist	10 $\mu$ M	100 $\mu$ M	
KA	97.90 $\pm$ 1.03	96.70 $\pm$ 2.50	
AMPA	95.34 $\pm$ 3.12	89.26 $\pm$ 3.01	
NMDA	93.56 $\pm$ 2.16	88.67 $\pm$ 1.86	

\* $P < 0.05$  as compared to untreated control

<sup>#</sup> $P < 0.01$  as compared to MeHg alone

**Part III: Effect of L-Glu on MeHg-induced toxicity in neuroblastoma cell line**

To clarify if the enhancing effect of L-Glu on MeHg toxicity occurred in HeLa S3 cells is applicable to neural cells, three neuroblastoma cell lines were used to examine the effects. The results showed that each neuroblastoma cell lines had different susceptibility to MeHg. As shown in Figure 18, Neuro2A is susceptible to MeHg toxicity than NIE115 and NG108-15. MeHg at 4  $\mu$ M decreased cell viability of Neuro2A, NIE115 and NG108-14 to  $83 \pm 4.17\%$ ,  $77.3 \pm 11.1\%$  and  $19.9 \pm 3.1\%$ , respectively. MeHg at 4  $\mu$ M and 2  $\mu$ M were used for further examining the enhancing effect of L-Glu in Neuro2A, NIE115 and NG108-14, respectively. All three neuroblastoma cell lines had higher susceptibility to MeHg toxicity than HeLa S3 cell. L-Glu (10 mM) significantly reduced the viability of cells when co-treated with MeHg, whereas L-Glu alone does not significantly affect the viability of all neuroblastoma cells (Figure 19).

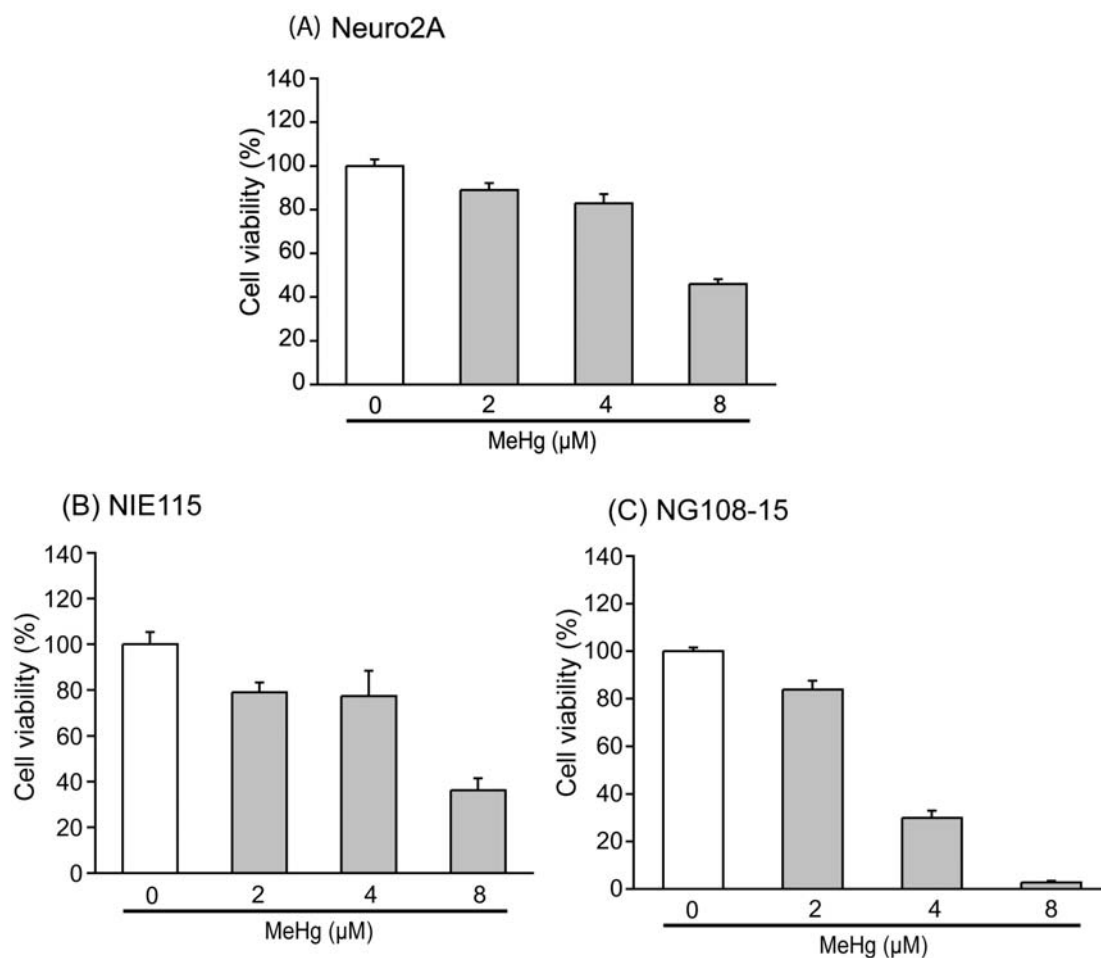


**Figure 18.** Concentration-dependent of MeHg cytotoxicity in neuroblastoma cell lines. Three neuroblastoma cell lines including Neuro2A cells (A), NIE115 cells (B) and NG108-15 cells (C) were treated with MeHg at 2 to 8  $\mu$ M for 12 h. At the end of incubation, cell viability was determined by using MTT assay. The values are expressed as percentage of untreated control.

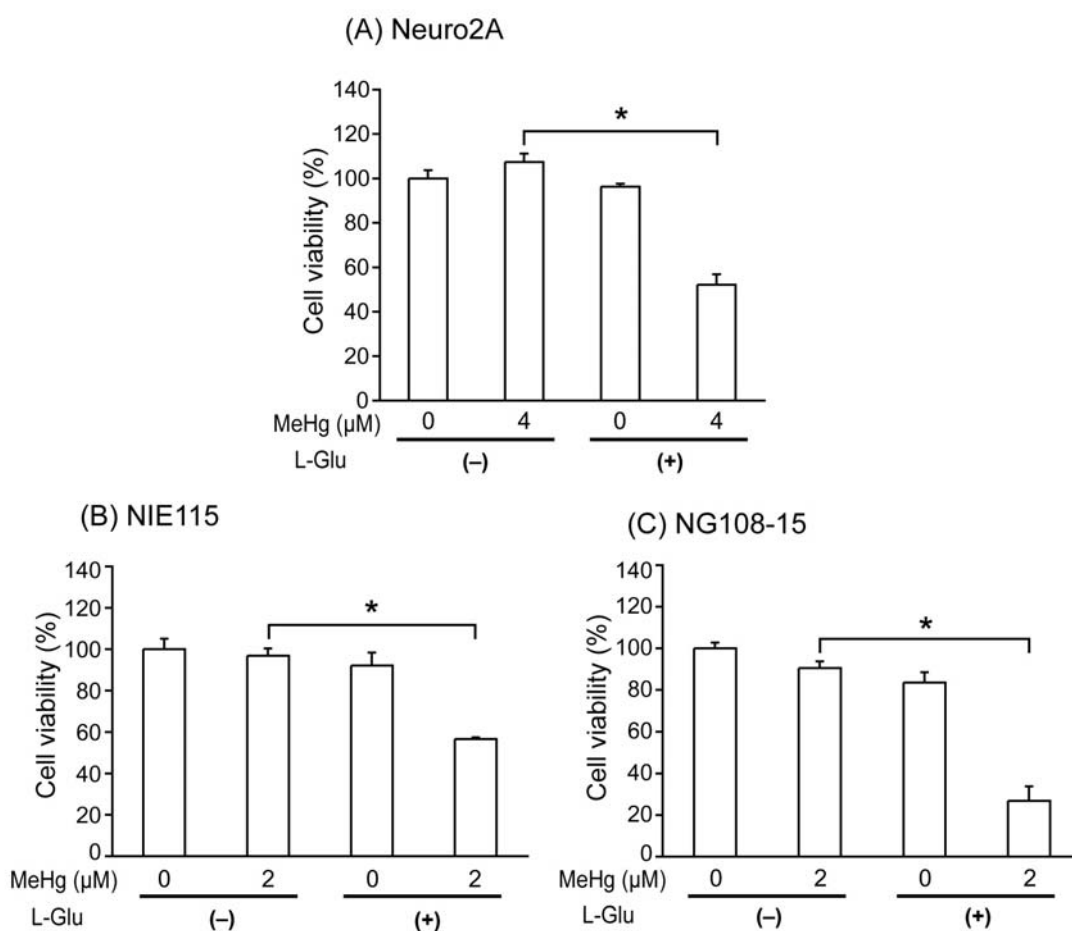


**Figure 19.** Effect of L-Glu on MeHg-induced cytotoxicity in neuroblastoma cells. Neuroblastoma cell lines Neuro2A cells (A), NIE115 cells (B) and NG108-15 cells (C) were treated with MeHg (2 or 4 μM) and/or L-Glu (10 mM) for 12 h. At the end of incubation, cell viability was determined by MTT assay. The values are expressed as percentage of untreated control [MeHg(0), L-Glu(-)].

\* $P < 0.01$  as compared to MeHg alone

## CHAPTER V

### DISCUSSION

The present study demonstrated that L-Glu unequivocally enhances MeHg-induced cytotoxicity. Among 20 naturally L-amino acids, only L-Glu was specifically and greatly enhanced MeHg toxicity in HeLa S3 cell. Additionally, the Glu-related amino acid, L-AAD gave similar effect to L-Glu on the MeHg toxicity whereas D-Glu, L- and D-Asp were not effective in enhancing the cytotoxicity. Furthermore, from the examination on the mechanism underlying the enhancing toxic effect by using the microarray analysis, the result of the gene expression profile and the Gene Ontology (GO) analysis suggested that the induction of stress and apoptosis process were involved in L-Glu enhanced MeHg toxicity. Indeed, L-Glu enhanced the induction of apoptotic cell death by MeHg by the loss of mitochondrial membrane potential ( $\Delta\Psi_m$ ), the externalization of phosphatidylserine (PS) as well as the activation of caspase-3 activity. Co-exposure of L-Glu with MeHg essentially enhanced the reactive oxygen species (ROS) production, decreased reduced glutathione (GSH) level and the antioxidant, *N*-acetylcysteine (NAC) greatly alleviated the cytotoxicity. All these lines of the obtained results suggested that enhanced oxidative stress was the underlying mechanism of the increased MeHg toxicity elicited by L-Glu.

The mechanism in detail on the enhancement of MeHg toxicity by L-Glu was further examined and indicated that it was associated with transport system  $x^-_C$ . Co-treatment of MeHg and L-Glu greatly enhanced the expression of light subunit xCT mRNA and transport activity of system  $x^-_C$ , which is the system known to be responsible to and being regulated by oxidative stress. In addition, the inhibitory effect of the competitive inhibitor on this transport system showed that [ $^{14}$ C]L-cystine uptake of the untreated cell, MeHg and/or L-Glu was strongly inhibited by L-Glu and L-AAD but not by L-Asp. Consistent with the involvement of the inhibition of amino acid transport system  $x^-$ , the glutamate receptor agonist (NMDA, KA, and AMPA) failed to



enhance MeHg toxicity. These characteristics were in consistent with the involvement of the inhibition of  $x_C^-$  activity. Therefore, L-Glu enhanced MeHg toxicity occurred via the oxidative glutamate toxicity by inhibition of  $x_C^-$  activity but not by the glutamate-receptor excitotoxicity.

### **1. Effect of L-Glu on MeHg cytotoxicity in HeLa S3 cell.**

A number of earlier studies have shown that MeHg exposure decreased cell viability in several cell models, such as primary cerebellar granule cell (Castoldi *et al.*, 2001), glial cell, neuronal cell lines (Kaur *et al.*, 2007) and in the striatal synaptosome (Ali *et al.*, 1992). In this study, we used a non-neuron-derived cell line, HeLa S3 (human cervical carcinoma), to examine the mechanism underlying the enhancement of L-Glu on MeHg toxicity. MeHg has little effect on the percent viability of HeLa S3 cells in the absence of L-Glu suggesting that this cell line was relatively resistant to MeHg toxicity. It allowed us to clearly observe the enhancing effect of L-Glu on MeHg toxicity. L-Glu concentration-dependently decreased the cell viability when the cells were co-exposed to MeHg (Figure 3). Moreover, in the presence of L-Glu, the toxic effect of MeHg was clearly dependent on the concentration of MeHg (Figure 2). These results indicated that L-Glu increased the sensitivity of the cells to MeHg toxicity in HeLa S3 cell. Furthermore, we confirmed that this enhancement of MeHg toxicity by L-Glu also occurred in three neuroblastoma cell lines including Neuro2A, NIE115 and NG108-15 but at different intense of toxicity (Figures 18 and 19).

### **2. Oxidative stress induction underlies the L-Glu enhanced MeHg-induced cytotoxicity.**

The underlying mechanism(s) mediated L-Glu-enhanced MeHg toxicity was initially examined using the microarray analysis to investigate whether co-exposure to MeHg plus L-Glu modified the expression of specific gene involved in the enhancing toxic effect of L-Glu. Gene profiling analysis and the Gene Ontology (GO) analysis were performed to gain an understanding of the molecular processes which might be affected by the changes of gene expression, and to further revealed information on mode of action and toxicity. The obtained results from the gene expression profiles of cells in co-treatment of MeHg and L-Glu revealed that several genes were

differentially expressed following co-exposure to MeHg and L-Glu as compared to MeHg alone. Total 71, 1491 and 401 genes whose the level of expression were altered at least 2-fold different from MeHg treatment for 3, 6 and 12 h, respectively. The Gene Ontology of 67 up-regulated genes at 3 h by co-treatment of MeHg plus L-Glu (Table 2) revealed that at least two processes, including the stress-response and apoptotic-related process might be the key processes in the enhancing toxic effect of L-Glu. Some of the genes identified in the present study have already been known to participate in these two processes (stress-response and apoptosis). For instance, HSPA1B (heat shock protein 1B) was the highest increased at 3 h and then declined at 6 and 12 h of exposure. High levels of the inducible heat shock protein 70 (Hsp70s) have been reported to prevent stress-induced apoptosis. It blocks caspase activity, mitochondrial damage, and nuclear fragmentation (Mosser *et al.*, 1997). Another interesting gene is the CTGF (connective tissue growth factor), which showed the different in the pattern of its expression with time. Its increased was higher at 6 h than that at 3 h of exposure, and then declined at 12 h. This connective tissue growth factor (CTGF/CCN2) is a cysteine-rich protein that promotes a broad range of cellular response including proliferation, chemotaxis, adhesion, migration, and extracellular matrix (ECM) production (Brigstock, 1999). Accumulated evidence has suggested that the alteration of CTGF expression might be regulated by the oxidative stress. In 2004, McCarthy reported that CTGF mRNA expression decreased after 24 h of hypoxia, whereas reoxygenation led to its prompt upregulation. The upregulation of CTGF was detected after oxidative stress exposure from paraquat (Matsuda *et al.*, 2006; McCarthy *et al.*, 2004). CTGF has been reported to participate in the induction of apoptosis and activation of caspase-3 activity (Hishikawa *et al.*, 1999). Even though the detail of mechanisms and the exact functions of these genes involved in the above processes are not clear, they may act in a coordinated manner to initiate and propagate apoptotic cell death which may lead the enhancement of toxic effect observed in cells co-exposed to MeHg and L-Glu. Consistent with the screening results of the microarray analysis in the present study, co-treatment of MeHg and L-Glu prominently induced cell death which accompanied by the loss of mitochondrial transmembrane potential, externalized phosphatidylserine, and the activation of caspase-3 activity.

## **2.1 L-Glu induced the increment of reactive oxygen species production by MeHg**

Oxidative stress has been implicated as an important mediator of apoptosis. Alteration in intracellular redox status as well as the generation of reactive oxygen species (ROS) have been shown to induce pathological processes, including apoptotic by many diverse cytotoxic stimuli (Gorman *et al.*, 1997; McGowan *et al.*, 1996). The deleterious effect of ROS is the activation of intracellular cascades at different phases of the apoptotic pathway, such as the induction of mitochondrial permeability transition and release of mitochondrial death amplification factors. Activation of intracellular caspase, and DNA damage has been also reported (Inoue *et al.*, 2004; Le Bras *et al.*, 2005). Many studies have shown that ROS acts as a potent mediator for cascade activation during MeHg toxicity (Ali *et al.*, 1992; Mundy & Freudenrich, 2000; Shanker & Aschner, 2003). For example, MeHg induced ROS production in cultured neurons (Mundy & Freudenrich, 2000), glial cell (Shanker & Aschner, 2003) as well as cerebellum synaptosome from MeHg treated rat and mice (LeBel *et al.*, 1990). In this study, it was evident that MeHg alone decreased cell viability at higher concentrations with long exposure time. This effect was accompanied by the increases in ROS and the decrease in GSH. Interestingly, we observed that L-Glu greatly increased MeHg-induced apoptotic cell death. It was mediated by the induction of oxidative stress process by which L-Glu dramatically enhanced the MeHg-induced ROS production and decreased GSH level (Figures 12 and 13). In addition, *N*-acetylcysteine (NAC) which is a known source of thiol groups and scavenger of free radicals such as  $\text{H}_2\text{O}_2$  and  $\cdot\text{OH}$  (Aruoma *et al.*, 1989) protected the enhancing toxic effect of L-Glu. It was suggested that the induction of oxidative stress underlies the enhanced cytotoxicity of Glu in MeHg co-treatment (Figure 14).

## **2.2 L-Glu enhanced the depletion of antioxidant glutathione (GSH) by MeHg**

GSH, the most abundant intracellular non-protein thiol, which plays an important role in maintaining cellular redox status, detoxifying sulfhydryl-reactive substances, and protecting cell against oxidative stress (Meister, 1995). Its depletion leads to accumulation of ROS within the cell (Choi *et al.*, 1996; Sarafian & Verity,

1991). Due to its extremely high affinity for thiol groups, MeHg binds to GSH leading to GSH depletion and exposing the cells to free-radical mediated damage (Gatti *et al.*, 2004; Yee & Choi, 1994). When GSH is reduced to approximately 20 to 30% of normal levels, the cell's ability to defend against oxidative damage is impaired, and this may eventually lead to cell injury and death (Reed, 1990). However, according to the present study of the level of GSH was transiently increased in cell co-exposed to MeHg plus L-Glu at 6 h of exposure, then significantly and dramatically decreased at 12 h by about 50% compared to MeHg alone. The upregulation of GSH synthesis as a transient adaptive response process of cells against the oxidative damage in mammalian cells and tissues have been described (Godwin *et al.*, 1992; Tian *et al.*, 1997; Woods & Ellis, 1995). Although, the elevated GSH levels occurred at 6 h but they failed to overcome the accumulation of ROS when cells were co-exposed to MeHg and L-Glu for 12 h (Figures 13 and 12). The increase in GSH at low or non-toxic dose and the decrease level at high or toxic dose after MeHg exposure were demonstrated by Zalups (2000) (Zalups, 2000). However, this adaptation might not be sufficient to overcome the oxidative stress insult from co-treatment of MeHg and L-Glu which ultimately lead to cell death by apoptosis. The decreased GSH levels at 12 h was accompanied by the increased oxidative stress measured by an increase in the level of ROS. All these data equivocally suggested to the GSH depletion in associated with the oxidative stress, which directly contributed to the enhancing effect of L-Glu on the MeHg-induced apoptotic cell death.

A number of detail mechanisms of L-Glu involved in the MeHg toxicity could be proposed. Firstly, MeHg may inhibit cellular L-Glu uptake by inhibiting glutamate transporters, which then elevates extracellular L-Glu concentration and induces cell death caused by overstimulation of glutamate receptors (excitotoxicity) (Aschner *et al.*, 2000; Juarez *et al.*, 2002). Secondly, MeHg may selectively inhibits the uptake systems for cystine and cysteine (Allen *et al.*, 2001; Shanker *et al.*, 2001) which is essential for glutathione (GSH) synthesis. It would ultimately increase the susceptibility of cells to ROS produced by the stimulation of glutamate receptor (Choi *et al.*, 1996). According to these two proposed mechanisms, neuronal cell death is caused by the excitotoxicity. In contrast, the third mechanism involves the oxidative

glutamate toxicity. The elevated extracellular L-Glu causes prolonged cell death due to a sustained oxidative stress resulting from the inhibition of amino acid transport system  $x^-_C$  and leading to a decrease in GSH synthesis (Lewerenz *et al.*, 2006; Tan *et al.*, 2001).

### 3. Role of the $x^-_C$ transport system on the enhancing toxic effect of L-Glu

The transport system  $x^-_C$  is the  $Na^+$ -independent transporter system, which is identified as the heterodimeric protein composed of a catalytic unit xCT and an accessory unit 4F2hc (Kanai & Endou, 2001; Verrey *et al.*, 2004). We showed that mRNA of xCT was present in the untreated control cells and increased after exposure to MeHg and MeHg plus L-Glu for 6 and 12 h. The xCT mRNA was also found to be upregulated by exposure to MeHg alone or co-exposure of MeHg and L-Glu for 12 h. Various stress stimuli including diethyl maleate (DEM) and  $H_2O_2$  (Sasaki *et al.*, 2002), oxygen (Sato *et al.*, 2001), lipopolysaccharide (LPS) (Sato *et al.*, 1995) as well as nitric oxide donor (Bridges *et al.*, 2001) have been reported to promote the upregulation of xCT expression. It is likely that cells compensated the loss of GSH by the induction of xCT expression. In addition, the increment of xCT expression in our study further confirmed that oxidative stress was the process underlying the enhancing toxic effect of L-Glu. Because the transport activity of system  $x^-_C$  is thought to be mediated by the light chain subunit (xCT) (Sato *et al.*, 1999), we examined the transport activity of system  $x^-_C$  after exposure to MeHg and/or L-Glu.

Several earlier reports have also shown that excitotoxicity-independent pathway which involves the induction of oxidative stress also plays a role in glutamate-induced cell death (Froissard *et al.*, 1997; Han *et al.*, 1997; Pereira & Oliveira, 1997). One of the underlying processes is the inhibition of cystine/glutamate transporter ( $x^-_C$ ), which results in glutathione depletion and cell death (Murphy *et al.*, 1990). System  $x^-_C$  is the cystine/glutamate exchanger that mediates the cellular uptake of cystine in exchange for L-Glu (Bannai, 1986; Christensen, 1990). Because the cytoplasm contains high concentration of L-Glu, cystine uptake by system  $x^-_C$  is driven by outwardly directed electrochemical gradient of L-Glu via the exchange mechanism. Cystine uptake by system  $x^-_C$  is, however, inhibited by L-Glu in a competitive manner, if L-Glu exists at high concentration at the *cis*-side (Christensen,

1990). The binding site of system  $x_C^-$  accepts cystine and L-form of acidic amino acids with longer side chains such as L-Glu and L-AAD, whereas acidic amino acids with shorter side chains such as L-Asp do not interact with system  $x_C^-$  (Kanai & Endou, 2001, 2003). In the present study, L-Glu and L-AAD were found to be effective, whereas D-Glu, L-Asp and D-Asp were not effective in enhancing MeHg cytotoxicity (Figure 4). In addition, cystine uptake of both untreated cells and cells treated with MeHg and/or L-Glu was strongly inhibited by L-Glu and L-AAD but not by L-Asp, suggesting that the background and the induced cystine uptake of HeLa S3 cells were mainly due to system  $x_C^-$  (Kanai & Endou, 2001, 2003). The property of cystine uptake of untreated HeLa cells was consistent with that of system xCT in its sensitivity to inhibitors. The xCT mRNA was upregulated by MeHg, and MeHg plus L-Glu (Figure 15). Cystine uptake was increased slightly by L-Glu or MeHg but largely augmented by the treatment of MeHg plus L-Glu. Cysteine is required for GSH synthesis. It is oxidized to cystine in the extracellular environment. The system  $x_C^-$  is important to provide cells with cystine (as cystine for GSH synthesis). Thus, the sustained inhibition of system  $x_C^-$  by L-Glu makes the cells liable to the accumulation of ROS and ultimately leads to cell death by oxidative stress. Cells usually respond to the oxidative glutamate toxicity by enhancing apoptosis (Lewerenz *et al.*, 2006; Tan *et al.*, 2001). Consistent with this, we observed that L-Glu greatly enhanced MeHg-induced apoptosis as monitored by the alteration of mitochondrial membrane potential, externalized phosphatidylserine and activated caspase-3 activity. Although the baseline system  $x_C^-$  activity of HeLa S3 cells is proposed to be inhibited by L-Glu (10 mM) in this study (Figure 17), L-Glu (10 mM) alone did not reduce GSH level (Figure 13). In the absence of MeHg, the GSH level can probably be maintained in the normal range even in the suppression of baseline system  $x_C^-$  activity through the supply of intracellular cystine via the other. Our result showed that no significant effect was detected for L-Glu alone on the ROS level and the GSH level. Because the adequate transport cystine into the cells is essential for the maintenance of intracellular cysteine levels and it is thought to be a rate limiting step process in GSH synthesis (Bannai & Tateishi, 1986). The transcription of xCT gene and  $x_C^-$  transport activities are induced by oxidative stress. Therefore, it was anticipated that besides transport of cystine via system  $x_C^-$  in the non-oxidative stress condition like L-Glu treatment, there

are other transport processes responsible for carrying the substrate for GSH synthesis. Cysteine may be directly transported into the cell by the  $\text{Na}^+$ -dependent (the ASC system and  $\text{X}_{\text{AG-}}$ ) (Knickelbein *et al.*, 1997) and  $\text{Na}^+$ -independent amino acid transport system (multifunctional ectoenzyme/amino acid transporter (GGT), and neutral amino acid L-system (Shanker & Aschner, 2001). However, the relative importance of each transporter system for cysteine and cystine may vary, depending on the extracellular redox status and the presence of certain amino acid. The present study also confirmed that L-Glu enhanced MeHg mediated by the oxidative glutamate toxicity because the agonists of glutamate receptors including kainic acid (KA),  $\alpha$ -amino-3-hydroxy-5-methyl-4-isoxazolepropionic acid (AMPA) and N-methyl-D-aspartate (NMDA) did not enhance MeHg toxicity at the concentrations of 10-100  $\mu\text{M}$  at which is supposed to fully activate non-NMDA and NMDA receptors (Sinor *et al.*, 2000; Verdaguer *et al.*, 2002). It is, thus, proposed that the enhancing effect of L-Glu to MeHg cytotoxicity observed in the present study was involved in the inhibition of system  $\text{x}_\text{C}^-$  by L-Glu. Although the profiles of mRNA was not high as the observed activity of cystine uptake, the upregulation of xCT activity essentially confirmed the contribution of oxidative stress in the phenomena observed in this study. The inhibitory effect of L-Glu on cystine transport together with the ROS production by MeHg concurrently caused the greater toxic effect to the cell, ultimately cell death.

In the present study, 8  $\mu\text{M}$  of MeHg exhibited minimal effects on HeLa cell viability. However, MeHg (8  $\mu\text{M}$ ) alone still slightly increased apoptosis and ROS level, and decreased GSH level at 12 h, confirming the oxidative stress induced by MeHg itself. This is consistent with the increase in xCT expression induced by MeHg alone. L-Glu (10 mM) alone did not show significant effect on most of parameters examined in this study. Interestingly, MeHg toxic effect was highly enhanced by 10 mM L-Glu. Therefore, the enhancement of toxicity by co-treatment with MeHg and L-Glu observed in this study was highly synergistic. Although the molecular mechanisms or specific contributions of this synergistic nature are not understood at this moment, it is possible that some other additional cellular events driven by L-Glu and MeHg could also contribute. These roles are needed to be elucidated in the future.

Although in this study, the non-neuronal cells were mainly used to characterize synergistic toxicity of MeHg and L-Glu, it was confirmed in neural cells

(neuroblastoma cell lines). Our results may be applicable to the toxicity of neurons in certain regions of brain tissues. One of the unsolved mysteries of MeHg neurotoxicity is the locality of the lesion. Discrete anatomical areas of the brain, such as visual cortex, other sensory cortex and the granule layers of the cerebellum have been reported to be highly prone to the damage by MeHg (Nagashima, 1997). These brain areas are proposed to be highly active in processing sensory signals and other neural signals. It is possible that the neurons in these areas could be exposed more to excitatory neurotransmitter L-Glu compared to other parts of the brain. Whether the enhancement of MeHg toxicity observed in this study is involved in the mechanisms of locality of MeHg lesion would be an interesting issue to be examined in the future.

In conclusion, we demonstrated that L-Glu enhanced MeHg toxicity by increasing the elevation of oxidative stress and inducing apoptotic cell death, which were resulted from the inhibition of system  $x_C^-$ . In addition, the present study provided a clue how to ameliorate MeHg toxicity on neural cells. To prevent more toxic effect from MeHg, we should avoid over exposure to extracellular glutamate. Second, the protective effect of NAC antioxidant therapy can be a one candidate for treatment of MeHg toxicity.



## CHAPTER VI

### CONCLUSION

The present study demonstrated that L-Glu specifically and greatly enhanced MeHg toxicity by the synergistic effect. The mechanism underlying the enhancing toxic effect of L-Glu was the increase in oxidative stress that induces apoptotic cell death probably due to the inhibition of cystine transport via system  $x_c^-$ .

1. HeLa S3 cells were relatively resistant to MeHg-induced toxicity. Treatment with MeHg alone exhibited slight cytotoxic to HeLa S3 cell. Only MeHg at very high concentration and long time could induce the cytotoxicity to HeLa S3 cells.
2. Co-treatment of MeHg (8  $\mu$ M) and L-Glu (10 mM) markedly decreased the viability of cells when compared to treatment with MeHg alone. The severity of toxicity was dependent on the concentration of L-Glu (1-10 mM). No toxic effect was observed in cell treated with L-Glu alone.
3. Among 20 naturally occurring L-amino acids, only L-Glu significantly decreased the viability of cells in the presence of MeHg. The specific toxic effect of L-Glu was further confirmed. Cells were co-treated with MeHg plus Glu-related acidic amino acids (D-Glu, L- and D-Asp and L-AAD), the result showed that L-AAD also enhanced MeHg toxicity as effective as that of L-Glu.
4. Co-treatment of MeHg and L-Glu was able to exert its effect on gene expression profile. Total of 71, 1490 and 401 genes were altered at least 2 folds, either up- or down-regulation as compared to MeHg alone at 3, 6, and 12 h of exposure, respectively.
5. Most of up-regulated genes were found at the early time point of exposure (3 h), and then the number of genes were declined at 6 and 12 h of exposure. Using the Gene Ontology (GO) analysis, the up-regulated gene at 3 h were classified into six functional groups, two of them are expected to be the process-related enhancing toxic effects of L-Glu including the stress-response and apoptotic-related process.

6. L-Glu-enhanced MeHg toxicity occurred via the induction of apoptotic cell death as accompanied by the loss of mitochondrial membrane potential ( $\Delta\Psi_m$ ), induction of phosphatidylserine (PS) externalization, and activation of caspase-3 activity.
7. Oxidative stress process was involved in the enhancing toxic effect of L-Glu on MeHg as indicated by the elevation of reactive oxygen species (ROS) level, depletion of reduced glutathione (GSH) as well as pretreatment with N-acetylcysteine (NAC) could prevent the cytotoxicity.
8. Expression of xCT mRNA in HeLa S3 cells was increased in a time-dependent manner after cells were treated with MeHg and MeHg plus L-Glu. Treatment with L-Glu alone tended to increase the xCT expression, however, though no statistically significant increase as compared to the untreated control.
9. Consistent with the expression of xCT mRNA, untreated HeLa S3 cells also exhibited x<sub>C</sub><sup>-</sup> transport system because the uptake of [<sup>14</sup>C]L-cystine was inhibited by the competitive inhibitor of x<sub>C</sub><sup>-</sup> transport system including L-cystine (L-Cyst.), L-glutamate (L-Glu), L- $\alpha$ -aminoadipate (L-AAD), but not by L-Asp. Moreover, x<sub>C</sub><sup>-</sup> transport activity was slightly increased in MeHg treatment and greatly increased when co-treatment with MeHg plus L-Glu.
10. Agonists of glutamate receptors including (NMDA, KA, and AMPA) did not enhance MeHg toxicity. The results implied that the enhancing toxic effect of L-Glu occurred via oxidative glutamate toxicity by inhibition of x<sub>C</sub><sup>-</sup> activity but not by the glutamate-receptor excitotoxicity.
11. Neuroblastoma cell lines had higher susceptibility to MeHg toxicity than HeLa S3 cell. Co-exposure to L-Glu significantly increased MeHg toxicity whereas L-Glu alone did not significantly affect the viability of all neuroblastoma cells.

## REFERENCES

- Alexander, J., & Aaseth, J. (1982). Organ distribution and cellular uptake of methyl mercury in the rat as influenced by the intra- and extracellular glutathione concentration. *Biochem Pharmacol*, 31(5), 685-690.
- Ali, S. F., LeBel, C. P., & Bondy, S. C. (1992). Reactive oxygen species formation as a biomarker of methylmercury and trimethyltin neurotoxicity. *Neurotoxicology*, 13(3), 637-648.
- Allen, J. W., Mutkus, L. A., & Aschner, M. (2001). Methylmercury-mediated inhibition of 3H-D-aspartate transport in cultured astrocytes is reversed by the antioxidant catalase. *Brain Res*, 902(1), 92-100.
- Alnemri, E. S., Livingston, D. J., Nicholson, D. W., Salvesen, G., Thornberry, N. A., Wong, W. W., et al. (1996). Human ICE/CED-3 protease nomenclature. *Cell*, 87(2), 171.
- Anuradha, B., & Varalakshmi, P. (1999). Protective role of DL-alpha-lipoic acid against mercury-induced neural lipid peroxidation. *Pharmacol Res*, 39(1), 67-80.
- Aruoma, O. I., Halliwell, B., Hoey, B. M., & Butler, J. (1989). The antioxidant action of N-acetylcysteine: its reaction with hydrogen peroxide, hydroxyl radical, superoxide, and hypochlorous acid. *Free Radic Biol Med*, 6(6), 593-597.
- Aschner, M., & Aschner, J. L. (1990). Mercury neurotoxicity: mechanisms of blood-brain barrier transport. *Neurosci Biobehav Rev*, 14(2), 169-176.
- Aschner, M., Yao, C. P., Allen, J. W., & Tan, K. H. (2000). Methylmercury alters glutamate transport in astrocytes. *Neurochem Int*, 37(2-3), 199-206.
- Atlante, A., Calissano, P., Bobba, A., Giannattasio, S., Marra, E., & Passarella, S. (2001). Glutamate neurotoxicity, oxidative stress and mitochondria. *FEBS Lett*, 497(1), 1-5.
- Bakir, F., Damluji, S. F., Amin-Zaki, L., Murtadha, M., Khalidi, A., al-Rawi, N. Y., et al. (1973). Methylmercury poisoning in Iraq. *Science*, 181(96), 230-241.
- Bannai, S. (1984). Transport of cystine and cysteine in mammalian cells. *Biochim Biophys Acta*, 779(3), 289-306.

- Bannai, S. (1986). Exchange of cystine and glutamate across plasma membrane of human fibroblasts. *J Biol Chem*, 261(5), 2256-2263.
- Bannai, S., Sato, H., Ishii, T., & Sugita, Y. (1989). Induction of cystine transport activity in human fibroblasts by oxygen. *J Biol Chem*, 264(31), 18480-18484.
- Bannai, S., & Tateishi, N. (1986). Role of membrane transport in metabolism and function of glutathione in mammals. *J Membr Biol*, 89(1), 1-8.
- Beal, M. F., Ferrante, R. J., Henshaw, R., Matthews, R. T., Chan, P. H., Kowall, N. W., et al. (1995). 3-Nitropropionic acid neurotoxicity is attenuated in copper/zinc superoxide dismutase transgenic mice. *J Neurochem*, 65(2), 919-922.
- Beissbarth, T., & Speed, T. P. (2004). GStat: find statistically overrepresented Gene Ontologies within a group of genes. *Bioinformatics*, 20(9), 1464-1465.
- Belletti, S., Orlandini, G., Vettori, M. V., Mutti, A., Uggeri, J., Scandroglio, R., et al. (2002). Time course assessment of methylmercury effects on C6 glioma cells: submicromolar concentrations induce oxidative DNA damage and apoptosis. *J Neurosci Res*, 70(5), 703-711.
- Bender, A. S., Reichelt, W., & Norenberg, M. D. (2000). Characterization of cystine uptake in cultured astrocytes. *Neurochem Int*, 37(2-3), 269-276.
- Bernardi, P., Scorrano, L., Colonna, R., Petronilli, V., & Di Lisa, F. (1999). Mitochondria and cell death. Mechanistic aspects and methodological issues. *Eur J Biochem*, 264(3), 687-701.
- Bernardi, P., Veronese, P., & Petronilli, V. (1993). Modulation of the mitochondrial cyclosporin A-sensitive permeability transition pore. I. Evidence for two separate  $\text{Me}_2^+$  binding sites with opposing effects on the pore open probability. *J Biol Chem*, 268(2), 1005-1010.
- Berridge, M. J., Lipp, P., & Bootman, M. D. (2000). The versatility and universality of calcium signalling. *Nat Rev Mol Cell Biol*, 1(1), 11-21.
- Bertran, J., Werner, A., Moore, M. L., Stange, G., Markovich, D., Biber, J., et al. (1992). Expression cloning of a cDNA from rabbit kidney cortex that induces a single transport system for cystine and dibasic and neutral amino acids. *Proc Natl Acad Sci U S A*, 89(12), 5601-5605.

- Bortner, C. D., Oldenburg, N. B., & Cidlowski, J. A. (1995). The role of DNA fragmentation in apoptosis. *Trends Cell Biol*, 5(1), 21-26.
- Bossy-Wetzel, E., & Green, D. R. (1999). Apoptosis: checkpoint at the mitochondrial frontier. *Mutat Res*, 434(3), 243-251.
- Bratton, D. L., Fadok, V. A., Richter, D. A., Kailey, J. M., Guthrie, L. A., & Henson, P. M. (1997). Appearance of phosphatidylserine on apoptotic cells requires calcium-mediated nonspecific flip-flop and is enhanced by loss of the aminophospholipid translocase. *J Biol Chem*, 272(42), 26159-26165.
- Bratton, S. B., Walker, G., Srinivasula, S. M., Sun, X. M., Butterworth, M., Alnemri, E. S., et al. (2001). Recruitment, activation and retention of caspases-9 and -3 by Apaf-1 apoptosome and associated XIAP complexes. *EMBO J*, 20(5), 998-1009.
- Brice, N. L., Varadi, A., Ashcroft, S. J., & Molnar, E. (2002). Metabotropic glutamate and GABA(B) receptors contribute to the modulation of glucose-stimulated insulin secretion in pancreatic beta cells. *Diabetologia*, 45(2), 242-252.
- Bridges, C. C., Kekuda, R., Wang, H., Prasad, P. D., Mehta, P., Huang, W., et al. (2001). Structure, function, and regulation of human cystine/glutamate transporter in retinal pigment epithelial cells. *Invest Ophthalmol Vis Sci*, 42(1), 47-54.
- Brigstock, D. R. (1999). The connective tissue growth factor/cysteine-rich 61/nephroblastoma overexpressed (CCN) family. *Endocr Rev*, 20(2), 189-206.
- Brosnan, J. T., Man, K. C., Hall, D. E., Colbourne, S. A., & Brosnan, M. E. (1983). Interorgan metabolism of amino acids in streptozotocin-diabetic ketoacidotic rat. *Am J Physiol*, 244(2), E151-158.
- Cain, K., Bratton, S. B., Langlais, C., Walker, G., Brown, D. G., Sun, X. M., et al. (2000). Apaf-1 oligomerizes into biologically active approximately 700-kDa and inactive approximately 1.4-MDa apoptosome complexes. *J Biol Chem*, 275(9), 6067-6070.
- Carty, A.J., Malone, S.F., The chemistry of mercury in biological systems. In: Nriagu JO, editor. *The Biogeochemistry of Mercury in Environment*. Amsterdam: Elsevier/North-Holland Biomedical Press; 1979. p. 433-70.
- Castoldi, A. F., Coccini, T., Ceccatelli, S., & Manzo, L. (2001). Neurotoxicity and

- molecular effects of methylmercury. *Brain Res Bull*, 55(2), 197-203.
- Chenu, C., Serre, C. M., Raynal, C., Burt-Pichat, B., & Delmas, P. D. (1998). Glutamate receptors are expressed by bone cells and are involved in bone resorption. *Bone*, 22(4), 295-299.
- Choi, B. H., Yee, S., & Robles, M. (1996). The effects of glutathione glycoside in methyl mercury poisoning. *Toxicol Appl Pharmacol*, 141(2), 357-364.
- Choi, D. W. (1988). Glutamate neurotoxicity and diseases of the nervous system. *Neuron*, 1(8), 623-634.
- Choi, D. W. (1992). Excitotoxic cell death. *J Neurobiol*, 23(9), 1261-1276.
- Christensen, H. N. (1990). Role of amino acid transport and countertransport in nutrition and metabolism. *Physiol Rev*, 70(1), 43-77.
- Clarkson, T. W. (1972). The pharmacology of mercury compounds. *Annu Rev Pharmacol*, 12, 375-406.
- Clarkson, T. W. (2002). The three modern faces of mercury. *Environ Health Perspect*, 110 Suppl 1, 11-23.
- Clarkson, T. W., & Magos, L. (2006). The toxicology of mercury and its chemical compounds. *Crit Rev Toxicol*, 36(8), 609-662.
- Clarkson, T. W., Magos, L., & Myers, G. J. (2003). The toxicology of mercury--current exposures and clinical manifestations. *N Engl J Med*, 349(18), 1731-1737.
- Cohen, G. M. (1997). Caspases: the executioners of apoptosis. *Biochem J*, 326 ( Pt 1), 1-16.
- Cory, S., & Adams, J. M. (2002). The Bcl2 family: regulators of the cellular life-or-death switch. *Nat Rev Cancer*, 2(9), 647-656.
- Cowling, V., & Downward, J. (2002). Caspase-6 is the direct activator of caspase-8 in the cytochrome c-induced apoptosis pathway: absolute requirement for removal of caspase-6 prodomain. *Cell Death Differ*, 9(10), 1046-1056.
- Crespo-Lopez, M. E., Lima de Sa, A., Herculano, A. M., Rodriguez Burbano, R., & Martins do Nascimento, J. L. (2007). Methylmercury genotoxicity: a novel effect in human cell lines of the central nervous system. *Environ Int*, 33(2), 141-146.
- Danbolt, N. C. (2001). Glutamate uptake. *Prog Neurobiol*, 65(1), 1-105.

- Debes, F., Budtz-Jorgensen, E., Weihe, P., White, R. F., & Grandjean, P. (2006). Impact of prenatal methylmercury exposure on neurobehavioral function at age 14 years. *Neurotoxicol Teratol*, 28(5), 536-547.
- Degterev, A., Boyce, M., & Yuan, J. (2003). A decade of caspases. *Oncogene*, 22(53), 8543-8567.
- Denny, M. F., Hare, M. F., & Atchison, W. D. (1993). Methylmercury alters intrasynaptosomal concentrations of endogenous polyvalent cations. *Toxicol Appl Pharmacol*, 122(2), 222-232.
- Desagher, S., Osen-Sand, A., Nichols, A., Eskes, R., Montessuit, S., Lauper, S., et al. (1999). Bid-induced conformational change of Bax is responsible for mitochondrial cytochrome c release during apoptosis. *J Cell Biol*, 144(5), 891-901.
- Dong, Z., Saikumar, P., Weinberg, J. M., & Venkatachalam, M. A. (2006). Calcium in cell injury and death. *Annu Rev Pathol*, 1, 405-434.
- Duchen, M. R. (2000). Mitochondria and  $\text{Ca}^{2+}$  in cell physiology and pathophysiology. *Cell Calcium*, 28(5-6), 339-348.
- Dugan, L. L., Sensi, S. L., Canzoniero, L. M., Handran, S. D., Rothman, S. M., Lin, T. S., et al. (1995). Mitochondrial production of reactive oxygen species in cortical neurons following exposure to N-methyl-D-aspartate. *J Neurosci*, 15(10), 6377-6388.
- Ermak, G., & Davies, K. J. (2002). Calcium and oxidative stress: from cell signaling to cell death. *Mol Immunol*, 38(10), 713-721.
- Eto, K. (1997). Pathology of Minamata disease. *Toxicol Pathol*, 25(6), 614-623.
- Eto, K., Oyanagi, S., Itai, Y., Tokunaga, H., Takizawa, Y., & Suda, I. (1992). A fetal type of Minamata disease. An autopsy case report with special reference to the nervous system. *Mol Chem Neuropathol*, 16(1-2), 171-186.
- Fabisiak, J. P., Tyurina, Y. Y., Tyurin, V. A., Lazo, J. S., & Kagan, V. E. (1998). Random versus selective membrane phospholipid oxidation in apoptosis: role of phosphatidylserine. *Biochemistry*, 37(39), 13781-13790.
- Fadok, V. A., Voelker, D. R., Campbell, P. A., Cohen, J. J., Bratton, D. L., & Henson, P. M. (1992). Exposure of phosphatidylserine on the surface of apoptotic

- lymphocytes triggers specific recognition and removal by macrophages. *J Immunol*, 148(7), 2207-2216.
- Fibach, E. (1998). Techniques for studying stimulation of fetal hemoglobin production in human erythroid cultures. *Hemoglobin*, 22(5-6), 445-458.
- Froissard, P., Monrocq, H., & Duval, D. (1997). Role of glutathione metabolism in the glutamate-induced programmed cell death of neuronal-like PC12 cells. *Eur J Pharmacol*, 326(1), 93-99.
- Fuchs, E., Kim, K. H., Hanukoglu, I., & Tanese, N. (1983). The evolution and complexity of the genes encoding the cytoskeletal proteins of human epidermal cells. *Curr Probl Dermatol*, 11, 27-44.
- Fujiyama, J., Hirayama, K., & Yasutake, A. (1994). Mechanism of methylmercury efflux from cultured astrocytes. *Biochem Pharmacol*, 47(9), 1525-1530.
- Gabai, V. L., Meriin, A. B., Mosser, D. D., Caron, A. W., Rits, S., Shifrin, V. I., et al. (1997). Hsp70 prevents activation of stress kinases. A novel pathway of cellular thermotolerance. *J Biol Chem*, 272(29), 18033-18037.
- Ganther, H. E. (1978). Modification of methylmercury toxicity and metabolism by selenium and vitamin E: possible mechanisms. *Environ Health Perspect*, 25, 71-76.
- Gasso, S., Cristofol, R. M., Selema, G., Rosa, R., Rodriguez-Farre, E., & Sanfeliu, C. (2001). Antioxidant compounds and Ca(2+) pathway blockers differentially protect against methylmercury and mercuric chloride neurotoxicity. *J Neurosci Res*, 66(1), 135-145.
- Gatti, R., Belletti, S., Uggeri, J., Vettori, M. V., Mutti, A., Scandroglio, R., et al. (2004). Methylmercury cytotoxicity in PC12 cells is mediated by primary glutathione depletion independent of excess reactive oxygen species generation. *Toxicology*, 204(2-3), 175-185.
- Gerhardsson L., Skerfving S. Concepts on biological markers and biomonitoring for metal toxicity. In: Chang WL, Magos L, Suzuki T, editors. Toxicology of metals. Florida: CRC Lewis; 1996. p. 95-96.
- Gill, S. S., & Pulido, O. M. (2001). Glutamate receptors in peripheral tissues: current knowledge, future research, and implications for toxicology. *Toxicol Pathol*, 29(2), 208-223.



- Godwin, A. K., Meister, A., O'Dwyer, P. J., Huang, C. S., Hamilton, T. C., & Anderson, M. E. (1992). High resistance to cisplatin in human ovarian cancer cell lines is associated with marked increase of glutathione synthesis. *Proc Natl Acad Sci U S A*, 89(7), 3070-3074.
- Golstein, P. (1997). Controlling cell death. *Science*, 275(5303), 1081-1082.
- Gonoi, T., Mizuno, N., Inagaki, N., Kuromi, H., Seino, Y., Miyazaki, J., et al. (1994). Functional neuronal ionotropic glutamate receptors are expressed in the non-neuronal cell line MIN6. *J Biol Chem*, 269(25), 16989-16992.
- Gorman, A., McGowan, A., & Cotter, T. G. (1997). Role of peroxide and superoxide anion during tumour cell apoptosis. *FEBS Lett*, 404(1), 27-33.
- Gunter, K. K., & Gunter, T. E. (1994). Transport of calcium by mitochondria. *J Bioenerg Biomembr*, 26(5), 471-485.
- Han, D., Sen, C. K., Roy, S., Kobayashi, M. S., Tritschler, H. J., & Packer, L. (1997). Protection against glutamate-induced cytotoxicity in C6 glial cells by thiol antioxidants. *Am J Physiol*, 273(5 Pt 2), R1771-1778.
- Hanley, D. F., & Varelas, P. (1999). Glutamate in parenteral nutrition. *Crit Care Med*, 27(10), 2319-2320.
- Harada, M. (1995). Minamata disease: methylmercury poisoning in Japan caused by environmental pollution. *Crit Rev Toxicol*, 25(1), 1-24.
- Hengartner, M. O. (2000). The biochemistry of apoptosis. *Nature*, 407(6805), 770-776.
- Hinoi, E., Takarada, T., Ueshima, T., Tsuchihashi, Y., & Yoneda, Y. (2004). Glutamate signaling in peripheral tissues. *Eur J Biochem*, 271(1), 1-13.
- Hishikawa, K., Nakaki, T., & Fujii, T. (1999). Transforming growth factor-beta(1) induces apoptosis via connective tissue growth factor in human aortic smooth muscle cells. *Eur J Pharmacol*, 385(2-3), 287-290.
- Hollmann, M., O'Shea-Greenfield, A., Rogers, S. W., & Heinemann, S. (1989). Cloning by functional expression of a member of the glutamate receptor family. *Nature*, 342(6250), 643-648.
- Hosoya, K., Tomi, M., Ohtsuki, S., Takanaga, H., Saeki, S., Kanai, Y., et al. (2002). Enhancement of L-cystine transport activity and its relation to xCT gene induction at the blood-brain barrier by diethyl maleate treatment. *J Pharmacol*

*Exp Ther*, 302(1), 225-231.

- Howell, J. A., Matthews, A. D., Swanson, K. C., Harmon, D. L., & Matthews, J. C. (2001). Molecular identification of high-affinity glutamate transporters in sheep and cattle forestomach, intestine, liver, kidney, and pancreas. *J Anim Sci*, 79(5), 1329-1336.
- Hughes, W.L. (1957). A physicochemical rationale for the biological activity of mercury and its compounds. *Ann N Y Acad Sci*, 65(5), 454-460.
- Igney, F. H., & Krammer, P. H. (2002). Death and anti-death: tumour resistance to apoptosis. *Nat Rev Cancer*, 2(4), 277-288.
- Inoue, M., Sato, E. F., Nishikawa, M., Hiramoto, K., Kashiwagi, A., & Utsumi, K. (2004). Free radical theory of apoptosis and metamorphosis. *Redox Rep*, 9(5), 237-247.
- InSug, O., Datar, S., Koch, C. J., Shapiro, I. M., & Shenker, B. J. (1997). Mercuric compounds inhibit human monocyte function by inducing apoptosis: evidence for formation of reactive oxygen species, development of mitochondrial membrane permeability transition and loss of reductive reserve. *Toxicology*, 124(3), 211-224.
- Ishii, T., Nakayama, K., Sato, H., Miura, K., Yamada, M., Yamada, K., et al. (1991). Expression of the mouse macrophage cystine transporter in *Xenopus laevis* oocytes. *Arch Biochem Biophys*, 289(1), 71-75.
- Juarez, B. I., Martinez, M. L., Montante, M., Dufour, L., Garcia, E., & Jimenez-Capdeville, M. E. (2002). Methylmercury increases glutamate extracellular levels in frontal cortex of awake rats. *Neurotoxicol Teratol*, 24(6), 767-771.
- Kanai, Y., & Endou, H. (2001). Heterodimeric amino acid transporters: molecular biology and pathological and pharmacological relevance. *Curr Drug Metab*, 2(4), 339-354.
- Kanai, Y., & Endou, H. (2003). Functional properties of multispecific amino acid transporters and their implications to transporter-mediated toxicity. *J Toxicol Sci*, 28(1), 1-17.
- Kanai, Y., & Hediger, M. A. (1992). Primary structure and functional characterization of a high-affinity glutamate transporter. *Nature*, 360(6403), 467-471.
- Kao, C. H., Kao, T. Y., Huang, W. T., & Lin, M. T. (2007). Lipopolysaccharide- and

- glutamate-induced hypothalamic hydroxyl radical elevation and fever can be suppressed by N-methyl-D-aspartate-receptor antagonists. *J Pharmacol Sci*, 104(2), 130-136.
- Kato, S., Ishita, S., Sugawara, K., & Mawatari, K. (1993). Cystine/glutamate antiporter expression in retinal Muller glial cells: implications for DL-alpha-amino adipate toxicity. *Neuroscience*, 57(2), 473-482.
- Kaur, P., Aschner, M., & Syversen, T. (2007). Role of glutathione in determining the differential sensitivity between the cortical and cerebellar regions towards mercury-induced oxidative stress. *Toxicology*, 230(2-3), 164-177.
- Kershaw, T. G., Clarkson, T. W., & Dhahir, P. H. (1980). The relationship between blood levels and dose of methylmercury in man. *Arch Environ Health*, 35(1), 28-36.
- Kim, J. Y., Kanai, Y., Chairoungdua, A., Cha, S. H., Matsuo, H., Kim, D. K., et al. (2001). Human cystine/glutamate transporter: cDNA cloning and upregulation by oxidative stress in glioma cells. *Biochim Biophys Acta*, 1512(2), 335-344.
- Knickelbein, R. G., Seres, T., Lam, G., Johnston, R. B., Jr., & Warshaw, J. B. (1997). Characterization of multiple cysteine and cystine transporters in rat alveolar type II cells. *Am J Physiol*, 273(6 Pt 1), L1147-1155.
- Kroemer, G., & Reed, J. C. (2000). Mitochondrial control of cell death. *Nat Med*, 6(5), 513-519.
- Kroemer, G., Zamzami, N., & Susin, S. A. (1997). Mitochondrial control of apoptosis. *Immunol Today*, 18(1), 44-51.
- Le Bras, M., Clement, M. V., Pervaiz, S., & Brenner, C. (2005). Reactive oxygen species and the mitochondrial signaling pathway of cell death. *Histol Histopathol*, 20(1), 205-219.
- LeBel, C. P., Ali, S. F., McKee, M., & Bondy, S. C. (1990). Organometal-induced increases in oxygen reactive species: the potential of 2',7'-dichlorofluorescein diacetate as an index of neurotoxic damage. *Toxicol Appl Pharmacol*, 104(1), 17-24.
- Leist, M., & Jaattela, M. (2001). Four deaths and a funeral: from caspases to alternative mechanisms. *Nat Rev Mol Cell Biol*, 2(8), 589-598.
- Levesque, P. C., & Atchison, W. D. (1991). Disruption of brain mitochondrial calcium

- sequestration by methylmercury. *J Pharmacol Exp Ther*, 256(1), 236-242.
- Lewerenz, J., Klein, M., & Methner, A. (2006). Cooperative action of glutamate transporters and cystine/glutamate antiporter system Xc<sup>-</sup> protects from oxidative glutamate toxicity. *J Neurochem*, 98(3), 916-925.
- Li, H., Marshall, Z. M., & Whorton, A. R. (1999). Stimulation of cystine uptake by nitric oxide: regulation of endothelial cell glutathione levels. *Am J Physiol*, 276(4 Pt 1), C803-811.
- Limke, T. L., & Atchison, W. D. (2002). Acute exposure to methylmercury opens the mitochondrial permeability transition pore in rat cerebellar granule cells. *Toxicol Appl Pharmacol*, 178(1), 52-61.
- Limke, T. L., Otero-Montanez, J. K., & Atchison, W. D. (2003). Evidence for interactions between intracellular calcium stores during methylmercury-induced intracellular calcium dysregulation in rat cerebellar granule neurons. *J Pharmacol Exp Ther*, 304(3), 949-958.
- Lipton, S. A., & Rosenberg, P. A. (1994). Excitatory amino acids as a final common pathway for neurologic disorders. *N Engl J Med*, 330(9), 613-622.
- Loeffler, M., & Kroemer, G. (2000). The mitochondrion in cell death control: certainties and incognita. *Exp Cell Res*, 256(1), 19-26.
- Lu, H. F., Sue, C. C., Yu, C. S., Chen, S. C., Chen, G. W., & Chung, J. G. (2004). Diallyl disulfide (DADS) induced apoptosis undergo caspase-3 activity in human bladder cancer T24 cells. *Food Chem Toxicol*, 42(10), 1543-1552.
- Lund, B. O., Miller, D. M., & Woods, J. S. (1993). Studies on Hg(II)-induced H<sub>2</sub>O<sub>2</sub> formation and oxidative stress in vivo and in vitro in rat kidney mitochondria. *Biochem Pharmacol*, 45(10), 2017-2024.
- Marchetti, P., Decaudin, D., Macho, A., Zamzami, N., Hirsch, T., Susin, S. A., et al. (1997). Redox regulation of apoptosis: impact of thiol oxidation status on mitochondrial function. *Eur J Immunol*, 27(1), 289-296.
- Martin, S. J., Reutelingsperger, C. P., McGahon, A. J., Rader, J. A., van Schie, R. C., LaFace, D. M., et al. (1995). Early redistribution of plasma membrane phosphatidylserine is a general feature of apoptosis regardless of the initiating stimulus: inhibition by overexpression of Bcl-2 and Abl. *J Exp Med*, 182(5), 1545-1556.

- Marty, M. S., & Atchison, W. D. (1997). Pathways mediating  $\text{Ca}^{2+}$  entry in rat cerebellar granule cells following in vitro exposure to methyl mercury. *Toxicol Appl Pharmacol*, 147(2), 319-330.
- Marty, M. S., & Atchison, W. D. (1998). Elevations of intracellular  $\text{Ca}^{2+}$  as a probable contributor to decreased viability in cerebellar granule cells following acute exposure to methylmercury. *Toxicol Appl Pharmacol*, 150(1), 98-105.
- Matsuda, S., Gomi, F., Katayama, T., Koyama, Y., Tohyama, M., & Tano, Y. (2006). Induction of connective tissue growth factor in retinal pigment epithelium cells by oxidative stress. *Jpn J Ophthalmol*, 50(3), 229-234.
- Matsuo, H., Kanai, Y., Kim, J. Y., Chairoungdua, A., Kim, D. K., Inatomi, J., et al. (2002). Identification of a novel  $\text{Na}^{+}$ -independent acidic amino acid transporter with structural similarity to the member of a heterodimeric amino acid transporter family associated with unknown heavy chains. *J Biol Chem*, 277(23), 21017-21026.
- McBean, G. J. (2002). Cerebral cystine uptake: a tale of two transporters. *Trends Pharmacol Sci*, 23(7), 299-302.
- McCarthy, S., Somayajulu, M., Sikorska, M., Borowy-Borowski, H., & Pandey, S. (2004). Paraquat induces oxidative stress and neuronal cell death; neuroprotection by water-soluble Coenzyme Q10. *Toxicol Appl Pharmacol*, 201(1), 21-31.
- McGowan, A. J., Ruiz-Ruiz, M. C., Gorman, A. M., Lopez-Rivas, A., & Cotter, T. G. (1996). Reactive oxygen intermediate(s) (ROI): common mediator(s) of poly(ADP-ribose)polymerase (PARP) cleavage and apoptosis. *FEBS Lett*, 392(3), 299-303.
- Meister, A. (1995). Glutathione metabolism. *Methods Enzymol*, 251, 3-7.
- Meldrum, B. S. (2000). Glutamate as a neurotransmitter in the brain: review of physiology and pathology. *J Nutr*, 130(4S Suppl), 1007S-1015S.
- Mori, N., Yasutake, A., & Hirayama, K. (2007). Comparative study of activities in reactive oxygen species production/defense system in mitochondria of rat brain and liver, and their susceptibility to methylmercury toxicity. *Arch Toxicol*, 81(11), 769-776.
- Morimoto, R. I., Sarge, K. D., & Abravaya, K. (1992). Transcriptional regulation of

- heat shock genes. A paradigm for inducible genomic responses. *J Biol Chem*, 267(31), 21987-21990.
- Mosser, D. D., Caron, A. W., Bourget, L., Denis-Larose, C., & Massie, B. (1997). Role of the human heat shock protein hsp70 in protection against stress-induced apoptosis. *Mol Cell Biol*, 17(9), 5317-5327.
- Mullaney, K. J., Fehm, M. N., Vitarella, D., Wagoner, D. E., Jr., & Aschner, M. (1994). The role of -SH groups in methylmercuric chloride-induced D-aspartate and rubidium release from rat primary astrocyte cultures. *Brain Res*, 641(1), 1-9.
- Mundy, W. R., & Freudenrich, T. M. (2000). Sensitivity of immature neurons in culture to metal-induced changes in reactive oxygen species and intracellular free calcium. *Neurotoxicology*, 21(6), 1135-1144.
- Murphy, T. H., Miyamoto, M., Sastre, A., Schnaar, R. L., & Coyle, J. T. (1989). Glutamate toxicity in a neuronal cell line involves inhibition of cystine transport leading to oxidative stress. *Neuron*, 2(6), 1547-1558.
- Murphy, T. H., Schnaar, R. L., & Coyle, J. T. (1990). Immature cortical neurons are uniquely sensitive to glutamate toxicity by inhibition of cystine uptake. *FASEB J*, 4(6), 1624-1633.
- Naganuma, A., Miura, K., Tanaka-Kagawa, T., Kitahara, J., Seko, Y., Toyoda, H., et al. (1998). Overexpression of manganese-superoxide dismutase prevents methylmercury toxicity in HeLa cells. *Life Sci*, 62(12), PL157-161.
- Nagashima, K. (1997). A review of experimental methylmercury toxicity in rats: neuropathology and evidence for apoptosis. *Toxicol Pathol*, 25(6), 624-631.
- Nagata, S. (2000). Apoptotic DNA fragmentation. *Exp Cell Res*, 256(1), 12-18.
- Nakatsu, N., Yoshida, Y., Yamazaki, K., Nakamura, T., Dan, S., Fukui, Y., et al. (2005). Chemosensitivity profile of cancer cell lines and identification of genes determining chemosensitivity by an integrated bioinformatical approach using cDNA arrays. *Mol Cancer Ther*, 4(3), 399-412.
- Namiki, M., Mori, T., Sawaguchi, T., Ito, S., & Suzuki, T. (2005). Underlying mechanism of combined effect of methamphetamine and morphine on lethality in mice and therapeutic potential of cooling. *J Pharmacol Sci*, 99(2), 168-176.
- Nedergaard, M., Takano, T., & Hansen, A. J. (2002). Beyond the role of glutamate as

- a neurotransmitter. *Nat Rev Neurosci*, 3(9), 748-755.
- Ou, Y. C., White, C. C., Krejsa, C. M., Ponce, R. A., Kavanagh, T. J., & Faustman, E. M. (1999). The role of intracellular glutathione in methylmercury-induced toxicity in embryonic neuronal cells. *Neurotoxicology*, 20(5), 793-804.
- Pacheco, R., Oliva, H., Martinez-Navio, J. M., Climent, N., Ciruela, F., Gatell, J. M., et al. (2006). Glutamate released by dendritic cells as a novel modulator of T cell activation. *J Immunol*, 177(10), 6695-6704.
- Pereira, C. M., & Oliveira, C. R. (1997). Glutamate toxicity on a PC12 cell line involves glutathione (GSH) depletion and oxidative stress. *Free Radic Biol Med*, 23(4), 637-647.
- Ralphe, J. C., Bedell, K., Segar, J. L., & Scholz, T. D. (2005). Correlation between myocardial malate/aspartate shuttle activity and EAAT1 protein expression in hyper- and hypothyroidism. *Am J Physiol Heart Circ Physiol*, 288(5), H2521-2526.
- Ran, R., Lu, A., Zhang, L., Tang, Y., Zhu, H., Xu, H., et al. (2004). Hsp70 promotes TNF-mediated apoptosis by binding IKK gamma and impairing NF-kappa B survival signaling. *Genes Dev*, 18(12), 1466-1481.
- Ravagnan, L., Gurbuxani, S., Susin, S. A., Maise, C., Daugas, E., Zamzami, N., et al. (2001). Heat-shock protein 70 antagonizes apoptosis-inducing factor. *Nat Cell Biol*, 3(9), 839-843.
- Reed, D. J. (1990). Glutathione: toxicological implications. *Annu Rev Pharmacol Toxicol*, 30, 603-631.
- Reynolds, I. J., & Hastings, T. G. (1995). Glutamate induces the production of reactive oxygen species in cultured forebrain neurons following NMDA receptor activation. *J Neurosci*, 15(5 Pt 1), 3318-3327.
- Sagara, Y., & Schubert, D. (1998). The activation of metabotropic glutamate receptors protects nerve cells from oxidative stress. *J Neurosci*, 18(17), 6662-6671.
- Sakamoto, M., Ikegami, N., & Nakano, A. (1996). Protective effects of Ca<sup>2+</sup> channel blockers against methyl mercury toxicity. *Pharmacol Toxicol*, 78(3), 193-199.
- Sandstrom, P. A., Tebbey, P. W., Van Cleave, S., & Buttke, T. M. (1994). Lipid hydroperoxides induce apoptosis in T cells displaying a HIV-associated glutathione peroxidase deficiency. *J Biol Chem*, 269(2), 798-801.

- Sanfeliu, C., Sebastia, J., & Ki, S. U. (2001). Methylmercury neurotoxicity in cultures of human neurons, astrocytes, neuroblastoma cells. *Neurotoxicology*, 22(3), 317-327.
- Sarafian, T., & Verity, M. A. (1991). Oxidative mechanisms underlying methylmercury neurotoxicity. *Int J Dev Neurosci*, 9(2), 147-153.
- Sarafian, T. A., Bredesen, D. E., & Verity, M. A. (1996). Cellular resistance to methylmercury. *Neurotoxicology*, 17(1), 27-36.
- Sasaki, H., Sato, H., Kuriyama-Matsumura, K., Sato, K., Maebara, K., Wang, H., et al. (2002). Electrophile response element-mediated induction of the cystine/glutamate exchange transporter gene expression. *J Biol Chem*, 277(47), 44765-44771.
- Sato, H., Fujiwara, K., Sagara, J., & Bannai, S. (1995). Induction of cystine transport activity in mouse peritoneal macrophages by bacterial lipopolysaccharide. *Biochem J*, 310 ( Pt 2), 547-551.
- Sato, H., Kuriyama-Matsumura, K., Hashimoto, T., Sasaki, H., Wang, H., Ishii, T., et al. (2001). Effect of oxygen on induction of the cystine transporter by bacterial lipopolysaccharide in mouse peritoneal macrophages. *J Biol Chem*, 276(13), 10407-10412.
- Sato, H., Takenaka, Y., Fujiwara, K., Yamaguchi, M., Abe, K., & Bannai, S. (1995). Increase in cystine transport activity and glutathione level in mouse peritoneal macrophages exposed to oxidized low-density lipoprotein. *Biochem Biophys Res Commun*, 215(1), 154-159.
- Sato, H., Tamba, M., Ishii, T., & Bannai, S. (1999). Cloning and expression of a plasma membrane cystine/glutamate exchange transporter composed of two distinct proteins. *J Biol Chem*, 274(17), 11455-11458.
- Senoo-Matsuda, N., Yasuda, K., Tsuda, M., Ohkubo, T., Yoshimura, S., Nakazawa, H., et al. (2001). A defect in the cytochrome b large subunit in complex II causes both superoxide anion overproduction and abnormal energy metabolism in *Caenorhabditis elegans*. *J Biol Chem*, 276(45), 41553-41558.
- Shanker, G., Allen, J. W., Mutkus, L. A., & Aschner, M. (2001). Methylmercury inhibits cysteine uptake in cultured primary astrocytes, but not in neurons. *Brain Res*, 914(1-2), 159-165.



- Shanker, G., & Aschner, M. (2001). Identification and characterization of uptake systems for cystine and cysteine in cultured astrocytes and neurons: evidence for methylmercury-targeted disruption of astrocyte transport. *J Neurosci Res*, 66(5), 998-1002.
- Shanker, G., & Aschner, M. (2003). Methylmercury-induced reactive oxygen species formation in neonatal cerebral astrocytic cultures is attenuated by antioxidants. *Brain Res Mol Brain Res*, 110(1), 85-91.
- Shanker, G., Syversen, T., Aschner, J. L., & Aschner, M. (2005). Modulatory effect of glutathione status and antioxidants on methylmercury-induced free radical formation in primary cultures of cerebral astrocytes. *Brain Res Mol Brain Res*, 137(1-2), 11-22.
- Shanker, G., Syversen, T., & Aschner, M. (2003). Astrocyte-mediated methylmercury neurotoxicity. *Biol Trace Elem Res*, 95(1), 1-10.
- Shenker, B. J., Guo, T. L., & Shapiro, I. M. (1998). Low-level methylmercury exposure causes human T-cells to undergo apoptosis: evidence of mitochondrial dysfunction. *Environ Res*, 77(2), 149-159.
- Shenker, B. J., Pankoski, L., Zekavat, A., & Shapiro, I. M. (2002). Mercury-induced apoptosis in human lymphocytes: caspase activation is linked to redox status. *Antioxid Redox Signal*, 4(3), 379-389.
- Sinor, J. D., Du, S., Venneti, S., Blitzblau, R. C., Leszkiewicz, D. N., Rosenberg, P. A., et al. (2000). NMDA and glutamate evoke excitotoxicity at distinct cellular locations in rat cortical neurons in vitro. *J Neurosci*, 20(23), 8831-8837.
- Skerry, T. M., & Genever, P. G. (2001). Glutamate signalling in non-neuronal tissues. *Trends Pharmacol Sci*, 22(4), 174-181.
- Smith, P. K., Krohn, R. I., Hermanson, G. T., Mallia, A. K., Gartner, F. H., Provenzano, M. D., et al. (1985). Measurement of protein using bicinchoninic acid. *Anal Biochem*, 150(1), 76-85.
- Stankiewicz, A. R., Lachapelle, G., Foo, C. P., Radicioni, S. M., & Mosser, D. D. (2005). Hsp70 inhibits heat-induced apoptosis upstream of mitochondria by preventing Bax translocation. *J Biol Chem*, 280(46), 38729-38739.
- Stejskal, V. D., Forsbeck, M., Cederbrant, K. E., & Asteman, O. (1996). Mercury-specific lymphocytes: an indication of mercury allergy in man. *J Clin Immunol*,

16(1), 31-40.

- Takano, T., Lin, J. H., Arcuino, G., Gao, Q., Yang, J., & Nedergaard, M. (2001). Glutamate release promotes growth of malignant gliomas. *Nat Med*, 7(9), 1010-1015.
- Takarada, T., & Yoneda, Y. (2008). Pharmacological topics of bone metabolism: glutamate as a signal mediator in bone. *J Pharmacol Sci*, 106(4), 536-541.
- Tan, S., Sagara, Y., Liu, Y., Maher, P., & Schubert, D. (1998). The regulation of reactive oxygen species production during programmed cell death. *J Cell Biol*, 141(6), 1423-1432.
- Tan, S., Schubert, D., & Maher, P. (2001). Oxytosis: A novel form of programmed cell death. *Curr Top Med Chem*, 1(6), 497-506.
- Tan, S., Wood, M., & Maher, P. (1998). Oxidative stress induces a form of programmed cell death with characteristics of both apoptosis and necrosis in neuronal cells. *J Neurochem*, 71(1), 95-105.
- Tanabe, Y., Masu, M., Ishii, T., Shigemoto, R., & Nakanishi, S. (1992). A family of metabotropic glutamate receptors. *Neuron*, 8(1), 169-179.
- Thornberry, N. A., & Lazebnik, Y. (1998). Caspases: enemies within. *Science*, 281(5381), 1312-1316.
- Tian, L., Shi, M. M., & Forman, H. J. (1997). Increased transcription of the regulatory subunit of gamma-glutamylcysteine synthetase in rat lung epithelial L2 cells exposed to oxidative stress or glutathione depletion. *Arch Biochem Biophys*, 342(1), 126-133.
- Tong, Q., Ouedraogo, R., & Kirchgessner, A. L. (2002). Localization and function of group III metabotropic glutamate receptors in rat pancreatic islets. *Am J Physiol Endocrinol Metab*, 282(6), E1324-1333.
- Trotti, D., Danbolt, N. C., & Volterra, A. (1998). Glutamate transporters are oxidant-vulnerable: a molecular link between oxidative and excitotoxic neurodegeneration? *Trends Pharmacol Sci*, 19(8), 328-334.
- Turrens, J. F., & Boveris, A. (1980). Generation of superoxide anion by the NADH dehydrogenase of bovine heart mitochondria. *Biochem J*, 191(2), 421-427.
- Usuki, F., & Ishiura, S. (1998). Expanded CTG repeats in myotonin protein kinase increase susceptibility to oxidative stress. *Neuroreport*, 9(10), 2291-2296.

- Van Cruchten, S., & Van Den Broeck, W. (2002). Morphological and biochemical aspects of apoptosis, oncosis and necrosis. *Anat Histol Embryol*, 31(4), 214-223.
- Verdaguer, E., Garcia-Jorda, E., Jimenez, A., Stranges, A., Sureda, F. X., Canudas, A. M., et al. (2002). Kainic acid-induced neuronal cell death in cerebellar granule cells is not prevented by caspase inhibitors. *Br J Pharmacol*, 135(5), 1297-1307.
- Vermes, I., Haanen, C., Steffens-Nakken, H., & Reutelingsperger, C. (1995). A novel assay for apoptosis. Flow cytometric detection of phosphatidylserine expression on early apoptotic cells using fluorescein labelled Annexin V. *J Immunol Methods*, 184(1), 39-51.
- Verrey, F., Closs, E. I., Wagner, C. A., Palacin, M., Endou, H., & Kanai, Y. (2004). CATs and HATs: the SLC7 family of amino acid transporters. *Pflugers Arch*, 447(5), 532-542.
- Vijayalakshmi, K., & Sood, P. P. (1994). Ameliorative capacities of vitamins and monothiol post therapy in the restoration of methylmercury altered glutathione metabolism. *Cell Mol Biol (Noisy-le-grand)*, 40(2), 211-224.
- Walczak, H., & Krammer, P. H. (2000). The CD95 (APO-1/Fas) and the TRAIL (APO-2L) apoptosis systems. *Exp Cell Res*, 256(1), 58-66.
- Wang, X. (2001). The expanding role of mitochondria in apoptosis. *Genes Dev*, 15(22), 2922-2933.
- WHO (1990). Environmental Health Criteria 101: Methylmercury. World Health Organization. Geneva.
- Wilke, R. A., Kolbert, C. P., Rahimi, R. A., & Windebank, A. J. (2003). Methylmercury induces apoptosis in cultured rat dorsal root ganglion neurons. *Neurotoxicology*, 24(3), 369-378.
- Woods, J. S., & Ellis, M. E. (1995). Up-regulation of glutathione synthesis in rat kidney by methyl mercury. Relationship to mercury-induced oxidative stress. *Biochem Pharmacol*, 50(10), 1719-1724.
- Wu, G., Fang, Y. Z., Yang, S., Lupton, J. R., & Turner, N. D. (2004). Glutathione metabolism and its implications for health. *J Nutr*, 134(3), 489-492.
- Yee, S., & Choi, B. H. (1994). Methylmercury poisoning induces oxidative stress in

- the mouse brain. *Exp Mol Pathol*, 60(3), 188-196.
- Yee, S., & Choi, B. H. (1996). Oxidative stress in neurotoxic effects of methylmercury poisoning. *Neurotoxicology*, 17(1), 17-26.
- Yin, Z., Milatovic, D., Aschner, J. L., Syversen, T., Rocha, J. B., Souza, D. O., et al. (2007). Methylmercury induces oxidative injury, alterations in permeability and glutamine transport in cultured astrocytes. *Brain Res*, 1131(1), 1-10.
- Zalups, R. K. (2000). Molecular interactions with mercury in the kidney. *Pharmacol Rev*, 52(1), 113-143.
- Zeiss, C. J. (2003). The apoptosis-necrosis continuum: insights from genetically altered mice. *Vet Pathol*, 40(5), 481-495.
- Zerangue, N., Arriza, J. L., Amara, S. G., & Kavanaugh, M. P. (1995). Differential modulation of human glutamate transporter subtypes by arachidonic acid. *J Biol Chem*, 270(12), 6433-6435.
- Zoratti, M., & Szabo, I. (1995). The mitochondrial permeability transition. *Biochim Biophys Acta*, 1241(2), 139-176.

## **APPENDIX**

## APPENDIX A

### COMPOSITION OF BUFFERS

Buffer	Composition
<b>Cell culture</b>	
25X PBS (-) (pH 7.4)	- Dissolve 200 g of NaCl, 28.75 g of Na <sub>2</sub> HPO <sub>4</sub> , 5 g of KH <sub>2</sub> PO <sub>4</sub> , and 5 g of KCl in distilled water to total volume of 1 liter, keep at room temperature
PBS containing Ca <sup>2+</sup> and Mg <sup>2+</sup> (pH7.4)	- Dissolve 0.9 g D-glucose in 40 ml 25X PBS(-) and 800 ml distilled water - Add 5 ml 100 mM MgCl <sub>2</sub> , and 10 ml 100 mM CaCl <sub>2</sub> - Adjust pH to 7.4, and fill up volume to 1 liter with distilled water, keep at room temperature
MEM with 10% FBS, pH 7.2	- Dissolve 1 bottle of MEM powder, and 2.2 g of NaHCO <sub>3</sub> in 800 ml of distilled water - Add 100 ml of FBS, then adjust pH and add additional distilled water to total volume of 1 liter, filtrate using bottle-top filter (0.45 Micron), keep at 4 °C
<b>Uptake experiment</b>	
Na <sup>+</sup> -free Hanks' balanced salt solution: HBSS (-) (pH 7.4)	- Compose of 125 mM Choline Chloride, 4.8 mM KCl, 1.2 mM MgSO <sub>4</sub> ·7H <sub>2</sub> O, 1.2 mM KH <sub>2</sub> PO <sub>4</sub> , 1.3 mM CaCl <sub>2</sub> ·H <sub>2</sub> O, 25 mM HEPES, and 5.6 mM glucose in distilled water, and adjust pH to pH 7.4 with 2 M Tris base, Freshly prepare

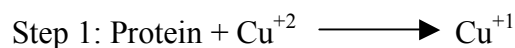
## APPENDIX B

### PROTEIN DETERMINATION USING BICINCHONINIC ACID (BCA) ASSAY (Smith *et al.*, 1985)

#### Principle

BCA act as the detection reagent for cuprous cation ( $\text{Cu}^{+1}$ ), which is formed when cupric cation ( $\text{Cu}^{+2}$ ) is reduced by protein in an alkaline. The reaction starts with the reduction of  $\text{Cu}^{+2}$ , from cupric sulfate to  $\text{Cu}^{+1}$  by protein. One molecule cuprous cation ( $\text{Cu}^{+1}$ ) is interacted with two molecules of BCA, which results in the production of purple-colored product that exhibits a strong absorbance at 562 nm.

#### BCA-Protein Reaction Scheme:



#### BCA™ Protein Assay (Pierce Biotechnology, Rockford, IL, USA)

Reagent A contains sodium carbonate, sodium bicarbonate, bicinchoninic acid (BCA) and sodium tartate in 0.1 M sodium hydroxid.

Reagent B contains 4% cupric sulfate.

Albumin Standard Ampules contain bovine serum albumin (BSA) at 2 mg/ml in 0.9% saline and 0.05% sodium azide.

#### Procedure

1. Prepare a working solution by mixing Reagent A with Reagent B (50:1).
2. Prepare BSA standard as follows.

BSA (μg)	2 mg/ml BSA (μl)	DW (μl)	Mixture of A and B (μl)
0	0	15	500
2	1	14	500
4	2	13	500
8	4	11	500
16	8	7	500

3. Prepare sample as follows.

Samples ( $\mu$ l)	DW ( $\mu$ l)	Mixture of A and B ( $\mu$ l)
1	14	500

4. The samples were mixed well and then incubated at 37 °C for 30 minutes.
5. Read absorbance at 562 nm by BECKMAN DU<sup>®</sup> 640 Spectrophotometer (Beckman Industries, Inc., CA. USA).
6. Standard curve was plotted between absorbance (Y-axis) and amount ( $\mu$ g) of standard BSA (X-axis).



## BIOGRAPHY

<b>NAME</b>	Miss Sirirat Amonpatumrat
<b>DATE OF BIRTH</b>	January 18 <sup>th</sup> , 1982
<b>PLACE OF BIRTH</b>	Bangkok, Thailand
<b>INSTUTION ATTENED</b>	Mahidol University, 1999-2003 Bachelor of Science (Biology) Mahidol University, 2003-2008 Doctor of Philosophy (Toxicology)
<b>RESEARCH GRANTS</b>	1) Development and Promotion of Science and Technology (DPST) Scholarship 2) The Post-graduate Education, Training and Research Program in Environmental Science, Technology and Management (ESTM) Scholarship 3) The Japanese Ministry of Education, Culture, Sports, Science and Technology; Research Promotion Fund of Japan Private School Promotion Foundation (MEXT)
<b>HOME ADDRESS</b>	41, Ramkhamhaeng Rd., Minburi Distinct, Bangkok, Thailand 10510
<b>E-MAIL ADDRESS</b>	sirirat543@gmail.com